NEUROIMAGING AND GENETICS STUDIES OF THE ROLE OF RIGHT PREFRONTAL CORTEX IN CONTROLLED ATTENTION

by

Anne Shively Berry

A dissertation submitted in partial fulfillment
of the requirements for the degree of
Doctor of Philosophy
(Neuroscience)
in the University of Michigan
2014

Doctoral Committee:

Associate Professor Cindy Lustig, Co-Chair
Professor Martin Sarter, Co-Chair
Professor William J. Gehring
Professor John Jonides
Professor Terry E. Robinson

DEDICATION

For Donald Howard Shively

TABLE OF CONTENTS

LIST OF FIGURES

LIST OF TABLES

LIST OF ABBREVIATIONS

ACC	anterior cingulate cortex
ACh	acetylcholine
ASL	arterial spin labeling
BA	Brodmann's area
CHT	choline transporter
dSAT	distractor condition Sustained Attention Task
EEG	electroencephalography
ERP	event-related potential
FEF	frontal eye fields
fMRI	functional magnetic resonance imaging
IFG	inferior frontal gyrus
MFG	middle frontal gyrus
PFC	prefrontal cortex
SAT	Sustained Attention Task
SPL	superior parietal lobule

ABSTRACT

Maintaining goal-relevant behavior requires controlled attention, especially when attention is challenged by distraction. Deficits in controlled attention are characteristic of a number of disorders, including schizophrenia. Here I present three studies investigating the human neural correlates of successful attentional control, specifically those associated with stabilizing performance during distractor challenge. To optimize the translational potential of this work, the present studies used the Sustained Attention Task (SAT) and its distractor condition (dSAT) which has been validated for use in both humans and rodent models, and has been identified as a promising tool for understanding attention deficits in schizophrenia (Luck et al., 2012). The first study, using BOLD fMRI, found that a region in right inferior frontal gyrus approximating Broadmann's Area (BA) 9 showed increased activation in response to the distractor. This right mid-dorsal/dorsolateral prefrontal cortex region is part of the frontoparietal cognitive control network, and multivariate analyses charting its functional connections to other regions revealed that increases in connectivity between BA 9 and posterior parietal cortex were associated with successful behavioral resistance to distraction. A second study using electrophysiological methods complemented these findings by showing a similar correlation between increases in theta phase-

locking during distractor challenge and optimal performance. Finally, the third study used genetic variation to probe the role of the cholinergic system, which rodent studies employing SAT and dSAT suggest is critical for attention. Specifically, in rodents, the maintenance of performance during distraction is associated with increases in acetylcholine in right prefrontal cortex. Consistent with rodent findings, the present work in humans suggested a role of acetylcholine in distractor-related activation increases in right BA 9. Participants with a genetic polymorphism thought to limit cholinergic release capacity showed diminished distractor-evoked right BA 9 activation increases. Together, these findings further specify the neural correlates of controlled attention in humans, and take the first steps in linking these measures to the human cholinergic system. The ultimate goal of this research is to capitalize on the strengths of both human-based and animal model-based investigations of attention to contribute to the identification of therapeutic targets to treat deficits where they may exist.

Chapter I

INTRODUCTION

Performing attention-demanding tasks is made more difficult in the presence of distraction. For example, imagine driving into a sudden thunderstorm. The pouring rain and flashing lightning make it difficult to see the road ahead, much less the street sign marking your intended turn. However, high levels of performance can be maintained during such challenging conditions through increased cognitive control. Cognitive control may act to stabilize performance by supporting the maintenance of task goals over time, by modulating the processing of relevant and irrelevant sensory inputs according to these goals, and by facilitating the activation of appropriate task rules. Prefrontal cortex (PFC) is thought to mediate these cognitive control functions (reviewed in Dehaene, Kerszberg, & Changeux, 1998; Miller & Cohen, 2001).

The three studies presented here investigated the role of right PFC approximating Brodmann area (BA) 9 in cognitive control. These studies used a visual signal detection task, the Sustained Attention Task (SAT), and its distractor condition (dSAT). The dSAT includes a global visual distractor, which was designed to increase the task's cognitive control demands, much like a thunderstorm may increase the cognitive control demands of an otherwise

routine drive home. The first fMRI study examined how distractor challenge may influence the hemodynamic response in right BA 9, shape its functional network activity, and how these functional responses relate to the preservation of attentional performance (Chapter II). The second fMRI study examined a possible role of the neurotransmitter acetylcholine (ACh) in cognitive control and right BA 9 activation by testing a population with a genetic variant affecting the cholinergic system (Chapter III). The third study used electroencephalography (EEG) to define the temporal dynamics of visual, parietal, and PFC responses associated with optimal dSAT performance (Chapter IV).

Below I provide background on SAT and dSAT and its use in previous human fMRI and behavioral studies, as well as its use in rodent studies for which original support for the critical contribution of ACh to dSAT performance was demonstrated.

Human SAT and dSAT task.

The SAT was originally designed to study the neural mechanisms of controlled attention in rodent models (McGaughy & Sarter, 1995), and has been adapted and validated for human research (Demeter, Sarter, & Lustig, 2008). The basic SAT is a visual signal detection task. Participants monitor for the appearance of a small, centrally presented signal, which appears for approximately half of the trials. The monitoring times and signal durations vary,

introducing temporal uncertainty and increasing need for the maintenance of controlled attention over time (c.f. Parasuraman & Davies, 1977; Parasuraman & Mouloua, 1987; Parasuraman, Warm, & Dember, 1987). After the signal (or nonsignal) period, participants are cued to respond. Responses are required for both signal and nonsignal trials and are followed by accuracy feedback. dSAT trials are identical to SAT trials with the addition of a global distractor, a flashing background screen. The successful control of attention is indexed by the "distractor effect," the impact of distraction on performance (SAT performance – dSAT performance), such that small behavioral decrements during dSAT reflect optimal control.

SAT validation studies established that the presence of distraction impairs performance. This behavioral decrement during dSAT is also found in rodents, though with greater effect sizes (Demeter et al., 2008). Such differences may be driven by interspecies differences in cognitive control capacity. Experimental manipulations in humans have shown that the distractor's effect on performance can be altered by imposing monetary penalties for missed trials (Demeter et al., 2008). Specifically, introducing penalties impacts the distribution of miss vs false alarm errors. The ability of distractor performance to be modified via shifting reward contingencies is an important indicator that dSAT performance is sensitive to the engagement of cognitive control, and serves as validation of dSAT as a high cognitive control condition.

Human neural correlates of dSAT.

A previous arterial spin labeling (ASL) study explored the neural correlates of SAT and dSAT performance (Demeter, Hernandez-Garcia, Sarter, & Lustig, 2011). This study employed long blocks of sustained task performance to identify possible cognitive control regions characterized by greater increases in perfusion for dSAT relative to SAT blocks. This analysis revealed increased demands on cognitive control were accompanied by enhanced perfusion in right middle frontal gyrus (MFG) approximating BA 9. Increased right BA 9 perfusion was significant after controlling for the visual stimulation of the distractor, which indicated prefrontal perfusion increases were not induced by the flashing stimulus *per se*, but increased in association with the attentional demands of the task.

Further suggesting perfusion increases were functionally relevant, right BA 9 perfusion during distractor challenge correlated with the distractor's effect on performance. Specifically, participants with the greatest drops in performance showed the greatest perfusion increases during dSAT. The direction of this neural-behavioral relationship is opposite to what is often reported: increased activation in cognitive control regions positively correlating with high levels of performance. Instead of tracking behavioral resistance to distraction, right BA 9 perfusion during dSAT may be a marker of attentional effort in demanding conditions. *Chapter II replicated these findings and tested the hypothesis that*

increases in BA 9's functional network activity boosts behavioral resistance to distraction.

Clinical translational use.

The SAT has strong potential to contribute to translational research efforts both because of its close ties to complementary rodent studies (to be discussed in the next section), as well as the specific deficits it reveals in clinical populations. The primary clinical population our research has focused on to date is schizophrenia, which is characterized by prominent deficits in the control of attention. Consistent with this focus, SAT and dSAT were identified by the Cognitive Neuroscience Initiative to Improve Cognition in Schizophrenia (CNTRICS) as a useful translational research tool for promoting our understanding of these deficits (Luck, Ford, Sarter, & Lustig, 2012).

Behavioral studies in people with schizophrenia revealed specific dSAT performance deficits relative to SAT (Demeter, Guthrie, Taylor, Sarter, & Lustig, 2013), which is in agreement with behavioral studies in rodent models of schizophrenia (Kozak et al., 2007, Sarter, Martinez, & Kozak, 2009). An fMRI study in patients with schizophrenia is currently underway to determine whether distractor vulnerability is associated with disrupted right BA 9 activation. Supporting this prediction, an fMRI meta-analysis specifically identified right BA 9

as a region disproportionally affected by the disorder (Minzenberg, Laird, Thelen, Carter, & Glahn, 2009).

Rodent studies implicating acetylcholine in controlled attention.

Rodent studies have demonstrated the critical contribution of cholinergic inputs from the basal forebrain to right medial PFC in controlled attention. Specifically, selective cholinergic lesions of these structures cause robust performance declines in SAT and dSAT tasks (Martinez & Sarter, 2004; McGaughy, Decker, & Sarter, 1999; McGaughy, Kaiser, & Sarter, 1996; McGaughy & Sarter, 1998, 1999). Critical in establishing the translational value of the present cross-species studies, rodents and humans show parallel patterns of task-related ACh/fMRI effects in PFC. Performance of SAT increases rodent ACh concentrations in right PFC relative to baseline, and the heightened attentional challenge of dSAT augments ACh levels further (St. Peters, Demeter, Lustig, Bruno, & Sarter). There is also cross-species agreement in the right lateralization of these effects—unilateral lesion studies and choline transporter assays in rodents have indicated right-lateralized specialization of the cholinergic contribution to task performance (Apparsundaram, Martinez, Parikh, Kozak, & Sarter, 2005; Martinez & Sarter, 2004).

As was found in the human fMRI study, the degree of right PFC augmentation during dSAT correlated the distractor's impact on performance. In

rodents, the greater the ACh concentration, the better the performance (St Peters et al., 2011). Though the direction of the correlation with behavior is opposite for humans and rodents, the significant neural-behavioral relationship supports the idea that enhancement of right PFC activity is functionally relevant to the controlled attention processes engaged during distractor challenge. An intriguing possibility that emerges from the correspondence of findings across species is that the cholinergic system supports controlled attention processes in humans, and that cholinergic signaling in right PFC contributes to our observed right BA 9 increases in fMRI signal. *Chapter III takes the first steps in exploring these possibilities.*

Final remarks.

The three studies presented here further delineate the functional role of right BA 9 in supporting performance during attentional challenge. We provide replication of previous findings linking right BA 9 to increased cognitive control demands during dSAT performance (Chapter II). Connecting to research in rodents, we found an association between genetic variation in the cholinergic system and right BA 9 activation (Chapter III). We demonstrate BA 9 functional coupling with posterior regions is associated with successful distractor resistance (Chapters II and IV). Finally, we propose a timecourse by which controlled attention may modulate processing in posterior cortices (Chapter IV). The results

of these studies provide a basic understanding of the neural correlates associated with nondisordered attentional function, and will be relevant to the interpretation of ongoing and future studies investigating alterations in the neural correlates of cognitive control in clinical populations including schizophrenia and Parkinson's disease (Kim, Muller, Bohnen, Sarter, & Lustig, 2014).

References

Apparsundaram, S., Martinez, V., Parikh, V., Kozak, R., & Sarter, M. (2005). Increased capacity and density of choline transporters situated in synaptic membranes of the right medial prefrontal cortex of attentional task-performing rats. *J Neurosci, 25*(15), 3851-3856.

Dehaene, S., Kerszberg, M., & Changeux, J. P. (1998). A neuronal model of a global workspace in effortful cognitive tasks. Proc Natl Acad Sci U S A, 95(24), 14529-14534.

Demeter, E., Guthrie, S. K., Taylor, S. F., Sarter, M., & Lustig, C. (2013). Increased distractor vulnerability but preserved vigilance in patients with schizophrenia: evidence from a translational Sustained Attention Task. Schizophr Res, 144(1-3), 136-141.

Demeter, E., Hernandez-Garcia, L., Sarter, M., & Lustig, C. (2011). Challenges to attention: a continuous arterial spin labeling (ASL) study of the effects of distraction on sustained attention. Neuroimage, 54(2), 1518-1529.

Demeter, E., Sarter, M., & Lustig, C. (2008). Rats and humans paying attention: cross-species task development for translational research. Neuropsychology, 22(6), 787-799.

Kim, K., Muller, M., Bohnen, N., Sarter, M., & Lustig, C. (2014). Vulnerability to distraction in patients with Parkinson's disease is linked to low cortical cholinergic function. Paper presented at the Annual meeting of the Cogntive Neuroscience Society.

Kozak, R., Martinez, V., Young, D., Brown, H., Bruno, J. P., & Sarter, M. (2007). Toward a neuro-cognitive animal model of the cognitive symptoms of schizophrenia: disruption of cortical cholinergic neurotransmission following repeated amphetamine exposure in attentional task-performing, but not non-performing, rats. *Neuropsychopharmacology, 32*(10), 2074-2086.

Luck, S. J., Ford, J. M., Sarter, M., & Lustig, C. (2012). CNTRICS final biomarker selection: Control of attention. Schizophrenia bulletin, 38(1), 53-61.

Martinez, V., & Sarter, M. (2004). Lateralized attentional functions of cortical cholinergic inputs. Behav Neurosci, 118(5), 984-991.

McGaughy, J., Decker, M. W., & Sarter, M. (1999). Enhancement of sustained attention performance by the nicotinic acetylcholine receptor agonist ABT-

418 in intact but not basal forebrain-lesioned rats. Psychopharmacology, 144(2), 175-182.

McGaughy, J., Kaiser, T., & Sarter, M. (1996). Behavioral vigilance following infusions of 192 IgG-saporin into the basal forebrain: selectivity of the behavioral impairment and relation to cortical AChE-positive fiber density. Behav Neurosci, 110(2), 247-265.

McGaughy, J., & Sarter, M. (1995). Behavioral vigilance in rats: task validation and effects of age, amphetamine, and benzodiazepine receptor ligands. Psychopharmacology, 117(3), 340-357.

McGaughy, J., & Sarter, M. (1998). Sustained attention performance in rats with intracortical infusions of 192 IgG-saporin-induced cortical cholinergic deafferentation: effects of physostigmine and FG 7142. Behav Neurosci, 112(6), 1519-1525.

McGaughy, J., & Sarter, M. (1999). Effects of ovariectomy, 192 IgG-saporin-induced cortical cholinergic deafferentation, and administration of estradiol on sustained attention performance in rats. Behav Neurosci, 113(6), 1216-1232.

Miller, E. K., & Cohen, J. D. (2001). An integrative theory of prefrontal cortex function. Annu Rev Neurosci, 24, 167-202.

Minzenberg, M. J., Laird, A. R., Thelen, S., Carter, C. S., & Glahn, D. C. (2009). Meta-analysis of 41 functional neuroimaging studies of executive function in schizophrenia. Arch Gen Psychiatry, 66(8), 811-822.

Parasuraman, R., & Davies, D. R. (1977). A taxonomic analysis of vigilance performance. In R. R. Mackie (Ed.), Vigilance: Theory, operational performance, and physiological correlates (pp. 559-574). New York: Plenum Press.

Parasuraman, R., & Mouloua, M. (1987). Interaction of signal discriminability and task type in vigilance decrement. Perception & psychophysics, 41(1), 17-22.

Parasuraman, R., Warm, J. S., & Dember, W. N. (Eds.). (1987). Vigilance: Taxonomy and utility. New York: Springer.

Sarter, M., Martinez, V., & Kozak, R. (2009). A neurocognitive animal model dissociating between acute illness and remission periods of schizophrenia. *Psychopharmacology (Berl), 202*(1-3), 237-258.

St Peters, M., Demeter, E., Lustig, C., Bruno, J. P., & Sarter, M. (2011). Enhanced control of attention by stimulating mesolimbic-corticopetal cholinergic circuitry. J Neurosci, 31(26), 9760-9771.

Chapter II

FRONTOPARIETAL CORRELATES OF ATTENTIONAL EFFORT VERSUS DISTRACTOR RESISTANCE DURING CHALLENGES TO ATTENTION

INTRODUCTION

The ability to detect and respond to relevant signals in the environment is critical for survival. Detection of sudden onset signals may be mediated largely through stimulus-driven "bottom-up" processes in the absence of competing stimuli, while the presence of distraction increases the demand for "top-down" cognitive control for successful detection. Increasing cognitive control may facilitate detection by enhancing the processing of targets, filtering distractors, and maintaining task set (Corbetta & Shulman, 2002; Kanwisher & Wojciulik, 2000; Kastner & Ungerleider, 2000; Sarter, Gehring, & Kozak, 2006; Sarter, Givens, & Bruno, 2001). The present study specifically examined the role of right prefrontal cortex (PFC) approximating Brodmann's area (BA) 9 in stabilizing performance during challenges to attention.

Our previous research using the Sustained Attention Task (SAT) and its distractor condition (dSAT) identified a region in right middle frontal gyrus (MFG) approximating BA 9 that increased activation during distractor challenge (Demeter, Hernandez-Garcia, Sarter, & Lustig, 2011). The arterial spin labeling

(ASL) study employed long blocks of sustained task performance with and without distraction, implemented via a strobing background screen. Right BA 9 showed small activity increases during standard task performance when cognitive load was limited, with greater augmentation of activity during distractor challenge. Enhanced perfusion in this region was prominent after controlling for the visual stimulation of the distractor, indicating elevated activity was not induced by the strobing background *per se* but was elevated in association with attentional challenge. The strong right lateralization of the observed BA 9 activity is consistent with other studies of sustained attention in both humans (Cabeza & Nyberg, 2000; Coull, Frackowiak, & Frith, 1998; Kim et al., 2006, Lim et al., 2010; Sturm et al., 1999) and rodents (Gill, Sarter, & Givens, 2000; Kozak et al., 2006; St Peters et al., 2011). The present study assessed a more general role of right BA 9 in cognitive control during distractor challenge independent of challenges driven by time-on-task. Specifically, the event-related design used in the present BOLD fMRI study interrupted continuous performance by introducing short task-free fixation periods among SAT and dSAT trials, thereby reducing the sustained element of task performance.

BA 9 lies in mid-dorsal/dorsolateral PFC and is part of the frontoparietal cognitive control network strongly implicated in functions including the representation of task goals or rules, biasing activity in functionally connected regions, monitoring the outcome of behavior, and maintaining and updating task representations (reviewed in Dehaene et al., 1998; Miller & Cohen, 2001).

Supporting the role of BA 9 in directing these functions, it is highly connected with sensory, motor, parietal, other PFC regions as well as midbrain and limbic structures. Relevant to detection processes specifically, it is situated between the dorsal and ventral attention networks thought to comprise the respective "top-down" and "bottom-up" components of attentional orienting (Corbetta & Shulman, 2002; Kanwisher & Wojciulik, 2000; Kastner & Ungerleider, 2000). In turn, defining the role of mid-dorsal PFC in flexibly coupling with these networks and mediating communication between them is an active topic of cognitive neuroscience research (Cole et al., 2013; Miller & Cohen, 2001). Our hope is that defining the mechanisms by which this region acts to preserve detection performance in the face of attentional challenge may reveal general principals relevant to understanding disorders where cognitive control is compromised such as in schizophrenia (Demeter, Guthrie, Taylor, Sarter, & Lustig, 2013; Minzenberg, Laird, Thelen, Carter, & Glahn, 2009).

Increased engagement of cognitive control regions may not always be sufficient to maintain performance in the face of challenges, even in non-clinical populations. In healthy older adults, robustly elevated PFC activation relative to young adults is often accompanied by equivalent or diminished performance on tasks with moderate executive function demands (Cappell, Gmeindl, & Reuter-Lorenz, 2010; Grady et al., 1994; Langenecker & Nielson, 2003; Langenecker, Nielson, & Rao, 2004). Such "overactivations" are thought to be compensatory and have been attributed to enhanced neural recruitment due to processing

inefficiency (e.g. Compensation-Related Utilization of Neural Circuits Hypothesis (CRUNCH), Reuter-Lorenz & Cappell, 2008).

In our own research, we found increased perfusion in right BA 9 was not sufficient to mitigate the impact of distraction on performance in young adults. On an individual subject level, participants whose performance was most negatively affected by the distractor showed the greatest right BA 9 increases. This pattern suggested right BA 9 perfusion increases did not reflect the successful recovery of declining performance, but tracked attentional effort in the face of challenge. In the present study we sought to determine whether right BA 9 activation scaled with attentional effort rather than successful distractor resistance once sustained attention challenges were removed.

The question remains, how, if at all, does right BA 9 act to successfully benefit performance during distractor challenge? To answer this question, we examined functional connectivity during task performance to determine whether right BA 9's coupling within attention networks may act to rescue declines in performance and promote distractor resistance. Our analyses across individuals revealed distinct patterns of functional connectivity between right BA 9 and other cognitive control regions that were associated with both successful and unsuccessful preservation of performance during distractor challenge.

Though our primary questions focused on investigating the role of right BA 9 during task performance, we next examined whether successful distractor resistance could be predicted based on individual differences in intrinsic BA 9

network activity measured before task performance. Task-relevant attention networks can be observed in patterns of functional connectivity measured at rest (Fox, Corbetta, Snyder, Vincent, & Raichle, 2006), and individual differences in the spontaneous organization of these networks may be useful in understanding individual differences in task-related attentional function. Increasingly, intrinsic and/or baseline measures of neural activity have been considered a powerful tool for predicting behavioral outcomes (Cole, Yarkoni, Repovs, Anticevic, & Braver, 2012; Li et al., 2013; Lim et al., 2010; Song et al., 2008; van den Heuvel, Stam, Kahn, & Hulshoff Pol, 2009), and are particularly promising from a translational perspective. Specifically, patterns of resting brain activity have been used to predict future gains following cognitive training interventions (Varkuti et al., 2013; Wu, Srinivasan, Kaur, & Cramer, 2014), and to identify post-training markers of functional plasticity (Buschkuehl, Hernandez-Garcia, Jaeggi, Bernard, & Jonides, 2014; Chapman et al., 2013; Urner, Schwarzkopf, Friston, & Rees, 2013; reviewed in Guerra-Carrillo, Mackey, & Bunge, 2014). Understanding how spontaneous network activity measured at rest relates to task-induced activity and predicts performance may significantly enhance our understanding of neural signatures of state and trait attention, may help identify potential biomarkers for the detection of cognitive control deficits, and may represent important targets for cognitive enhancement through training approaches or transcranial magnetic stimulation.

In the present study we took early steps in these efforts by characterizing the functional role of right BA 9 in stabilizing attentional performance, and by assessing the performance-predicting value of its functional connections. We tested specific hypotheses that univariate activation in this region during distractor challenge scales with attentional effort rather than successful distractor resistance, and that right BA 9 acts to successfully rescue performance through synchronized activity with other regions in the frontoparietal cognitive control network.

METHODS

Participants.

18 young adult participants (9 female, mean age = 22.78 yr, range = 18-27 yr) were included in the analysis. All participants were right-handed as determined by the Edinburgh Handedness Scale (Oldfield, 1971), had normal or corrected-to-normal vision, and scored at least a nine on the Extended Range Vocabulary Test (EVRT, Version 3, Educational Testing Services (ETS), 1976; mean score = 21.22, range = 9.00 - 32.25). Participants had no history of psychological or psychiatric disorder, and did not take medications that affect cognition. Data from 2 participants were excluded from analyses of functional runs collected during task performance due to excessive head motion (> 3 mm in x, y, z

direction or 3° pitch, roll, yaw). Their resting state scans, collected at the beginning of the fMRI session, were included in analysis as their head motion was under threshold.

Behavioral task.

Participants performed the Sustained Attention Task (SAT) and its distractor condition (dSAT) as previously described (Demeter et al., 2013; Demeter et al., 2011; Demeter, Sarter, & Lustig, 2008), implemented using E-prime software (Psychological Software Tools, Pittsburg, PA). SAT and dSAT trials consisted of signal and nonsignal trials (Figure 2.1). The signal was a small dark gray square centrally presented for a variable duration (17 – 64 ms). Trials consisted of a period of monitoring (1000, 2000, or 3000 ms), at the end of which a signal did (signal event) or did not (nonsignal event) appear. The signal occurred for 50% of the trials. Participants were cued to respond by a 700 ms low-frequency auditory response tone. Participants had up to 1000 ms after the tone to make a keypress response indicating whether or not the signal had been presented on that trial (response-hand mapping was counterbalanced across subjects). A high-frequency tone lasting 700 ms followed correct responses. Responses were classified as hits (correct signal trials), misses (incorrect signal trials), correct rejections (CR; correct nonsignal trials), false alarms (FA; incorrect nonsignal trials), and omissions. dSAT trials were identical to SAT trials except

the background screen flashed from gray to black at 10 Hz. Participants were provided monetary incentive. For each task run, participants were paid 1 cent for each percent correct, but penalized 5 cents for the percent of missed trials.

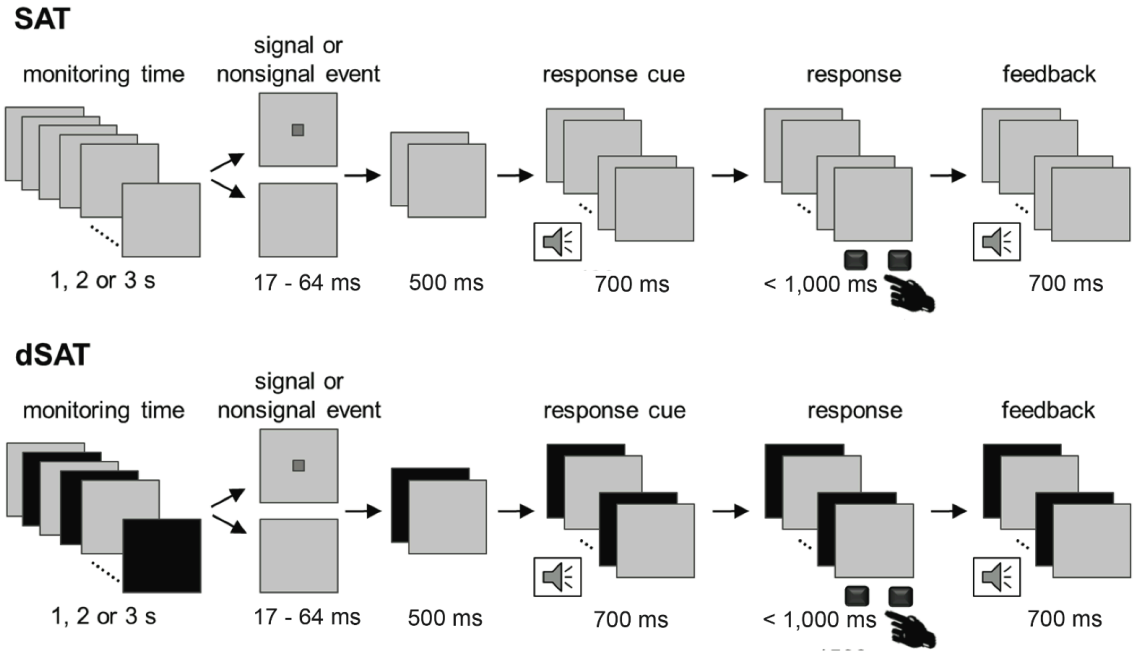

Figure 2.1. Sustained Attention Task (SAT). Each trial consisted of a variable duration monitoring interval followed by the presentation of a signal or nonsignal event. The signal was a gray square on a silver background and varied in duration. Signal and nonsignal events were pseudorandomized and occurred with equal frequency. After the auditory cue, participants responded via buttonpress using one index finger for signal trials and the other index finger for nonsignal trials (left-right key assignment counterbalanced across participants). Correct responses were followed by a high frequency feedback tone; incorrect responses or omissions did not result in feedback. The distractor condition, dSAT, increased the attentional control demands of the task by adding a global, continuous visual distractor. During dSAT trials, the screen flashed from gray to black at 10 Hz. SAT, dSAT, and fixation (not pictured) trials were pseudorandomly intermixed.

Behavioral analysis.

Our primary accuracy measure was SAT score, a measure of performance across both signal and nonsignal trials. For completeness, Appendix I reports the standard signal-detection measures of sensitivity (d') and bias (Swets, Tanner, & Birdsall, 1961). However, for our primary analyses, SAT score was preferred to d' because SAT score does not make assumptions about equal variance of positive and negative responses, which are often violated (see discussion by Frey & Colliver, 1973). In this regard, the SAT score is similar to the nonparametric similarity index (SI) but unlike SI is not confounded by errors of omission. SAT score was calculated for each condition (SAT, dSAT) using the formula SAT score = (hits – FAs)/[2(hits + FAs) – (hits + FAs)^2]. SAT score varies from + 1 to -1 with + 1 indicating all responses were hits or CRs and -1 indicating all responses were misses or FAs. Data were analyzed with SPSS, version 21. We assessed the effects of distraction on performance using paired *t* tests with effect sizes computed using Cohen's d.

fMRI data acquisition and preprocessing.

Resting state. All imaging data were collected using a 3 T General Electric Signa scanner with a standard quadrature head coil. Participants used mirrored glasses to view stimuli that were projected on a screen behind them. Functional

images were acquired during rest using a spiral-in sequence with 43 slices and voxel size 3.44 x 3.44 x 3 mm (TR = 2 s, TE = 30 ms, flip angle = 90°, FOV = 22 mm^2). During resting state fMRI acquisition (~ 6 min), a white fixation cross on a black background was displayed in the center of the screen. Participants were asked to remain awake with their eyes open and focused on the cross. Heart rate and respiration were recorded. Resting state scans were acquired in the beginning of the scanning session before task runs. Motion during scanning was minimal. No subject moved more than 0.20 mm in x, y, or z directions or rotated more than 1.57° along pitch, roll, or yaw axes.

Task runs. Six experimental runs consisted of equal numbers of SAT signal, dSAT signal, SAT nonsignal, dSAT nonsignal and fixation trials. During fixation periods (duration 2.2 s – 12.6 s), participants were instructed to relax and focus on a centrally presented fixation cross (background screen flashed from gray to black at 10 Hz). Each experimental run consisted of 75 trials. Trials were pseudorandomized to ensure that all possible sequences occurred with equal probability. Prior to functional runs, participants performed in-scanner practice trials to confirm they remembered task instructions, and the response and feedback tones were audible.

Functional images were acquired during task performance using a spiral-in sequence with 35 slices and voxel size 3.44 x 3.44 x 3 mm (TR = 2 s, TE = 30 ms, flip angle = 90°, FOV = 22 mm^2). T1-weighted anatomical overlay was acquired in the same functional space (TR = 225 ms, TE = 3.8 ms, flip angle =

90°). A 148-slice high-resolution T1-weighted anatomical scan was collected using spoiled-gradient-recalled acquisition (SPGR) in steady-state imaging (TR = 9 ms, TE = 1.8 ms, flip angle = 15°, FOV = 25 x 26 cm, slice thickness = 1.2 mm).

During preprocessing, structural images were skull-stripped using the Brain Extraction Tool in FSL (FMRIB Software Library; www.fmrib.ox.ac.uk/fsl; Smith et al., 2004) and corrected for signal inhomogeneity. SPGR images were normalized to the Montreal Neurological Institute (MNI) template using SPM 8 (Wellcome Department of Cognitive Neurology, London). To spatially normalize functional images to the MNI template, the functional overlay and SPGR were used as intermediates. All functional images were corrected for differences in slice timing (Oppenheim, Schafer, & Buck, 1999) and head movement using the MCFLIRT algorithm (Jenkinson, Bannister, Brady, & Smith, 2002). Functional images were smoothed with an 8-mm full width/half-maximum isotropic Gaussian kernel and high-pass filtered (128 s).

fMRI univariate analysis.

General Linear Model. Data were analyzed using a multisession General Linear Model (GLM) implemented in SPM8. SAT and dSAT hits, CRs, and fixation onsets were modeled as separate predictors. All omissions, misses, and FAs were modeled together as a separate predictor and are not included in the

present analysis. Predictors were time-locked to onset of the signal or nonsignal period and convolved with the canonical hemodynamic response function. To correct for the effect of motion artifact, six motion regressors derived from individual subject realignment were included in the model.

A priori region of interest analysis. To assess how data from the present study corresponded with findings from the ASL study by Demeter et al. (2011), we conducted a region of interest (ROI) analysis. Demeter et al. (2011) identified a region in right MFG, approximating BA 9 that showed increased perfusion during dSAT challenge (peak Montreal Neurological Institute (MNI) coordinates 35, 9, 33). To determine whether activation in this region was greater for dSAT trials relative to SAT trials in the present study, we extracted percent signal-change values from an 8 mm spherical ROI centered on the ASL peak coordinates. Percent signal-change values for each participant were extracted using MarsBar software (http://marsbar.sourceforge.net; Brett, Anton, Valabregue, & Poline, 2002) and subjected to paired *t* test.

Exploratory whole brain voxel-wise analysis. The use of *a priori* ROIs from independent datasets provides the strictest test of reproducibility across studies. However, the *a priori* ROI method does not allow the detection of other potentially important activations. Furthermore, in the present case, the use of different imaging modalities (ASL vs BOLD) and protocols (block vs event-related designs) might be expected to lead to some differences in the measurement of the location of peak activations. We therefore also conducted a whole brain

voxel-wise analysis using the contrast: all dSAT (hits + CRs) > all SAT (hits + CRs). Whole brain analyses used a combined height threshold of $p < .001$, uncorrected and extent threshold of greater than 20 voxels. Clusters surviving an AlphaSim cluster-level threshold $p < .05$ are denoted with asterisks in Tables 2.2 and 2.3. AlphaSim analysis, implemented using the REST toolbox v1.8 (Song et al., 2011), was used to determine the minimum cluster size that would limit false detection rates to below alpha = .05. 1,000 Monte Carlo simulations were performed excluding voxels in the ventricles, cerebellum, pons and medulla.

Neural-behavioral correlations. To evaluate the relationship between neural activity and performance, we tested whether activation increases in right BA 9 during distractor challenge correlated with distractor-related performance decrements. This analysis further tested the convergence of findings between the present event-related BOLD study and the previous block design ASL study, which found greater right BA 9 perfusion was associated with poor performance. Pearson correlations probed the relationship between increased activation (dSAT – SAT) and the impact of distraction on performance (SAT score – dSAT score). Percent signal-change was extracted for 8 mm ROIs defined by Demeter et al. (2011) coordinates as described above. To improve sensitivity of correlational analyses, an additional analysis defined ROIs for each participant individually. Separate 8 mm spheres were drawn for each participant centered on their peak voxel (dSAT – SAT) within the *a priori* ROI.

Finally, to test the selectivity of the neural-behavioral correlation, we assessed whether percent signal change in a visual region correlated with performance. For this control analysis, we used a previously defined ROI in right cuneus (BA 7 centered on MNI coordinates 9, -67, 31; Demeter et al., 2011). Similar to the analysis described above, correlations were tested for the single *a priori* ROI as well as individually defined ROIs.

Task-based functional connectivity analysis.

Psychophysiological interaction analysis during distractor performance. Previous studies have found mid-dorsal/dorsolateral PFC regions couple with other cognitive control regions such as posterior parietal cortex and anterior cingulate cortex (ACC) during attention tasks (Brazdil, Mikl, Maracek, Krupa, & Rektor, 2007; Wang et al., 2010). To determine which regions showed significant increases in functional connectivity with right BA 9 during dSAT performance, we generated whole-brain psychophysiological interaction (PPI) (Friston et al., 1997) maps implemented in SPM 8. A ROI based on the peak right BA 9 activation in the present study was used as the seed region (dSAT > SAT contrast). The ROI was an 8 mm sphere drawn around the peak coordinates in right inferior frontal gyrus (IFG), MNI 46, 2, 30. The seed region included only voxels within this ROI that reached significance level of $p < .05$ for the contrast all task > fixation for each participant. The first-level model contained separate regressors for seed

region time series, dSAT > SAT contrast, and interaction (the multiplication of the deconvolved BOLD time series from the seed and the contrast regressor). For each subject, voxel-wise PPI effects were estimated, and statistical parametric maps were generated for the interaction term. The resulting contrast images were used in second-level PPI group analysis.

Secondary analyses of functional connectivity results: correlation with performance. We conducted follow-up tests of the results from the PPI analyses described above. To preview our PPI results, we found significant increases in connectivity between the right BA 9 seed region and ACC during distractor challenge. ACC is a cognitive control region with known structural connections with BA 9 (reviewed in Bush, Luu, & Posner, 2000), and functional interactions between these regions are thought to reflect the engagement of cognitive control (reviewed in Ridderinkhof, Ullsperger, Crone, & Nieuwenhuis, 2004).

To determine whether functional connectivity was related to successful distractor resistance, we determined whether BA 9 – ACC connectivity strength correlated with the distractor's effect on performance and BA 9 activation. We used Pearson's correlations to determine which account, successful resistance or attentional effort, best applied to our data. Connectivity values within the significant ACC cluster were extracted using the REX toolbox (http://web.mit.edu/swg/software.htm), and were correlated with the distractor effect (SAT – dSAT score), and percent signal change values (dSAT – SAT)

within the right IFG ROI (8 mm sphere, MNI 46, 2, 30) used as a seed region for the PPI analysis.

Secondary analyses of functional connectivity results: multivariate regression analysis. Results of the above correlation analysis revealed a trend-level relationship between right BA 9 – ACC connectivity and performance favoring an attentional effort account of connectivity increases during dSAT.

Our next analysis probed the PPI maps specifically for BA 9 connections associated with successful distractor resistance. In other words, we aimed to identify regions where network activity may serve to mitigate the impact of distraction on performance to produce smaller distraction effects (SAT - dSAT score). We performed a whole-brain voxel-wise multivariate regression analysis to determine where BA 9 functional connectivity predicted successful preservation of performance during distraction. Individual PPI interaction contrasts were submitted to second-level multivariate regression analyses in SPM with the distractor effect (SAT - dSAT score) entered as a regressor.

Resting state functional connectivity analysis.

Pre task functional connectivity. Frontoparietal attention networks can be detected during rest by measuring their synchronized, spontaneous activity. We aimed to determine whether intrinsic frontoparietal network activity could be used to predict subsequent attentional performance. We first created resting state

functional connectivity maps for each participant using the right BA 9 ROI identified in the present study's univariate analysis as a seed region (8 mm sphere centered at MNI 46, 2, 30). Next, we performed regression analyses to determine whether patterns of functional connectivity between the right BA 9 seed region and the whole brain could predict the impact of distraction on performance (SAT – dSAT score) across individuals. We performed an exploratory whole brain analysis as well as targeted analyses of BA 9 – ACC connectivity and BA 9 – right precuneus/superior parietal lobule (SPL) connectivity based on PPI regression results. Masks for ACC and right precuneus/SPL were defined using WFU PickAtlas v3.0 (www.fmri.wfubmc.edu/software/PickAtlas; Lancaster et al., 1997; Lancaster et al., 2000; Maldjian, Laurienti, Kraft, & Burdette, 2003). Regression analyses were conducted using the Pattern Recognition for Neuroimaging Toolbox (PRoNTo) (www.mlnl.cs.ucl.ac.uk/pronto; Schrouff et al., 2013). We conducted this analysis using Relevance Vector Regression (Tipping, 2001) and a leave one subject out cross-validation scheme. Specifically, we trained a regression model to predict individual participant performance (SAT - dSAT score) based on the patterns of right BA 9 – whole brain connectivity, right BA 9 – ACC connectivity, and right BA 9 – right precuneus/SPL connectivity. We report the correlation value between predicted and target (actual) performance for each participant. Significance levels were calculated for 100 permutation tests.

RESULTS

Behavior.

Distraction impaired performance (Figure 2.2). Analysis of SAT score revealed significantly lower performance for dSAT trials relative to SAT trials, $t(17) = 4.62$, $p < .0001$, $dz = 1.11$. These behavioral effects replicated our previous studies (Demeter et al., 2013; Demeter et al., 2011; Demeter et al., 2008).

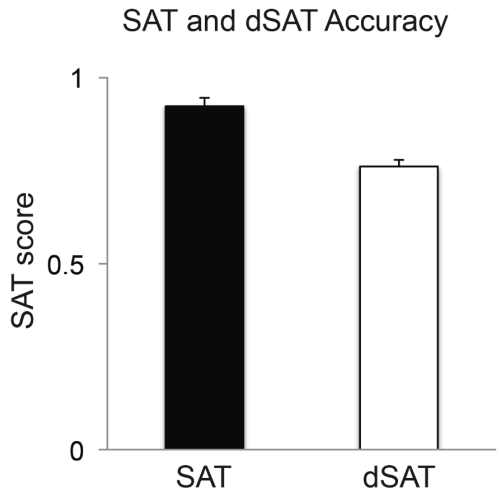

Figure 2.2. Effect of distraction on SAT scores. Data shown are from 6 experimental runs. Black bars display performance data for SAT trials without distraction; white bars display performance data for dSAT trials with distraction. Participants showed significant performance decrements with distraction ($p < .0001$).

d' analyses revealed similar results and are reported in Appendix I. The hit and FA data from which the SAT score and d' are derived are reported in Table 2.1. Omissions were generally low with a trend for higher omission rates during dSAT

trials (t(17) = 1.82, p = .09, dz = 0.35; SAT M = .02, SD = .01; dSAT M = .03, SD = .01).

Table 2.1. Hit and false alarm proportions for SAT and dSAT trials. Data are means (standard error around the mean).

	Hits	false alarms
SAT	.93 (.01)	.02 (.00)
dSAT	.80 (.03)	.06 (.01)

Univariate analysis

A priori region of interest analysis. In the *a priori* ROI drawn from Demeter et al. (2011), distractor challenge was associated with a trend for greater activation, but this fell short of traditional significance levels, t(15) = 1.86, p = .08, dz = 0.48.

Exploratory whole brain voxel-wise analysis. Voxel-wise analyses revealed dSAT performance significantly increased right BA 9 activation, strengthening the trend-level findings shown in the above ROI analysis. Peak activation in the present study was found in right inferior frontal gyrus (IFG) (MNI 46, 2, 30, approximating BA 9), the gyrus just posterior to MFG where the peak from the previous ASL study was located (MNI 35, 9, 33, approximating BA 9; Demeter et al., 2011). As noted above, the differences in imaging modality (ASL vs BOLD) and design (block vs event-related) may have contributed to the variation in the location of the peak activation across studies. Figure 2.3 shows 8mm ROIs from Demeter et al. (2011), the present study, and a previous ASL study by Kim et al. (2006) using a different sustained attention task. Although

there is some variation in the location of the peak activation across studies, overall they converge to suggest that right BA 9 (specifically IFG/MFG) is involved in controlled attention under challenging conditions.

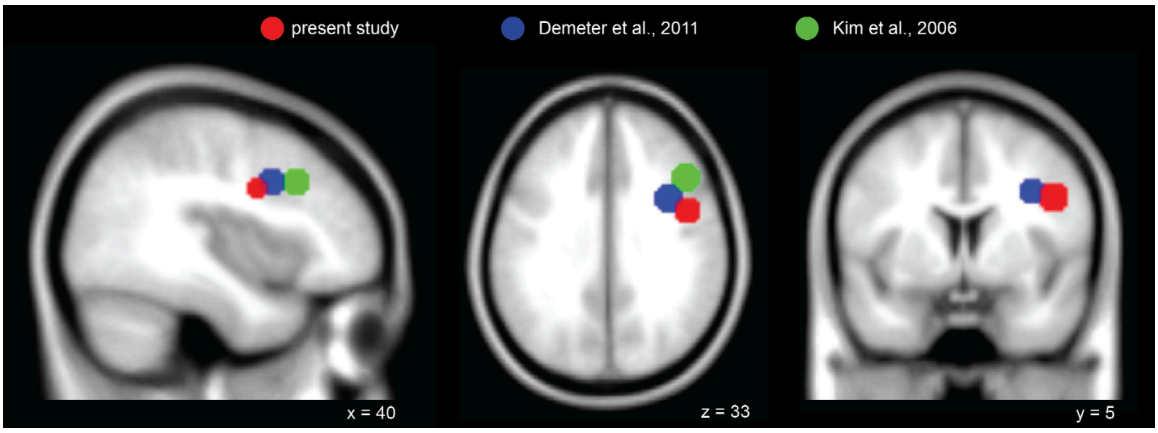

Figure 2.3. Comparison of right BA 9 peak activations across studies. Regions of interest (8 mm spheres) were drawn to surround the peak activation in right BA 9 for the present study, Demeter et al. (2011), and Kim et al. (2006). Though the imaging modality (BOLD vs ASL) and design (block vs event-related) varied across study, the findings generally converge to suggest a role of right BA 9 (specifically IFG/MFG) in controlled attention under challenging conditions. ROIs are displayed on an SPM template average of 152 normalized T1 anatomical scans.

In addition to increasing right IFG activation, dSAT performance was associated with greater activation in other frontoparietal cognitive control regions including right anterior insula/IFG, right superior frontal gyrus/frontal eye fields (FEF), and bilateral superior parietal lobule. (Figure 2.4, Table 2.2). Increased activation was also found in cuneus, most likely related to the visual stimulation from the flashing distractor.

Table 2.2 Univariate results. List of regions showing a significant activation applying a height threshold of $p < .001$ uncorrected, and a cluster volume threshold of greater than 20 voxels. Regions surviving AlphaSim correction $p < .05$ are marked with an asterisk.

Size (voxels)	Anatomical label	BA	MNI coordinates			T- score
dSAT > SAT						
15453*	cuneus	18	-2	-80	6	10.71
337*	left superior parietal lobule	7	-28	-56	60	6.77
176*	right superior parietal lobule	7	26	-56	52	6.36
135*	right superior frontal gyrus/frontal eye fields	6	12	6	58	6.42
111*	left middle frontal gyrus	6	-30	-2	54	5.41
53	right middle frontal gyrus	6	38	-6	50	4.89
64*	right inferior frontal gyrus	9	46	2	30	4.41
31	right insula/inferior frontal gyrus	47	32	16	-12	4.01
SAT > dSAT						
No significant clusters						

Neural-behavioral correlations. Distraction reduced performance and increased activation in right BA 9. Correlation analyses were generally consistent with previous ASL findings. Greater right BA 9 activation increases during dSAT (dSAT – SAT percent signal-change) were associated with greater distractor-related performance declines (SAT – dSAT score), though the strength of this relationship varied based on which ROI was evaluated ($r = .38$ - $.52$).

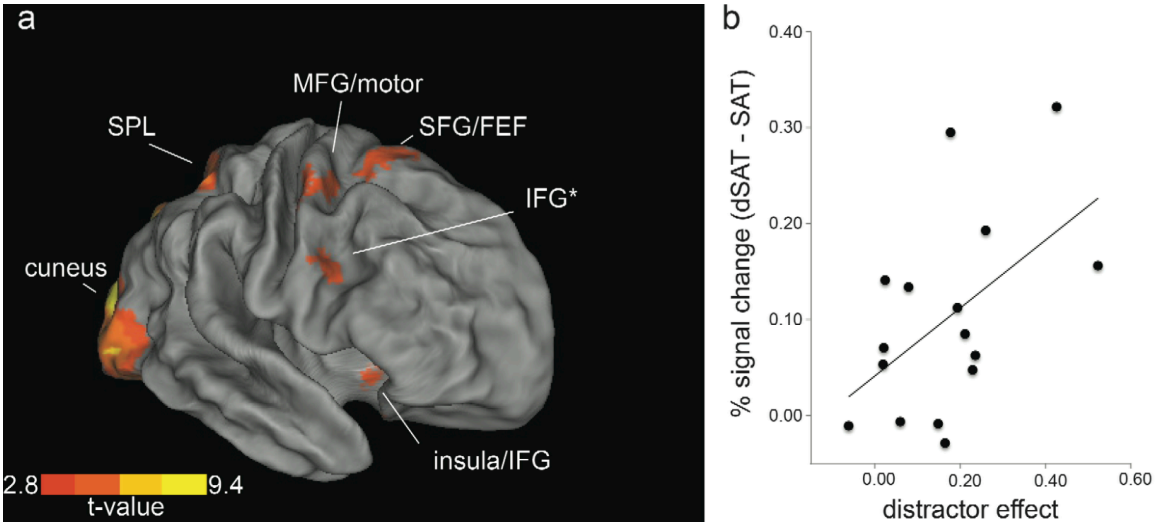

Figure 2.4. Univariate activation for distractor challenge and neural-behavioral correlation. (a) The contrast dSAT > SAT revealed activation in regions associated with cognitive control and top-down modulation of attentional orienting. Activation in right inferior frontal gyrus (IFG) approximating BA 9, highlighted with an asterisk, generally replicated our previous ASL findings (Demeter et al., 2011). The peak coordinates for this IFG region were used to define the seed region for subsequent functional connectivity analyses. Enhanced activation during distractor challenge was also found in superior parietal lobule (SPL), middle frontal gyrus (MFG), superior frontal gyrus (SFG)/frontal eye fields (FEF), anterior insula, and cuneus. The t-map is displayed on a CARET slightly inflated surface representation at a slightly reduced threshold to aid in the visualization of activations at the cortical surface ($p < .05$, FDR corrected). (b) There was a correlation between enhanced right BA 9 activation (dSAT – SAT) and the distractor effect on performance (SAT – dSAT score), $r = .52$, $p = .04$. Increased right BA 9 activation was measured from individualized ROIs based on the *a priori* region of interest identified in Demeter et al., 2011 and replicated previous findings that participants with the greatest performance decrements during dSAT showed the greatest increase in activation.

When the *a priori* ROI from Demeter et al. (2011) was used, the correlation between distractor-related performance and activation changes followed the same pattern seen in that earlier study, but did not meet traditional significance levels, $r = .38$, $p = .15$. To increase sensitivity, we also created individual ROIs for each participant centered on their peak voxel for the dSAT vs SAT contrast within the *a priori* ROI (see Methods for details). Note that although

this method allows greater sensitivity in the measurement of each individual's dSAT vs SAT activation contrast, the ROIs are still defined independently of the correlation (c.f., Vul, Harris, Winkielman, & Pashler, 2009). Using this method, the correlation between distraction-related activation increases and performance decreases was significant, $r = .52$, $p = .04$.

We conducted further control analyses to strengthen our interpretation that the relationship between right BA 9 activation increases and performance reflected attentional effects and was not an artifact of simple visual stimulation during dSAT. The effect of distraction on performance was not correlated with increases in right cuneus activation during distractor challenge (individualized ROIs: $r = -.18$, $p = .50$). The lack of correlation in visual cortex is consistent with the proposal that the relationship between right BA 9 activation and performance reflected increased demands on attention during the distractor and was not an artifact of visual stimulation during dSAT. These data converge to suggest right BA 9 activation increases reflect individual sensitivity to attentional challenge and increases in attentional effort.

We tested the neural-behavioral correlations for other regions with increased activation during distractor challenge to complement the *a priori* correlation analyses described above. Right superior frontal gyrus/FEF, and bilateral SPL did not correlate with performance (all $r < .28$, $p > .29$). Right anterior insula/IFG activation increases showed a marginal relationship with the behavioral distractor effect ($r = .49$, $p = .054$). However, this correlation was

driven by a single data point which, when removed, lowered the r-value to .26. Together, these correlational data suggest the patterns seen in right BA 9 were specific to that region.

Task-based functional connectivity

Psychophysiological interaction analysis during distractor performance. Univariate analyses demonstrated activation increases in right IFG approximating BA 9 in agreement with our previous research (Demeter et al., 2011). To further investigate the role of this region in cognitive control during distractor challenge, we conducted an exploratory whole brain voxel-wise analysis of PPI functional connectivity using IFG as a seed region (see Methods). We found increased functional connectivity for dSAT relative to SAT in ACC, right medial frontal gyrus/supplementary motor area, and right superior temporal gyrus (Figure 2.5, Table 2.3). ACC connectivity findings are in agreement numerous studies demonstrating PFC-ACC coactivation (e.g. Daheane et al., 1998; Duncan & Owen, 2000) as well as their functional connectivity (e.g. Brazdil et al., 2007; Wang et al., 2010). Increased connectivity with supplementary motor and superior temporal auditory regions may reflect enhanced response preparation and auditory cue monitoring to support performance.

Secondary analyses of functional connectivity results: correlation with performance. We probed the relationship between BA 9 – ACC connectivity strength, distractor-related performance decrements, and BA 9 activation. We found that connectivity strength was related to both performance decrements and BA 9 activation, though the correlation between functional connectivity and performance was only marginal (Figure 2.5). Specifically, stronger connectivity during dSAT showed a marginal correlation with greater impact of distraction (SAT – dSAT score; $r = .47$, $p = .07$). The trend was such that participants with the strongest BA 9 – ACC connectivity were those with the greatest performance declines during dSAT. Stronger BA 9 – ACC connectivity during dSAT was correlated with greater enhancement of right BA 9 activation ($r = .53$, $p = .03$). As would be predicted from the direction of the marginal correlation between connectivity and performance, participants with the greatest BA 9 – ACC connectivity showed the greatest activation increases in right BA 9.

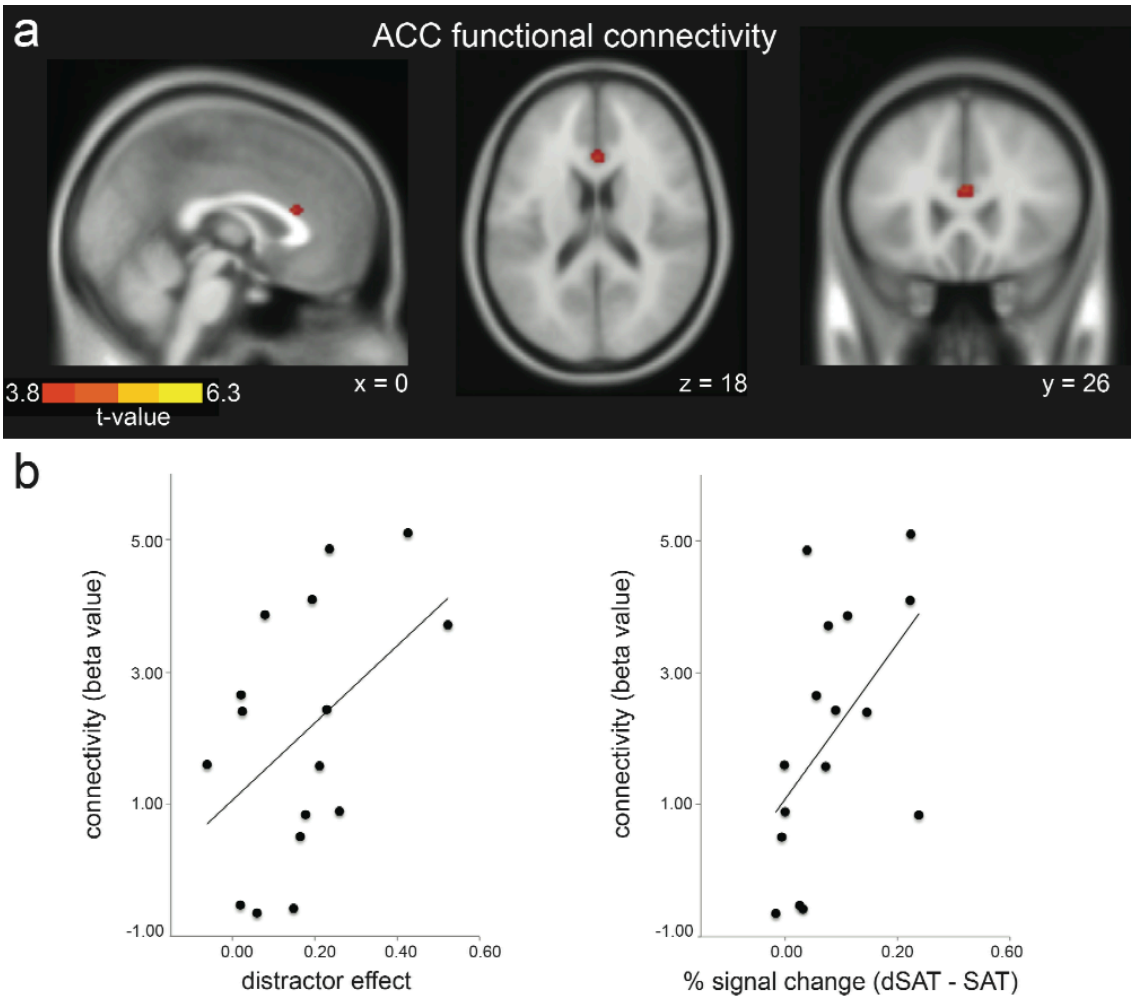

Figure 2.5 PPI functional connectivity during distractor challenge. (a) Psychophysiological interaction (PPI) analyses revealed greater functional connectivity between the right BA 9 seed region (8 mm sphere centered on IFG peak coordinates MNI 46, 2, 30) and anterior cingulate cortex (ACC) during distractor challenge. Right BA 9 also showed increased connectivity with regions listed in Table 2.3, medial frontal gyrus/supplementary motor area and superior temporal gyrus (not displayed). T-maps are displayed on an SPM template average of 152 normalized T1 anatomical scans. (b) Increased right BA 9 – ACC functional connectivity was associated with greater performance declines during distractor challenge and greater increases in right BA 9 activation. Functional connectivity strength showed a modest relationship between the distractor effect on performance (SAT – dSAT score), r = .47, p = .07, and increased BA 9 activation, r = .53, p = .03.

Greater BA 9 – ACC connectivity strength may be associated the processing of more numerous errors by ACC and signal increased demand for

cognitive control in participants with declining performance. The direction of the relationship with performance suggests that increased activation within right BA 9 and connectivity with ACC was not sufficient to rescue performance. Instead, they may serve as neural markers of individual sensitivity to distraction and likely scale with attentional effort. In contrast to ACC connectivity findings, connectivity with medial frontal gyrus/supplementary motor area and superior temporal gyrus did not correlate with performance or right BA 9 activation, all $r < .30$, $p > .26$.

Secondary analyses of functional connectivity results: multivariate regression analysis. We found functional connectivity between right BA 9 and right precuneus/SPL (MNI 18, -68, 48) approximating BA 7 was strongest for individuals least affected by distraction (Figure 2.6, Table 2.3). These findings are in agreement with previous studies implicating superior parietal cortex in cognitive control processes specifically supporting visual detection (Corbetta & Shulman, 2002; Kanwisher & Wojciulik, 2000; Kastner & Ungerleider, 2000).

Table 2.3 Multivariate results. List of regions showing significant functional connectivity applying a height threshold of $p < .001$ uncorrected, cluster volume threshold greater than 20 voxels. Regions surviving AlphaSim correction $p < .05$ are marked with an asterisk.

Size (voxels)	Anatomical label	BA	MNI coordinates			T- score
PPI: dSAT > SAT			x	y	z	
50	right medial frontal gyrus	6	14	-2	56	6.34
25	right superior temporal gyrus	41	46	-22	10	4.88
23	anterior cingulate gyrus	24	0	24	16	4.41
PPI: dSAT > SAT regression						
56	right precuneus/superior parietal lobule	7	18	-68	48	4.74
BA 9 resting state connectivity						
4435*	right inferior frontal/precentral gyrus	6/9	44	2	32	30.35
5911*	right precuneus/superior and inferor parietal lobe	7	28	-54	50	14.14
2647*	left inferior frontal gyrus/precentral gyrus	6/9	-46	0	32	12.68
2817*	left precuneus/superior and inferior parietal lobe	7	-32	-48	48	10.58
364*	cingulate gyrus	24	0	0	32	6.95
341*	superior frontal gyrus	8	4	18	56	6.92
462*	left inferior temporal gyrus	37	-46	-64	-6	6.81
33	right middle frontal gyrus/superior orbital gyrus	11	22	34	-18	4.85

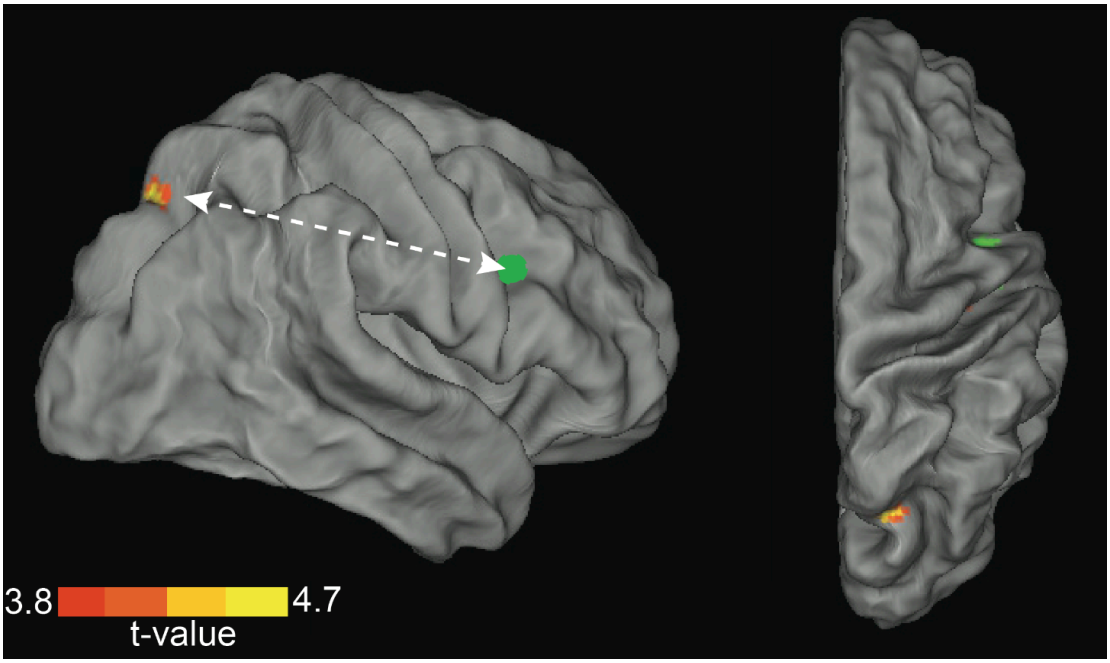

Figure 2.6. Frontoparietal functional connectivity associated with preserved performance during distractor challenge. Multivariate regression analyses identified a region in right precuneus/superior parietal lobule (SPL, warm colors) whose functional connectivity with right BA 9 was greatest for individuals with low behavioral impact of distraction. Green indicates the location of the right BA 9 seed region.

Resting state functional connectivity

Pre task functional connectivity. Before task performance, the right BA 9 seed region (8 mm sphere, MNI 46, 2, 30) showed significant functional connectivity with other task-positive frontoparietal regions including superior and inferior parietal lobe, precuneus, cingulate cortex, and superior frontal gyrus (Figure 2.7, Table 2.3).

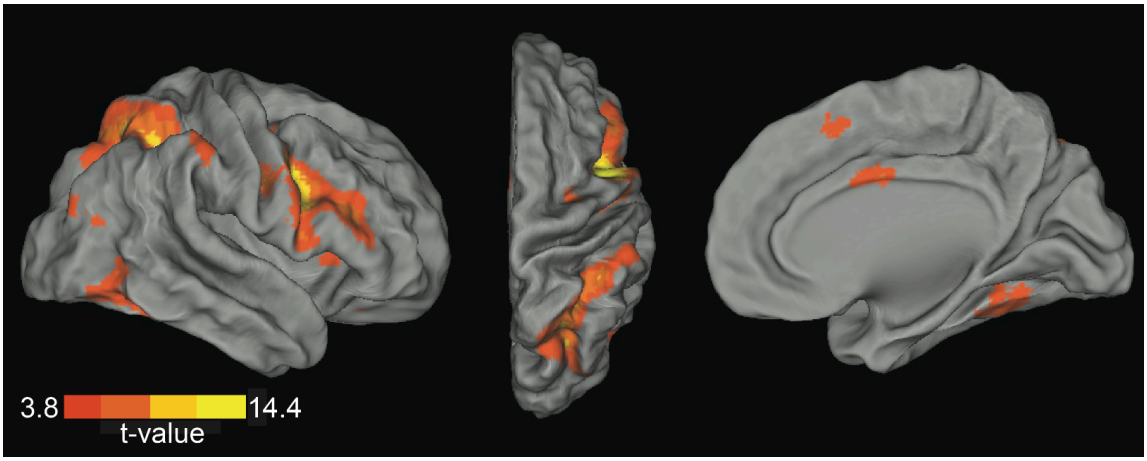

Figure 2.7. Resting state functional connectivity before task performance. Regions showing positive synchronization with the right BA 9 seed region (8 mm sphere centered on IFG peak coordinates MNI 46, 2, 30) during the resting state scan collected prior to task performance are displayed. Activity in IFG was correlated with other task positive regions including superior and inferior parietal cortex, middle frontal gyrus, inferior temporal gyrus (lateral and dorsal views), and cingulate cortex (medial view).

Patterns of whole-brain connectivity with right BA 9 during rest predicted subsequent performance (SAT – dSAT score) with marginal significance (correlation between target and predicted value r = .34, p = .08). Targeted analyses revealed that patterns of resting connectivity between right BA 9 – precuneus/SPL predicted performance at traditional significance levels (correlation r = .59, p = .02), while patterns of right BA9 – ACC connectivity did not (correlation r = -.68, p = .99) (Figure 2.8).

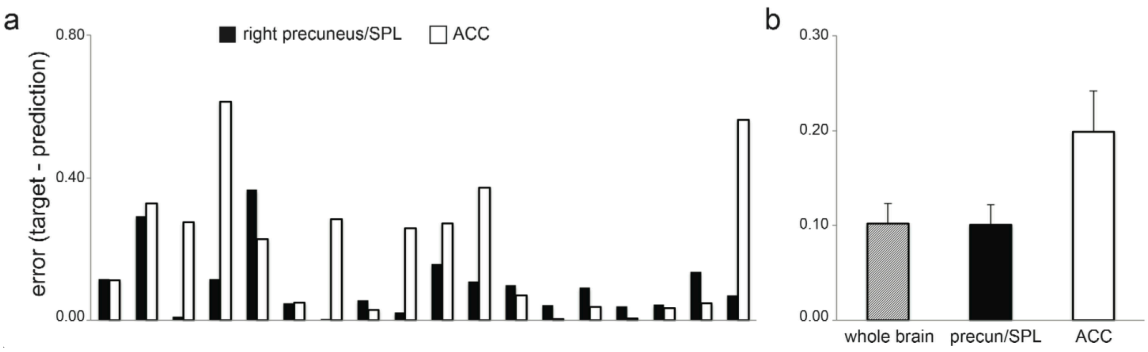

Figure 2.8. Resting frontoparietal connectivity predicts behavioral distractor effect. A relevance vector regression model significantly predicted subsequent task performance (SAT – dSAT score) based on patterns of connectivity between the right BA 9 seed region (8 mm sphere centered on IFG peak coordinates MNI 46, 2, 30) and right precuneus/superior parietal lobule (SPL), but not anterior cingulate cortex (ACC). Parietal and ACC masks were structurally defined. (a) Results for individual participants are displayed for right precuneus/SPL connectivity in black and ACC connectivity in white. Results are plotted as the difference between the actual behavioral performance of the participants, and the performance predicted by the model (target-prediction). (b) Average model error was greatest when only ACC connectivity was used to predict subsequent performance. Though error was similar for models including whole brain and right precuneus/SPL connectivity, whole brain prediction was only marginally significant (correlation r = .34, p = .08).

DISCUSSION

Attentional challenge caused declines in performance and increased the demand for cognitive control. Consistent with our previous research, a region in right PFC approximating BA 9 showed enhanced activation during distractor challenge (Demeter et al., 2011), and increased functional connectivity with other frontoparietal cognitive control regions. Analysis of individual subject differences revealed some distractor-related activity increases were associated with successful resistance against performance decrements, while some showed the opposite pattern and were associated with the greater sensitivity to the distractor. Specifically, functional connectivity between right BA 9 and right superior parietal cortex was associated with greater distractor resistance, while overall BA 9

univariate activation and connectivity with ACC were associated with the greatest impairment during distraction. These patterns suggest there are distinct components of frontoparietal control networks that can scale with successful maintenance of performance, and components that scale with attentional effort. Below we discuss how these distinct components may work together to support signal detection specifically, and discuss the utility of studying these task-active networks using intrinsic connectivity measures.

Distractor challenge reduced performance and increased univariate activation in right BA 9 and dorsal attention network regions including bilateral superior parietal cortex and FEF (Corbetta & Shulman, 2002). Parietal and FEF activation increases were not found in the previous ASL study and may be have been prominent in the present study because of the intermixing of SAT and dSAT trials within task runs (SAT and dSAT trials were not blocked, but alternated pseudorandomly). Shifting from SAT trials to dSAT trials in which the screen flashed may have increased demand for the reengagement of top-down orienting responses if, for example, the onset of the distractor caused participants to lose central fixation. It is possible sustained performance of dSAT trials in the previous study allowed for the establishment of a stable task set with diminished demand for dorsally mediated spatial orienting.

Enhanced engagement of right BA 9 during challenges to attention, measured via univariate activation increases during dSAT, replicated our previous ASL findings. Further, the relationship between activation increases in

this region and performance declines adds support for the view that right BA 9 activation reported attentional effort during the engagement of cognitive control. The agreement across studies is noteworthy considering they employed different fMRI imaging methods and designs, and strongly implicates right BA 9 in the cognitive control mechanisms engaged during attentional challenge.

Paralleling univariate findings, greater functional connectivity between right BA 9 and ACC was associated with greater distractor-related performance decrements (though this relationship met only trend-level significance). We propose these regions were engaged in concert to mitigate the behavioral impact of distraction, and though not an indication of successful recovery of performance, reflected the enhancement of attentional effort. We believe these subjects maintained motivation throughout the session with no significant motivational differences between high and low performers as all participants volunteered, were paid for their time, and were given the same monetary incentives for good performance. Further, there were low omission rates, and no significant time-on-task effects suggesting participants maintained high levels of motivated performance throughout the experimental session.

The tight coupling of conflict detection and the allocation of cognitive control may explain the functional connectivity findings in the present study and the abundance of reports of univariate coactivation of ACC and dorsolateral and mid-dorsal PFC during cognitively demanding tasks (Botvinick, Nystrom, Fissell, Carter, & Cohen, 1999; Carter et al., 1998; Carter et al., 2000; reviewed in

Dehaene et al., 1998; Duncan & Owen, 2000). The ACC, associated with the monitoring of conflict and detection of errors, may recruit correction mechanisms by signaling other prefrontal control regions with which it shares rich reciprocal anatomical connections such as BA 9 and BA 46 as well as BA 7 parietal cortex (Devinsky, Morrell, & Vogt, 1995). Modeling work (Botvinick, Braver, Barch, Carter, & Cohen, 2001) has demonstrated that pairing a conflict signal (ACC signal) with adjustments in the allocation of control (PFC signal) can accurately simulate the trial-based adjustments in behavior made by subjects during attentional challenge (Botvinick et al., 1999; Gratton, Coles, & Donchin, 1992; Logan, Zbrodoff, & Fostey, 1983; Tzelgov, Henik, & Berger, 1992). ACC and PFC activity may therefore coordinate dynamically based on current task demand or in response to error feedback to modify behavior. In the present study, low performers who most needed to engage such corrective mechanisms showed the greatest connectivity and increased right BA 9 activation. Consistent with the view that coordinated BA 9 – ACC activity is engaged transiently, based on current demand, we found that resting connectivity between these regions in the absence of task demands could not predict subsequent performance.

In contrast to effects in ACC, we found connectivity between right BA 9 and precuneus/superior parietal lobule approximating BA 7 was associated with successful maintenance of performance levels during attentional challenge. Right precuneus/superior parietal cortex was recently identified as a core cognitive control region in a large (n = 93) fMRI study of working memory and executive

control that met criterion of increased activation during interference, increased activation for correct versus error trials and positive correlation with task accuracy (Cole et al., 2012). Together, these regions may have successfully improved performance through the coupling of top-down control processes specifically supporting attentional orienting and working memory in parietal cortex and those tracking fluctuations in attentional challenge and error feedback in right BA 9.

Right frontoparietal connectivity was a relatively stable predictor of performance such that resting connectivity between these regions predicted subsequent behavioral impact of distraction across individuals. Resting functional connectivity can be used to identify large-scale brain networks, and is thought to be an important marker of the integrity of connections between regions (Ghosh, Rho, McIntosh, Kotter, & Jirsa, 2008; Greicius, Supekar, Menon, & Dougherty, 2009). In a similar vein to what we report presently, others have demonstrated greater distractibility associated with weaker resting frontoparietal functional connectivity in older adults following task performance (Campbell, Grady, Ng, & Hasher, 2012).

The unique value of the present approach, however, is the potential significance of identifying predictive markers of attentional performance. These markers shed light onto the neural mechanisms most critical for task-evoked controlled attention and represent potential therapeutic targets. The frontoparietal connectivity marker identified in the present study may reflect state-dependent fluctuations in network activity, or may be a relatively stable trait measure.

Though further research is needed to resolve the state vs trait stability of right BA 9 – parietal connectivity, the crux of this question lies in resolving what is most strongly reflected in the intrinsic connectivity and to what extent it is modulated by factors such as recent cognitive processing, or expectation of future use (Foster & Wilson, 2006; Harmelech & Malach, 2013; Kenet, Bibitchkov, Tsodyks, Grinvald, & Arieli, 2003; Pouget, Dayan, & Zemel, 2003; discussed in Fox et al., 2006). Elements of distractibility are, however, considered trait measures that are partly hereditable (Boomsma, 1998), are associated with specific genetic polymorphisms (Berry et al., in press), have been linked to differences in superior parietal anatomy (Kanai, Dong, Bahrami, & Rees, 2011), and therefore may be related to large-scale network activity. Furthermore, frontoparietal functional connectivity measured at rest has previously been linked to trait measures (Jung & Haier, 2007; Song et al., 2008; van den Heuvel et al., 2009), and resting state connectivity has been shown to be relatively stable in task-negative default mode, and task positive regions in healthy adults (Shehzad et al., 2009) and children (Thomason et al., 2011).

It is unclear why increases in univariate right BA 9 activation and ACC connectivity were not associated with successful distractor resistance, though it is possible that the unique perceptual demands of the task contributed to these patterns. The presence of the distractor may have made signal detection *perceptually* more challenging on top of added attentional challenges. Controlled attention may have benefited performance to a point by, for example, enhancing

perceptual gain in the central signal region or by selecting for the square shape of the signal, but this benefit may be subject to individual limits and neural inefficiencies. Therefore, increasing engagement of attentional control may not correlate with better performance but may, instead, reflect the continued attentional effort associated with motivated performance. Future studies implementing auditory distraction or visual distraction outside of the signal location will help resolve this question.

SAT and dSAT have been used extensively to investigate the frontoparietal correlates of controlled attention in rodents (Broussard, Karelina, Sarter, & Givens, 2009; Gill et al., 2000; St Peters et al., 2011), and particularly the contribution of cortical inputs from the basal forebrain cholinergic system (St Peters et al., 2011). Research in rodents strongly implicates elevated acetylcholine release in right PFC in controlled attention during distractor challenge. Similar to patterns in humans, SAT performance is associated with increased PFC acetylcholine relative to baseline, with greatest augmentation during distractor challenge. Paralleling findings in humans, this effect is right-lateralized (Apparsundaram, Martinez, Parikh, Kozak, & Sarter, 2005; Martinez & Sarter, 2004), suggesting a role of the cholinergic system in human controlled attention processes. However, further studies are needed to examine the relationship between human cholinergic function and right BA 9 activation to help determine whether cholinergic signaling in PFC may contribute to the observed increase in BOLD signal and ASL perfusion.

By tightly integrating our cognitive neuroscience research with that conducted in rodent models, we are able to assess the correspondence of findings across species and neural measures. By continuing this line of research, our hope is to better understand how acetylcholine acts to maintain performance during attentional challenge in humans and assess how this neuromodulator may influence local prefrontal activation measures as well as long-range network activity. The emerging links across neuroscience sub-fields make SAT and dSAT a particularly useful task for clinical use and drug development to advance therapeutic interventions treating the dysregulation of attentional control characteristic of disorders such as schizophrenia (Luck et al., 2012; Lustig, Kozak, Sarter, Young, & Robbins, 2013).

APPENDIX I

METHODS

Behavioral analysis d'

d' was calculated from the proportions of hits and FAs using the standard formula: d' = z(hits) – z(FAs) (Green & Swets, 1966). The following substitution was made for hit rates of 100%: 1-1/(2N) where N is the total number of signals. For FA rates of 0, we used the percentage equivalent to half a FA (1/2N) where N is the total number of nonsignal stimuli. Bias measures were calculated using the formula: $B"_D$ = [(1 -hits)(1 - FAs) – (hits x FAs)]/[(1 - hits)(1 - FAs) + (hits x FAs)] (Donaldson, 1992). Bias scores range from -1 to +1, with -1 indicating a liberal response bias, and + 1 indicating a conservative response bias.

RESULTS

Behavior

d' signal detection measures. In line with SAT score findings, distraction significantly impaired performance, $t(17) = 4.93$, $p < .0001$, $dz = 1.17$, (SAT M = 3.77, SE = 0.14; dSAT M = 2.70, SE = 0.22).

Response bias was conservative with overall average bias > 0.52. In the present study, bias was not affected by distraction ($t < 1$), (SAT M = 0.54, SE = 0.03; dSAT M = 0.51, SD = 0.07).

Univariate analysis

Signal detection: exploratory whole brain voxel-wise analysis. We conducted exploratory analyses contrasting hit and CR trials to identify regions associated with signal detection. The contrast hits > CR (SAT hit + dSAT hit > SAT CR + dSAT CR) revealed significant clusters in superior frontal gyrus and inferior parietal cortex. (Fig 2.A.1, Table 2.A.1). Similar to detection results for hit > CR contrasts in memory studies, largest clusters were left-lateralized (Cabeza, Ciaramelli, Olson, & Moscovitch, 2008; Hutchinson, Uncapher, & Wagner, 2009; Hutchinson et al., 2014).

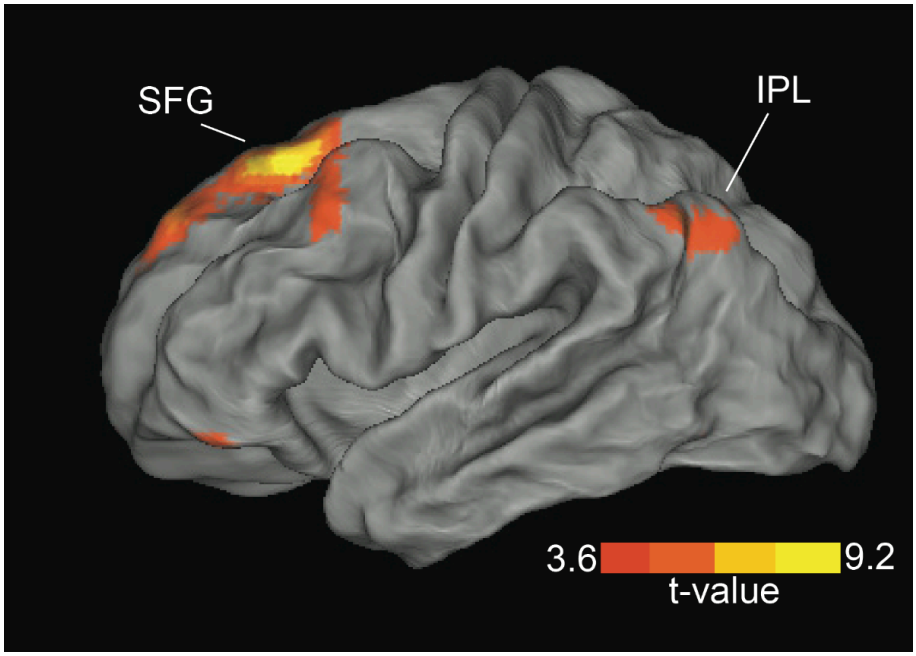

Figure 2.A.1. Univariate activation for signal detection. The contrast hits > CRs revealed bilateral activation in superior frontal gyrus (SFG) approximating BA 8 and inferior parietal lobule (IPL) approximating BA 40. Left-lateralized clusters were largest. The t-map is displayed on CARET slightly inflated surface representation at a peak voxel threshold of $p < .05$, FDR corrected and 20 voxel extent threshold to aid in the visualization of activations at the cortical surface.

Results for the contrast CR > hit revealed activations in visual and auditory cortex (Table 2.A.1), which may be associated with longer periods of monitoring for the signal during nonsignal trials. For hit trials, monitoring terminated after detection, but, for CR trials, active monitoring was sustained until the onset of the response cue. Activation increases were also found in right anterior insula, which may reflect greater cognitive control demands associated monitoring and response rule retrieval for CR trials.

Table 2.A.1 Univariate results: detection. List of regions showing a significant activation applying a height threshold of $p < .001$ uncorrected, and a cluster volume threshold of greater than 20 voxels. Regions surviving AlphaSim correction $p < .05$ are marked with an asterisk.

Size (voxels)	Anatomical label	BA	MNI coordinates			T-score
Hit > CR			x	y	z	
1403*	left superior frontal gyrus	8	-22	26	50	9.16
339*	right angular gyrus	40	58	-60	34	7.97
220*	right superior frontal gyrus	8	18	36	52	6.92
671*	left inferior parietal lobule	40	-48	-62	40	6.67
239*	left posterior cingulate	30	-6	-54	16	5.42
286*	right medial frontal gyrus	25	6	38	-16	5.41
180*	left middle frontal gyrus	11	-42	44	-10	5.34
210*	medial frontal gyrus	10	0	64	8	5.11
189*	right inferior temporal gyrus	37	58	-70	-2	4.86
CR > hit						
1878*	right middle occipital gyrus	18	36	-90	0	9.59
784*	left middle occipital gyrus	18	-26	-92	16	7.42
299*	right middle temporal gyrus	21	54	-12	-10	6.52

101*	left middle frontal gyrus	6	-34	-6	54	6.04
346*	right insula	47	34	26	2	5.92
206*	right medial frontal gyrus	8	4	20	52	5.51
211*	left superior temporal gyrus	22	-62	-14	0	5.44
154*	right precentral gyrus	6	40	-2	42	5.31
57*	left insula	13	-36	-36	18	5.20
66*	right precuneus	7	20	-66	38	5.19

DISCUSSION

Univariate analyses revealed activations for signal detection in inferior parietal cortex consistent with the ventral attention network supporting orienting, though patterns of activation were not right hemisphere dominant as has been the prevailing view (Corbetta & Shulman, 2002). Detection activations were bilateral and, if anything, larger in the left hemisphere, particularly in the superior frontal gyrus, consistent with previous findings for successful memory retrieval using a similar hits > CRs contrast (Cabeza et al., 2008; Hutchinson et al., 2009; Hutchinson et al., 2014). Right lateralization in parietal cortex activations has been found largely in spatial cuing studies for the contrast invalid cue > valid cue in which the stimulus location is unexpected. Bilateral activation in the present study is in line with previous “oddball” target detection tasks in which, similar to the present study, the location of the stimulus is constant and not invalidly cued (Linden et al., 1999; Marois, Leung, & Gore, 2000; Menon, Ford, Lim, Glover, & Pfefferbaum, 1997). Doricchi et al., 2010 examined the nature of left inferior

parietal activation in a spatial cuing paradigm and discovered that left inferior parietal cortex responded to both validly and invalidly cued targets whereas right inferior parietal cortex only responded to invalidly cued targets. These findings may explain the common right-lateralized effect reported for invalid > valid contrasts and have contributed to the theory that left inferior parietal cortex responds to stimuli that “match” internally maintained attentional templates (Doricchi, Macci, Silvetti, & Macaluso, 2010).

Acknowledgements

This chapter presented research conducted in collaboration with Cindy Lustig and Martin Sarter. This research was supported by PHS grants R01MH086530 (MS, CL), and by a grant from the National Science Foundation (0726285, CL). Anne Berry was supported by NIDA T32DA728115 (PI: Terry E. Robinson), and by a NSF Graduate Research Fellowship. Additional thanks go to Elise Demeter and Mary Askren for helpful discussions and to Josh Carp for early PPI analysis efforts.

References

Apparsundaram, S., Martinez, V., Parikh, V., Kozak, R., & Sarter, M. (2005). Increased capacity and density of choline transporters situated in synaptic membranes of the right medial prefrontal cortex of attentional task-performing rats. *J Neurosci, 25*(15), 3851-3856.

Berry, A. S., Demeter, E., Sabhapathy, S., English, B. A., Blakely, R. D., Sarter, M., et al. (in press). Disposed to distraction: Genetic variation in the cholinergic system influences distractibility but not time-on-task effects. *J Cogn Neurosci*.

Boomsma, D. I. (1998). Genetic analysis of cognitive failures (CFQ): A study of Dutch adolescent twins and their parents. *European Journal of Personality, 12*(5), 321-330.

Botvinick, Braver, T. S., Barch, D. M., Carter, C. S., & Cohen, J. D. (2001). Conflict monitoring and cognitive control. *Psychol Rev, 108*(3), 624-652.

Botvinick, Nystrom, L. E., Fissell, K., Carter, C. S., & Cohen, J. D. (1999). Conflict monitoring versus selection-for-action in anterior cingulate cortex. *Nature, 402*(6758), 179-181.

Brazdil, M., Mikl, M., Marecek, R., Krupa, P., & Rektor, I. (2007). Effective connectivity in target stimulus processing: a dynamic causal modeling study of visual oddball task. *Neuroimage, 35*(2), 827-835.

Brett, M., Anton, J., Valabregue, R., & Poline, J. (2002). *Region of interest analysis using an SPM toolbox [abstract]*. Paper presented at the 8th International Conference on Functional Mapping of the Human Brain.

Broussard, J. I., Karelina, K., Sarter, M., & Givens, B. (2009). Cholinergic optimization of cue-evoked parietal activity during challenged attentional performance. *Eur J Neurosci, 29*(8), 1711-1722.

Buschkuehl, M., Hernandez-Garcia, L., Jaeggi, S. M., Bernard, J. A., & Jonides, J. (2014). Neural effects of short-term training on working memory. *Cognitive, affective & behavioral neuroscience*.

Bush, G., Luu, P., & Posner, M. I. (2000). Cognitive and emotional influences in anterior cingulate cortex. *Trends in cognitive sciences, 4*(6), 215-222.

Cabeza, R., & Nyberg, L. (2000). Imaging cognition II: An empirical review of 275 PET and fMRI studies. *J Cogn Neurosci, 12*(1), 1-47.

Cabeza, R., Ciaramelli, E., Olson, I. R., & Moscovitch, M. (2008). The parietal cortex and episodic memory: an attentional account. *Nat Rev Neurosci, 9*(8), 613-625.

Campbell, K. L., Grady, C. L., Ng, C., & Hasher, L. (2012). Age differences in the frontoparietal cognitive control network: implications for distractibility. *Neuropsychologia, 50*(9), 2212-2223.

Cappell, K. A., Gmeindl, L., & Reuter-Lorenz, P. A. (2010). Age differences in prefontal recruitment during verbal working memory maintenance depend on memory load. *Cortex, 46*(4), 462-473.

Carter, C. S., Braver, T. S., Barch, D. M., Botvinick, M. M., Noll, D., & Cohen, J. D. (1998). Anterior cingulate cortex, error detection, and the online monitoring of performance. *Science, 280*(5364), 747-749.

Carter, C. S., Macdonald, A. M., Botvinick, M., Ross, L. L., Stenger, V. A., Noll, D., et al. (2000). Parsing executive processes: strategic vs. evaluative functions of the anterior cingulate cortex. *Proc Natl Acad Sci U S A, 97*(4), 1944-1948.

Chapman, S. B., Aslan, S., Spence, J. S., Hart, J. J., Jr., Bartz, E. K., Didehbani, N., et al. (2013). Neural Mechanisms of Brain Plasticity with Complex Cognitive Training in Healthy Seniors. *Cereb Cortex*.

Cole, M. W., Reynolds, J. R., Power, J. D., Repovs, G., Anticevic, A., & Braver, T. S. (2013). Multi-task connectivity reveals flexible hubs for adaptive task control. *Nat Neurosci, 16*(9), 1348-1355.

Cole, M. W., Yarkoni, T., Repovs, G., Anticevic, A., & Braver, T. S. (2012). Global connectivity of prefrontal cortex predicts cognitive control and intelligence. *J Neurosci, 32*(26), 8988-8999.

Corbetta, M., & Shulman, G. L. (2002). Control of goal-directed and stimulus-driven attention in the brain. *Nat Rev Neurosci, 3*(3), 201-215.

Coull, J. T., Frackowiak, R. S., & Frith, C. D. (1998). Monitoring for target objects: activation of right frontal and parietal cortices with increasing time on task. *Neuropsychologia, 36*(12), 1325-1334.

Dehaene, S., Kerszberg, M., & Changeux, J. P. (1998). A neuronal model of a global workspace in effortful cognitive tasks. *Proc Natl Acad Sci U S A, 95*(24), 14529-14534.

Demeter, E., Guthrie, S. K., Taylor, S. F., Sarter, M., & Lustig, C. (2013). Increased distractor vulnerability but preserved vigilance in patients with schizophrenia: evidence from a translational Sustained Attention Task. *Schizophr Res, 144*(1-3), 136-141.

Demeter, E., Hernandez-Garcia, L., Sarter, M., & Lustig, C. (2011). Challenges to attention: a continuous arterial spin labeling (ASL) study of the effects of distraction on sustained attention. *Neuroimage, 54*(2), 1518-1529.

Demeter, E., Sarter, M., & Lustig, C. (2008). Rats and humans paying attention: cross-species task development for translational research. *Neuropsychology, 22*(6), 787-799.

Devinsky, O., Morrell, M. J., & Vogt, B. A. (1995). Contributions of anterior cingulate cortex to behaviour. *Brain : a journal of neurology, 118 (Pt 1)*, 279-306.

Duncan, J., & Owen, A. M. (2000). Common regions of the human frontal lobe recruited by diverse cognitive demands. *Trends Neurosci, 23*(10), 475-483.

Donaldson, W. (1992). Measuring recognition memory. *J Exp Psychol Gen, 121*(3), 275-277.

Doricchi, F., Macci, E., Silvetti, M., & Macaluso, E. (2010). Neural correlates of the spatial and expectancy components of endogenous and stimulus-driven orienting of attention in the Posner task. *Cereb Cortex, 20*(7), 1574-1585.

Dosenbach, N. U., Visscher, K. M., Palmer, E. D., Miezin, F. M., Wenger, K. K., Kang, H. C., et al. (2006). A core system for the implementation of task sets. *Neuron, 50*(5), 799-812.

Duncan, J., & Owen, A. M. (2000). Common regions of the human frontal lobe recruited by diverse cognitive demands. *Trends Neurosci, 23*(10), 475-483.

Foster, D. J., & Wilson, M. A. (2006). Reverse replay of behavioural sequences in hippocampal place cells during the awake state. *Nature, 440*(7084), 680-683.

Fox, M. D., Corbetta, M., Snyder, A. Z., Vincent, J. L., & Raichle, M. E. (2006). Spontaneous neuronal activity distinguishes human dorsal and ventral attention systems. *Proc Natl Acad Sci U S A, 103*(26), 10046-10051.

Frey, P. W., & Colliver, J. A. (1973). Sensitivity and responsivity measures for discrimination learning. *Learning and Motivation, 4*, 327-342.

Friston, K. J., Buechel, C., Fink, G. R., Morris, J., Rolls, E., & Dolan, R. J. (1997). Psychophysiological and modulatory interactions in neuroimaging. *Neuroimage, 6*(3), 218-229.

Ghosh, A., Rho, Y., McIntosh, A. R., Kotter, R., & Jirsa, V. K. (2008). Cortical network dynamics with time delays reveals functional connectivity in the resting brain. *Cognitive neurodynamics, 2*(2), 115-120.

Gill, T. M., Sarter, M., & Givens, B. (2000). Sustained visual attention performance-associated prefrontal neuronal activity: evidence for cholinergic modulation. *J Neurosci, 20*(12), 4745-4757.

Grady, C. L., Maisog, J. M., Horwitz, B., Ungerleider, L. G., Mentis, M. J., Salerno, J. A., et al. (1994). Age-related changes in cortical blood flow activation during visual processing of faces and location. *J Neurosci, 14*(3 Pt 2), 1450-1462.

Gratton, G., Coles, M. G., & Donchin, E. (1992). Optimizing the use of information: strategic control of activation of responses. *J Exp Psychol Gen, 121*(4), 480-506.

Green, D. M., & Swets, J. A. (1966). *Signal detection theory and psychophysics*. New York: Wiley.

Greicius, M. D., Supekar, K., Menon, V., & Dougherty, R. F. (2009). Resting-state functional connectivity reflects structural connectivity in the default mode network. *Cereb Cortex, 19*(1), 72-78.

Guerra-Carrillo, B., Mackey, A. P., & Bunge, S. A. (2014). Resting-State fMRI: A Window into Human Brain Plasticity. *The Neuroscientist : a review journal bringing neurobiology, neurology and psychiatry*.

Harmelech, T., & Malach, R. (2013). Neurocognitive biases and the patterns of spontaneous correlations in the human cortex. *Trends in cognitive sciences, 17*(12), 606-615.

Hutchinson, J. B., Uncapher, M. R., & Wagner, A. D. (2009). Posterior parietal cortex and episodic retrieval: convergent and divergent effects of attention and memory. *Learn Mem, 16*(6), 343-356.

Hutchinson, J. B., Uncapher, M. R., Weiner, K. S., Bressler, D. W., Silver, M. A., Preston, A. R., et al. (2014). Functional heterogeneity in posterior parietal cortex across attention and episodic memory retrieval. *Cereb Cortex, 24*(1), 49-66.

Jenkinson, M., Bannister, P., Brady, M., & Smith, S. (2002). Improved optimization for the robust and accurate linear registration and motion correction of brain images. *Neuroimage, 17*(2), 825-841.

Jung, R. E., & Haier, R. J. (2007). The Parieto-Frontal Integration Theory (P-FIT) of intelligence: converging neuroimaging evidence. *The Behavioral and brain sciences, 30*(2), 135-154; discussion 154-187.

Kanai, R., Dong, M. Y., Bahrami, B., & Rees, G. (2011). Distractibility in daily life is reflected in the structure and function of human parietal cortex. *J Neurosci, 31*(18), 6620-6626.

Kanwisher, N., & Wojciulik, E. (2000). Visual attention: insights from brain imaging. *Nat Rev Neurosci, 1*(2), 91-100.

Kastner, S., & Ungerleider, L. G. (2000). Mechanisms of visual attention in the human cortex. *Annu Rev Neurosci, 23*, 315-341.

Kenet, T., Bibitchkov, D., Tsodyks, M., Grinvald, A., & Arieli, A. (2003). Spontaneously emerging cortical representations of visual attributes. *Nature, 425*(6961), 954-956.

Kim, J., Whyte, J., Wang, J., Rao, H., Tang, K. Z., & Detre, J. A. (2006). Continuous ASL perfusion fMRI investigation of higher cognition: quantification of tonic CBF changes during sustained attention and working memory tasks. *Neuroimage, 31*(1), 376-385.

Kozak, R., Bruno, J. P., & Sarter, M. (2006). Augmented prefrontal acetylcholine release during challenged attentional performance. *Cereb Cortex, 16*(1), 9-17.

Lancaster, J. L., Rainey, L. H., Summerlin, J. L., Freitas, C. S., Fox, P. T., Evans, A. C., et al. (1997). Automated labeling of the human brain: a preliminary report on the development and evaluation of a forward-transform method. *Hum Brain Mapp, 5*(4), 238-242.

Lancaster, J. L., Woldorff, M. G., Parsons, L. M., Liotti, M., Freitas, C. S., Rainey, L., et al. (2000). Automated Talairach atlas labels for functional brain mapping. *Hum Brain Mapp, 10*(3), 120-131.

Langenecker, S. A., & Nielson, K. A. (2003). Frontal recruitment during response inhibition in older adults replicated with fMRI. *Neuroimage, 20*(2), 1384-1392.

Langenecker, S. A., Nielson, K. A., & Rao, S. M. (2004). fMRI of healthy older adults during Stroop interference. *Neuroimage, 21*(1), 192-200.

Li, N., Ma, N., Liu, Y., He, X. S., Sun, D. L., Fu, X. M., et al. (2013). Resting-state functional connectivity predicts impulsivity in economic decision-making. *J Neurosci, 33*(11), 4886-4895.

Lim, J., Wu, W. C., Wang, J., Detre, J. A., Dinges, D. F., & Rao, H. (2010). Imaging brain fatigue from sustained mental workload: an ASL perfusion study of the time-on-task effect. *Neuroimage, 49*(4), 3426-3435.

Linden, D. E., Prvulovic, D., Formisano, E., Vollinger, M., Zanella, F. E., Goebel, R., et al. (1999). The functional neuroanatomy of target detection: an fMRI study of visual and auditory oddball tasks. *Cereb Cortex, 9*(8), 815-823.

Logan, G. D., Zbrodoff, N. J., & Fostey, A. R. (1983). Costs and benefits of strategy construction in a speeded discrimination task. *Memory & cognition, 11*(5), 485-493.

Luck, S. J., Ford, J. M., Sarter, M., & Lustig, C. (2012). CNTRICS final biomarker selection: Control of attention. *Schizophrenia bulletin, 38*(1), 53-61.

Lustig, C., Kozak, R., Sarter, M., Young, J. W., & Robbins, T. W. (2013). CNTRICS final animal model task selection: control of attention. *Neuroscience and biobehavioral reviews, 37*(9 Pt B), 2099-2110.

Maldjian, J. A., Laurienti, P. J., Kraft, R. A., & Burdette, J. H. (2003). An automated method for neuroanatomic and cytoarchitectonic atlas-based interrogation of fMRI data sets. *Neuroimage, 19*(3), 1233-1239.

Marois, R., Leung, H. C., & Gore, J. C. (2000). A stimulus-driven approach to object identity and location processing in the human brain. *Neuron, 25*(3), 717-728.

Martinez, V., & Sarter, M. (2004). Lateralized attentional functions of cortical cholinergic inputs. *Behav Neurosci, 118*(5), 984-991.

Menon, V., Ford, J. M., Lim, K. O., Glover, G. H., & Pfefferbaum, A. (1997). Combined event-related fMRI and EEG evidence for temporal-parietal cortex activation during target detection. *Neuroreport, 8*(14), 3029-3037.

Miller, E. K., & Cohen, J. D. (2001). An integrative theory of prefrontal cortex function. *Annu Rev Neurosci, 24*, 167-202.

Minzenberg, M. J., Laird, A. R., Thelen, S., Carter, C. S., & Glahn, D. C. (2009). Meta-analysis of 41 functional neuroimaging studies of executive function in schizophrenia. *Arch Gen Psychiatry, 66*(8), 811-822.

Oldfield, R.C. (1971). Assessment and analysis of handedness- Edinburgh Inventory. *Neuropsychologia*, *9*, 97-113.

Oppenheim, A. V., Schafer, R. W., & Buck, J. R. (1999). *Discrete-time signal processing*. Englewood Cliffs, NJ: Prentice Hall.

Pouget, A., Dayan, P., & Zemel, R. S. (2003). Inference and computation with population codes. *Annu Rev Neurosci, 26*, 381-410.

Reuter-Lorenz, P. A., & Cappell, K. A. (2008). Neurocognitive aging and the compensation hypothesis. *Current Directions in Psychological Science, 17*(3), 177-182.

Ridderinkhof, K. R., Ullsperger, M., Crone, E. A., & Nieuwenhuis, S. (2004). The role of the medial frontal cortex in cognitive control. *Science, 306*(5695), 443-447.

Sarter, M., Gehring, W. J., & Kozak, R. (2006). More attention must be paid: the neurobiology of attentional effort. *Brain Res Rev, 51*(2), 145-160.

Sarter, M., Givens, B., & Bruno, J. P. (2001). The cognitive neuroscience of sustained attention: where top-down meets bottom-up. *Brain Res Brain Res Rev, 35*(2), 146-160.

Schrouff, J., Rosa, M. J., Rondina, J. M., Marquand, A. F., Chu, C., Ashburner, J., et al. (2013). PRoNTo: pattern recognition for neuroimaging toolbox. *Neuroinformatics, 11*(3), 319-337.

Shehzad, Z., Kelly, A. M., Reiss, P. T., Gee, D. G., Gotimer, K., Uddin, L. Q., et al. (2009). The resting brain: unconstrained yet reliable. *Cereb Cortex, 19*(10), 2209-2229.

Song, M., Zhou, Y., Li, J., Liu, Y., Tian, L., Yu, C., et al. (2008). Brain spontaneous functional connectivity and intelligence. *Neuroimage, 41*(3), 1168-1176.

Song, X. W., Dong, Z. Y., Long, X. Y., Li, S. F., Zuo, X. N., Zhu, C. Z., et al. (2011). REST: a toolkit for resting-state functional magnetic resonance imaging data processing. *PloS one, 6*(9), e25031.

St Peters, M., Demeter, E., Lustig, C., Bruno, J. P., & Sarter, M. (2011). Enhanced control of attention by stimulating mesolimbic-corticopetal cholinergic circuitry. *J Neurosci, 31*(26), 9760-9771.

Sturm, W., de Simone, A., Krause, B. J., Specht, K., Hesselmann, V., Radermacher, I., et al. (1999). Functional anatomy of intrinsic alertness: evidence for a fronto-parietal-thalamic-brainstem network in the right hemisphere. *Neuropsychologia, 37*(7), 797-805.

Swets, J., Tanner, W. P., Jr., & Birdsall, T. G. (1961). Decision processes in perception. *Psychol Rev, 68*, 301-340.

Thomason, M. E., Dennis, E. L., Joshi, A. A., Joshi, S. H., Dinov, I. D., Chang, C., et al. (2011). Resting-state fMRI can reliably map neural networks in children. *Neuroimage, 55*(1), 165-175.

Tipping, M. E. (2001). Sparse bayesian leaning and the relevance vector machine. *Journal of Machine Learning Research, 1*, 211-244.

Tzelgov, J., Henik, A., & Berger, J. (1992). Controlling Stroop effects by manipulating expectations for color words. *Memory & cognition, 20*(6), 727-735.

Urner, M., Schwarzkopf, D. S., Friston, K., & Rees, G. (2013). Early visual learning induces long-lasting connectivity changes during rest in the human brain. *Neuroimage, 77*, 148-156.

van den Heuvel, M. P., Stam, C. J., Kahn, R. S., & Hulshoff Pol, H. E. (2009). Efficiency of functional brain networks and intellectual performance. *J Neurosci, 29*(23), 7619-7624.

Varkuti, B., Guan, C., Pan, Y., Phua, K. S., Ang, K. K., Kuah, C. W., et al. (2013). Resting state changes in functional connectivity correlate with movement recovery for BCI and robot-assisted upper-extremity training after stroke. *Neurorehabilitation and neural repair, 27*(1), 53-62.

Vul, E., Harris, C., Winkielman, P., & Pashler, H. (2009). Puzzlingly high correlations in fMRI studies of emotion, parsonality, and social cognition. *Perspectives on Psychological Science, 4*, 274-290.

Wang, L., Liu, X., Guise, K. G., Knight, R. T., Ghajar, J., & Fan, J. (2010). Effective connectivity of the fronto-parietal network during attentional control. *Journal of cognitive neuroscience, 22*(3), 543-553.

Wu, J., Srinivasan, R., Kaur, A., & Cramer, S. C. (2014). Resting-state cortical connectivity predicts motor skill acquisition. *Neuroimage*.

Yarkoni, T., Barch, D. M., Gray, J. R., Conturo, T. E., & Braver, T. S. (2009). BOLD correlates of trial-by-trial reaction time variability in gray and white matter: a multi-study fMRI analysis. *PloS one, 4*(1), e4257.

Chapter III

A CHOLINE TRANSPORTER MINOR ALLELE IS ASSOCIATED WITH ATTENUATED HEMODYNAMIC RESPONSE IN RIGHT PREFRONTAL CORTEX DURING CHALLENGES TO ATTENTION

INTRODUCTION

Cholinergic projections from basal forebrain to prefrontal cortex (PFC) are necessary for attentional performance (Hasselmo & Sarter, 2011), and abnormalities in the cholinergic system have been implicated in the attentional deficits associated with a number neurodegenerative and psychiatric disorders (Counts & Mufson, 2005; Mesulam, 2004; Mufson et al., 2000; Sarter, Lustig, & Taylor, 2012; Xie & Guo, 2004). However, little is known about how non-pathologic variation of endogenous cholinergic signaling influences attention and modulates PFC function in humans. The present study used an imaging genetics approach in healthy adults to address this gap in our knowledge. Specifically, we assessed the link between a polymorphism thought to limit cholinergic capacity and reduced fMRI activation in an attentional control region in PFC.

The attention task used in the present study has been instrumental in documenting that cholinergic modulation of the frontoparietal cortex is essential for attentional performance, especially under challenging conditions (Broussard

et al., 2009; Gill et al., 2000; St Peters et al., 2011). In rodents, performance of the Sustained Attention Task (SAT) causes increases in acetylcholine (ACh) release in right medial PFC relative to baseline, with further augmentation during distractor challenge (dSAT; St Peters et al., 2011). The importance of elevated PFC cholinergic activity to performance has been shown to be largely right-lateralized (Apparsundaram et al., 2005; Martinez & Sarter, 2004). Understanding the mechanisms by which cholinergic inputs to right PFC act to stabilize performance under challenging conditions is currently a topic of intense research interest (reviewed in Hasselmo & Sarter, 2011; Sarter, Lustig, Howe, Gritton, & Berry, 2014). Research to date suggests cholinergic inputs are capable of modulating highly specified cortical circuitry in right PFC to enhance cue detection mechanisms, facilitate the filtering of distractors, and modify sensitivity and biases (Everitt & Robbins, 1997; Hasselmo, 1995; Hasselmo & McGaughy, 2004; Hasselmo & Sarter, 2011; Sarter & Bruno, 1997; St Peters et al., 2011).

As a first step in delineating the contribution of the human cholinergic system to controlled attention, the SAT and dSAT tasks were adapted and validated for use in humans (Demeter, Sarter, & Lustig, 2008). Though we have identified that the size and pattern of some behavioral effects are species-specific (for discussion see Demeter et al., 2008), neuroimaging studies have established consistent, replicable evidence of functional overlap across species (Berry, Sarter, & Lustig, in prep; Demeter, Hernandez-Garcia, Sarter, & Lustig, 2011). Thus far, the basic circuitry underlying task performance and response to

distractor challenge appears to be fairly well conserved across species (see Brown & Bowman, 2002 for a discussion of the homologies between rat and human PFC; Demeter et al., 2011).

Functional imaging studies in humans reveal challenges to attention increase right-lateralized PFC activation, paralleling ACh increases measured in rodents. An arterial spin labeling study employing long task blocks revealed SAT performance increased perfusion in right middle frontal gyrus (MFG) approximating Brodmann's area (BA) 9 relative to fixation baseline. Mirroring patterns of cholinergic release in rodents, greatest perfusion increases were found for dSAT blocks during which attentional demands were highest (Demeter et al., 2011). A recent BOLD event-related design study replicated these findings with peak activation found in neighboring right inferior frontal gyrus (IFG) approximating BA 9 (Berry et al., in prep). We speculated that enhanced cholinergic neurotransmission might have contributed to the increased right PFC activation during attentional challenge. Though the close ties between rodent and human versions of this task provide principled guidance for these speculations, the present study aimed to more directly examine the role of cholinergic signaling in right BA 9 activation by using genetic variation in the cholinergic system as an independent variable.

Cholinergic signaling capacity may be limited by the Ile89Val variant (rs1013940) of the high-affinity choline transporter (CHT gene *SLC5A7*). CHT transports choline from the extracellular space into presynaptic terminals, a rate-

limiting step in the synthesis of ACh (Simon, Atweh, & Kuhar, 1976; Yamamura & Snyder, 1972). In humans, the Ile89Val variant of the CHT gene *SLC5A7* reduces the rate of choline transport by approximately 40-60% compared to the major allele (Okuda, Okamura, Kaitsuka, Haga, & Gurwitz, 2002). Connecting suboptimal cholinergic capacity to specific deficits in attention, our previous research demonstrated greater self-reported distractibility in Ile89Val heterozygotes compared to controls with the dominant allele, and greater decrements in attentional performance in the presence of distraction (Berry et al., in press). Performance levels without distraction were equivalent across groups, suggesting the Ile89Val polymorphism is associated with a specific vulnerability to distraction.

Here we tested the hypothesis that distractor vulnerability in Ile89Val is accompanied by diminished enhancement of right BA 9 activation during distractor challenge. Supporting our hypothesis, mice with a heterozygous deletion of the CHT gene (CHT + /-) showed significantly attenuated ACh release in right PFC during SAT performance relative to controls (Paolone et al., 2013). The current study represents an important step in establishing a link between altered endogenous cholinergic capacity and human functional neural measures of cognitive control. The close correspondence between rodent and human tasks and the coordinated genetic approach allows the results of this research to have strong translational potential for better understanding the biological mechanisms

underlying attentional control during distractor challenge, and for understanding the contribution of cholinergic signaling to PFC activation in BOLD fMRI studies.

METHODS

Participants.

13 Ile89Val heterozygotes and 13 controls homozygous for the dominant allele participated in the fMRI study. Participants were matched for gender, age, years of education, and self-reported distractibility assessed using the Poor Attentional Control (PAC) scale (Huba, Singer, Aneshensel, & Antrobus, 1982) (see Table 3.1). Participants were right handed, had normal or corrected to normal vision, had no history psychiatric disorders including anxiety, depression or ADHD, and did not take medications that affect cognition.

Participants were selected from a sample of 617 individuals recruited from the greater Ann Arbor community. Participants contributed saliva samples for genotyping as previously described (Berry et al., in press). In total, 67 Ile89Val heterozygotes were identified from this sample. Recruitment procedures for initial genotyping did not disqualify participants based on history of psychiatric disorder or medication use. We took this inclusive recruitment approach to maximize the rate of identification of Ile89Val heterozygotes as the frequency of the Ile89Val variant in normal Caucasian subjects is only ~6% (English et al., 2009), and has been specifically linked with higher incidence of ADHD and greater severity of

depression (English et al., 2009; Hahn et al., 2008). Our previous behavioral studies included participants with history of psychiatric disorder and medication use. Compared to controls matched for these factors, we found Ile89Val heterozygotes showed selective vulnerability to distraction (Berry et al., in press).

For the present fMRI study, our primary question was how genotypic variance in the brain's cholinergic system impacts fMRI BOLD activation during attentional challenge. Therefore, we screened for conditions that could cause uncontrolled effects on BOLD signal. We recruited participants with no psychiatric diagnosis history, no significant vision problems and no use of psychoactive medication. Individuals with history of migraines were also excluded due to the flashing distractor task stimulus. Based on health information collected at genotyping, 25 Ile89Val heterozygotes were re-contacted. Of these individuals, 13 were interested in participating and passed further screening for fMRI contraindications.

We matched participants on self-reported PAC distractibility to reduce potential concerns that a finding of distractor-related BOLD differences in Ile89Val participants might be due to an artifact of selection bias. That is, if we had not matched the samples for the experiment on PAC score, there might have been concerns that we happened to pick low-distractibility participants from the control population and high-distractibility participants from the Ile89Val population and thereby inflated our chances of finding a group differences. Instead, by matching the groups on PAC score, we conducted a conservative test of the

impact of genotypic variance in the cholinergic system on performance and BOLD activation. Indeed, we have likely picked control participants relatively high in the distractibility distribution. Berry et al. (in press) compared PAC scores for groups of 67 Ile89Val and 67 controls matched for age and gender, and found significantly greater self-reported distractibility for Ile89Val. Mean PAC distractibility in this previous report was lower for controls (M = 13.43, SD = 4.04) than in the current control sample (below), while mean PAC distractibility scores for Ile89Val (M = 15.14, SD = 4.43) was comparable the current Ile89Val sample (below). Our results may thus underestimate the size of the group differences distraction's effect on dSAT performance and BOLD signal.

To address concerns that the relatively small sample size may increase type I errors (Button et al., 2013), we conducted *post hoc* analyses of achieved power. Power analyses were computed using G*Power 3.1 (Faul, Erdfelder, Buchner, & Lang, 2009) and are reported for the central claims made in the present study.

Table 3.1. Demographics and self-reported everyday attention function for Ile89Val participants and controls. Each group included 13 participants (6 females, 7 males). PAC attention measures are reported below (Huba et al., 1982).

		Control	Ile89Val	t-test	Effect size (Cohen's d)
Age (yrs)	M	44.00	43.69	t < 1	d = 0.02
	SD	*16.89*	*17.67*	p = .96	
Edu (yrs)	M	17.15	17.00	t < 1	d = 0.04
	SD	*2.97*	*3.76*	p = .91	
Distractibility	M	14.84	15.08	t < 1	d = 0.05
	SD	*5.11*	*4.17*	p = .90	
Mind-wandering	M	14.92	14.07	t < 1	d = 0.17
	SD	*4.21*	*5.69*	p = .67	
Boredom	M	13.23	12.62	t < 1	d = 0.17
	SD	*3.85*	*3.25*	p = .66	

Behavioral task.

Participants performed the Sustained Attention Task (SAT) and its distractor condition (dSAT) as previously described (Berry et al., in prep; Demeter, Guthrie, Taylor, Sarter, & Lustig, 2013; Demeter et al., 2011; Demeter et al., 2008), implemented using E-prime (Psychological Software Tools, Pittsburg, PA). SAT and dSAT trials consisted of signal and nonsignal trials (Figure 3.1). The signal was a small dark gray square centrally presented for a variable duration (17 – 64 ms). Trials consisted of a period of monitoring (1000, 2000, or 3000 ms), at the end of which a signal did (signal event) or did not (nonsignal event) appear. The signal occurred for 50% of the trials. Participants

were cued to respond by a 700 ms low-frequency auditory response tone. Participants had up to 1000 ms after the tone to make a keypress response indicating whether or not the signal had been presented on that trial (response-hand mapping was counterbalanced across subjects). A high-frequency tone lasting 700 ms followed correct responses. Responses were classified as hits (correct signal trials), misses (incorrect signal trials), correct rejections (CR; correct nonsignal trials), false alarms (FA; incorrect nonsignal trials), and omissions. dSAT trials were identical to SAT trials except the background screen flashed from gray to black at 10 Hz. Participants were provided monetary incentive. For each task run, participants were paid 1 cent for each percent correct, but penalized 5 cents for the percent of missed trials.

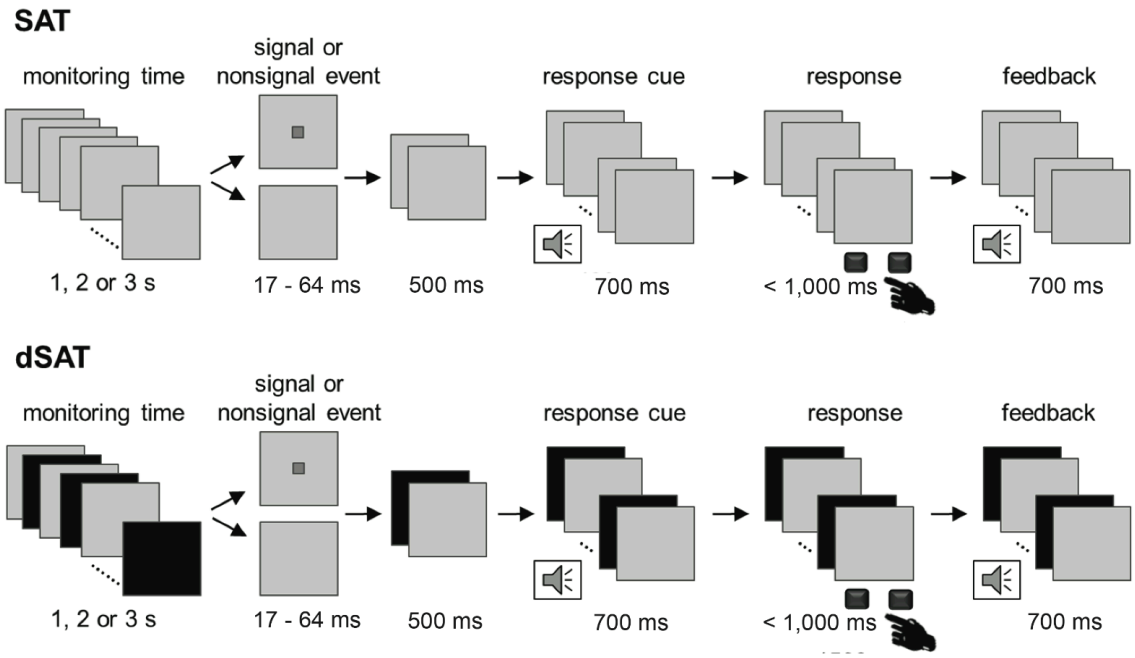

Figure 3.1. Sustained Attention Task (SAT). Each trial consisted of a variable duration monitoring interval followed by the presentation of a signal or nonsignal event. The signal was a gray square on a silver background and varied in duration. Signal and nonsignal events were pseudorandomized and occurred with equal frequency. Participants were cued to respond by a low frequency buzzer. Participants responded via buttonpress using one index finger for signal trials and the other index finger for nonsignal trials (left-right key assignment counterbalanced across participants). Correct responses were followed by a high frequency feedback tone; incorrect responses and omissions did not result in feedback. The distractor condition, dSAT, increased the attentional control demands of the task by adding a global, continuous visual distractor. During dSAT trials, the screen flashed from gray to black at 10 Hz. SAT, dSAT, and fixation (not pictured) trials were pseudorandomly intermixed.

Behavioral analysis.

Our primary accuracy measure was SAT score, a measure of performance across both signal and nonsignal trials. For completeness, Appendix II reports standard signal-detection measures of sensitivity (d') and bias (Swets, Tanner, & Birdsall, 1961). SAT score was calculated for each condition (SAT, dSAT) using the formula SAT score = (hits – FAs)/[2(hits + FAs) – (hits + FAs)^2]. SAT score

varies from + 1 to -1 with + 1 indicating all responses were hits or CRs and -1 indicating all responses were misses or FAs.

Data were analyzed with SPSS, version 21. Group comparisons were made using a mixed-design ANOVA with the between-subjects factor genotype (Ile89Val, control), and within-subjects factor distraction (SAT, dSAT). Greenhouse-Geisser sphericity correction was applied as needed for reporting p values, but degrees of freedom are reported as integers in the text for easier reading. Effect sizes are reported using η^2_G (Bakeman, 2005), which gives smaller values than the frequently-used η^2_P but is preferable as it reduces error when comparing across studies (Fritz, Morris, & Richler, 2012). *Post hoc t* tests were conducted with effect sizes computed using Cohen's d.

fMRI data acquisition, preprocessing, and GLM.

Methods for data acquisition, preprocessing, and GLM were identical to those reported in Berry et al. (in prep; Chapter II).

Data acquisition. Six experimental runs consisted of equal numbers of SAT signal, dSAT signal, SAT nonsignal, dSAT nonsignal and fixation trials. During fixation periods (duration 2.2 s – 12.6 s), participants were instructed to relax and focus on a centrally presented fixation cross (background screen flashed from gray to black at 10 Hz). Each experimental run consisted of 75 trials. Trials were pseudorandomized to ensure that all possible sequences occurred

with equal probability. Prior to scanning, participants performed in-scanner practice trials to confirm they remembered task instructions, and the response and feedback tones were audible.

Imaging data were collected using a 3 T General Electric Signa scanner with a standard quadrature head coil. Participants used mirrored glasses to view stimuli that were projected on a screen behind them. Functional images were acquired during task performance using a spiral-in sequence with 35 slices and voxel size 3.44 x 3.44 x 3 mm (TR = 2 s, TE = 30 ms, flip angle = 90°, FOV = 22 mm^2). A T1-weighted anatomical overlay was acquired in the same functional space (TR = 225 ms, TE = 3.8 ms, flip angle = 90°). A 148-slice high-resolution T1-weighted anatomical scan was collected using spoiled-gradient-recalled acquisition (SPGR) in steady-state imaging (TR = 9 ms, TE = 1.8 ms, flip angle = 15°, FOV = 26 x 20.8 cm, slice thickness = 1 mm).

Preprocessing. During preprocessing, structural images were skull-stripped using the Brain Extraction Tool in FSL (FMRIB Software Library; www.fmrib.ox.ac.uk/fsl; Smith et al., 2004) and corrected for signal inhomogeneity. SPGR images were normalized to the Montreal Neurological Institute (MNI) template using SPM 8 (Wellcome Department of Cognitive Neurology, London). To spatially normalize functional images to the MNI template, the functional overlay and SPGR were used as intermediates. All functional images were corrected for differences in slice timing (Oppenheim et al., 1999) and head movement using the MCFLIRT algorithm (Jenkinson et al.,

2002). Functional images were smoothed with an 8-mm full width/half-maximum isotropic Gaussian kernel and high-pass filtered (128 s).

General Linear Model. Data were analyzed using a multisession General Linear Model (GLM) implemented in SPM8. SAT and dSAT hits, CRs, and fixation onsets were modeled as separate predictors. All omissions, misses, and FAs were modeled together as a separate predictor and are not included in the present analysis. Predictors were time-locked to onset of the signal or nonsignal period and convolved with the canonical hemodynamic response function. To mitigate the effect of motion artifact, six motion regressors derived from individual subject realignment were included in the model.

fMRI data analysis methods and rationale.

Previous human imaging studies have suggested attentional challenge implemented during dSAT increases activation in human right BA 9 (Berry et al., in prep; Demeter et al., 2011) and increases right medial PFC ACh release in rodents (Arnold, Burk, Hodgson, Sarter, & Bruno, 2002; Kozak et al., 2006; St Peters et al., 2011). We hypothesized that controls, but not Ile89Val participants, would significantly increase right BA 9 activation during dSAT above levels of activation measured during standard SAT performance. Our primary hypothesis is supported by the observation that mice with genetically reduced CHT transporter expression (CHT +/-) release significantly less ACh during attentional

challenge than wild-type control mice (Paolone et al., 2013). We expected to find the same pattern of attenuated right PFC activity in Ile89Val heterozygotes.

Our univariate analyses tested our primary hypothesis, right prefrontal hypoactivation in Ile89Val heterozygotes, and were strongly motivated by previous empirical findings. To preview our results, we did, indeed, find significant group differences in the degree right BA 9 activation increased in response to distractor challenge. To provide additional support for our univariate findings, we used multivoxel pattern analysis (MVPA) to examine whether patterns of activation within right BA 9 were sufficient to discriminate Ile89Val participants and controls.

Next, we preformed exploratory MVPA analyses aimed to identify the possible regions Ile89Val heterozygotes differentially engaged during attentional challenge relative to controls. We believe the results of these analyses shed light on potential compensatory mechanisms that act to preserve performance when activity in prefrontal control regions is insufficient, and represent important targets for future investigation.

A priori region of interest analyses.

Univariate. Our region of interest (ROI) analyses focused on hypothesis-guided comparisons of right BA 9 activation during distractor challenge for Ile89Val participants versus controls. Percent signal change values were

submitted to mixed-design ANOVA with the between-subjects factor genotype (Ile89Val, control), and within-subjects factors distraction (SAT, dSAT). Methods for sphericity correction, effect size calculation, and post hoc testing were consistent with those described for the behavioral data.

We first used a functionally defined ROI based on the right PFC peak activation for the dSAT > SAT contrast from a study in young adults using the identical task and fMRI parameters (Berry et al., in prep). The ROI was centered on peak Montreal Neurological Institute (MNI) coordinates 46, 2, 30 in right IFG, approximating BA 9 (8 mm sphere). Percent signal-change values for each participant were extracted using MarsBar software (http://marsbar.sourceforge.net; Brett et al., 2002).

We preformed two complementary analyses to rigorously test our preferred hypothesis that modulation of activation in this region was attenuated in Ile89Val. First, we performed a single voxel analysis. A unique voxel was identified for each participant within the 8 mm sphere described above that showed the greatest increase in signal for the contrast dSAT > SAT for each participant. Percent signal change within this voxel was submitted to mixed-design ANOVA analysis as described above. Next, we tested group differences in activation within the anatomically defined right BA 9 region. We generated the right BA 9 mask using WFU PickAtlas v 3.0 (www.fmri.wfubmc.edu/software/PickAtlas; Lancaster et al., 1997; Lancaster et al., 2000; Maldjian et al., 2003).

Finally, we assessed percent signal change in a control region to test the specificity of genotype-related activation differences and to rule out the possibility of differences in global signal between groups. We tested activation within right motor cortex (M1; MNI 37, -25, 62, 8 mm sphere) (Mayka, Corcos, Leurgans, & Vaillancourt, 2006).

Multivariate: multivoxel pattern analysis. MVPA analyses were conducted using the Pattern Recognition for Neuroimaging Toolbox (PRoNTo) (www.mlnl.cs.ucl.ac.uk/pronto; Schrouff et al., 2013).

We tested whether the pattern of activation within the functionally defined right IFG ROI and anatomically defined right BA 9 could significantly discriminate Ile89Val vs controls. We submitted each participant's univariate contrast image dSAT > SAT to classification using the binary support vector machine (SVM; Burges, 1998 LIBSVM implementation, http://www.csie.ntu.edu.tw/~cijlin/libsvm/) with a leave one subject out cross-validation approach. Masks were identical to the ROIs used in the univariate analyses described above. However, we used 16 mm radius sphere ROIs rather than 8 mm radius spheres because of special considerations that arise from spatial smoothing (for discussion of smoothing in MVPA see Kamitani & Sawahata, 2010; Op de Beeck, 2010). We report classification accuracy and significance levels calculated for 100 permutation

tests for each mask. Additionally, we plot model prediction values for each participant[1].

Exploratory whole brain analyses.

Univariate: voxel-wise analysis. To determine whether there were activation differences between groups outside our *a priori* ROIs, we performed second-level, flexible factorial analyses, with genotype and condition as factors. Planned analyses were carried out to examine main effects of genotype (Ile89Val, control) and distraction (SAT, dSAT), and genotype by distraction interactions. SAT and dSAT trials were contrasted against fixation baseline for second-level analyses. For significance, a combined peak threshold of $p < .001$, uncorrected and extent threshold of 67 voxels was required (AlphaSim cluster-level threshold, $p < .05$). AphaSim was implemented using the REST toolbox v1.8 (Song et al., 2011).

Multivariate: multivoxel pattern analysis. To complement the exploratory univariate analysis described above, we used MVPA to determine whether

[1] Our FWHM smoothing kernel was 8 mm, the same size as our univariate ROIs. Smoothing data with a kernel that is approximately the same size as the ROI can reduce the *pattern* information contained within the ROI since all its voxels will have highly correlated values after smoothing. During MVPA, the classifier may largely base its classifications on the mean activity of the sphere rather than the distributed activation pattern within the sphere. As a result, the ROIs best able to discriminate Ile89Val vs controls would be those whose mean is consistently higher for one group than the other. To reduce this risk, ROIs twice the size of the smoothing kernel were used.

pattern classification could identify regions possibly engaged more by Ile89Val than controls in response to dSAT. Differential engagement of such regions could reflect a functional compensatory mechanism, or application of an alternative task strategy in the face of deficient right BA 9 activation. The MVPA approach has the advantage of detecting information coded across voxels in a multidimensional manner, and can be more sensitive than univariate measures (reviewed in Davis and Poldrack, 2013).

We performed binary support vector classification for dSAT vs SAT trials separately for Ile89Val and controls with a leave one subject out cross-validation approach. To identify the regions that were most important for classifying dSAT vs SAT performance, we generated separate weight vector images for Ile89Val and controls. We then contrasted the weight maps (Ile89Val – control) to determine which regions were preferentially weighted in Ile89Val classification. Because of the multivariate nature of the patterns, spatial inference on the weights cannot be performed using univariate statistics (The weight maps are displayed without a threshold or statistical test). Weight images can be used to identify the most discriminative regions, but should be interpreted with caution.

RESULTS

Behavior.

Ile89Val and controls showed equivalent performance for SAT and dSAT trials. For both groups, distraction impaired performance, which generally replicated the effects found in our previous studies (Berry et al., in prep; Demeter et al., 2013; Demeter et al., 2011; Demeter et al., 2008). Omissions were generally low (M = .05, SD = .06) and did not significantly differ for controls and Ile89Val participants ($t(24) = 0.43$, $p = .49$, $d = 0.17$).

Analysis of SAT score revealed the distractor reduced accuracy for both groups, $F(1,24) = 32.24$, $p < .001$, $\eta^2_G = 0.16$. There were no significant differences between groups in overall performance, $F(1,24) = 1.39$, $p = .25$, $\eta^2_G = 0.05$, and groups were equivalently impacted by distraction, $F < 1$.

Matching groups on PAC distractibility may have affected our ability to detect group differences in the dSAT distractor effect (as discussed in the Methods). Though there were no significant differences between groups, the average overall performance for Ile89Val was numerically greater than controls'. The direction of this numerical group difference was opposite to our prediction that Ile89Val would show greater sensitivity to the distractor based on previous research (Berry et al., in press). Therefore, we probed the behavioral data further.

Figure 3.2 shows the plots of individual participant SAT scores. Inspection of individual participant data revealed one control participant's performance was rather low, and contributed to lower mean performance for controls. Though their performance was low, their data were within 3 SD of average SAT and dSAT score. Removal of this participant's data (and their Ile89Val match's data) did not change overall statistical significance of our behavioral analyses, but did cause minor changes in effect size. For SAT score, all main effects and interactions showed the same pattern. The main effect of genotype remained nonsignficant $F < 1$ with a slight change in effect size (0.02 compared to 0.05), and the genotype by distraction interaction remained nonsignificant, $F(1,22) = 1.34$, $p = .30$, with a slight change in effect size (0.01 compared to 0.004). Similarly, removal of these two subjects from fMRI analyses did not change the major conclusions drawn from the current report. Therefore, the control and Ile89Val match were included in analyses to preserve sample size.

We conducted power analyses to determine the number of subjects that would be necessary to detect a significant difference between control and Ile89Val performance, if one were to exist, given present effect sizes. These analyses found that 196 total participants (98 per group) would be necessary to achieve .90 power, and 144 total participants (73 per group) to achieve .80 power. Because of the limited number of Ile89Val in our total sample (n = 67), we did not pursue additional behavioral testing.

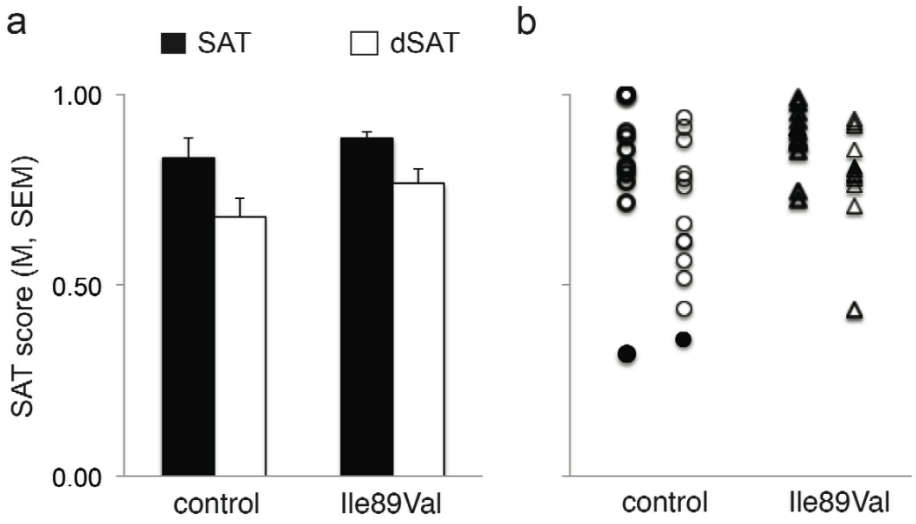

Figure 3.2. Effect of distraction on SAT scores for controls and Ile89Val. Data shown are from 6 experimental runs. Black bars and thick outlined shapes display performance data for SAT trials without distraction; white bars and thin outlined shapes display performance data for dSAT trials with distraction (a) The distractor impaired performance ($p < .001$), and had an equivalent effect on performance for both groups ($p = .44$) There was no difference between groups in overall performance ($p = .25$). (b) Individual data is plotted to illustrate the low performance of a control participant (filled circle). This participant was included in all analyses (performance was within 3 SD of group mean). Removal of this participant and their Ile89Val match from analyses did not change major conclusions of the present study.

fMRI a priori region of interest analyses.

A priori analyses showed strong and consistent differences in right BA 9 activation between groups. These results were consistent when applying both functionally defined ROIs as well as structurally defined ROIs. In reporting our results, we display group means as well as individual subject data to demonstrate the consistency of effects. Adding further support for our ROI results, group differences in right BA 9 activity were replicable through univariate and multivariate analysis approaches.

Univariate. ROI analyses of right PFC activation during SAT and dSAT indicated that controls more strongly increased activation during distractor challenge than Ile89Val participants. Controls did not differ from Ile89Val participants in overall activation, but showed greater enhancement of activation during distractor challenge (dSAT – SAT).

Inspection of percent signal change within the functionally defined right IFG ROI (MNI 46, 2, 30; 8 mm sphere) showed no overall effect of genotype, $F(1,24) = 0.15$, $p = .71$, $\eta^2_G < 0.01$. Percent signal change was greater during dSAT than SAT, $F(1,24) = 22.91$, $p < .001$, $\eta^2_G = 0.10$, but elevated activation during dSAT was more pronounced for controls, $F(1,24) = 10.94$, $p = .003$, $\eta^2_G = 0.05$. *Post hoc* paired *t* tests revealed only controls significantly increased activation in response to distractor challenge $t(12) = 4.72$, $p < .001$, $dz = 1.25$, while Ile89Val did not $t(12) = 1.44$, $p = .18$, $dz = 0.40$. Means and SE are displayed in Figure 3.3.

These results held for the single voxel analysis. For the voxel showing the greatest increase in activation for the dSAT > SAT contrast, there was no overall effect of genotype, $F(1,24) = 0.23$, $p = .63$, $\eta^2_G < 0.01$. Though both groups showed greater activation during dSAT (voxel selection was contingent on this fact), dSAT enhancement was still greater for controls, $F(1,24) = 10.68$, $p = .003$, $\eta^2_G = 0.05$. *Post hoc* paired *t* tests revealed controls strongly increased activation in response to distractor challenge $t(12) = 10.22$, $p < .001$, $dz = 2.80$, while

Ile89Val showed the same pattern with a smaller effect size $t(12) = 7.29$, $p < .001$, $dz = 2.03$.

Analysis of the anatomically defined right BA 9 ROI generally replicated our functionally defined ROI results. There was a marginal effect of genotype such that Ile89Val showed lower overall activation in right BA 9 than controls, $F(1,24) = 3.18$, $p = .09$, $\eta^2_G = 0.10$. For both groups combined, dSAT did not show greater activation than SAT, $F(1,24) = 2.22$, $p = .15$, $\eta^2_G = 0.01$. However, inspection of the significant interaction between genotype and distraction, $F(1,24) = 7.18$, $p = .01$, $\eta^2_G = 0.03$, revealed controls showed strong enhancement during dSAT, $t(12) = 3.17$, $p = .008$, $dz = 0.91$, while controls did not, $t(12) = .79$, $p = .45$, $dz = 0.22$. Means and SE are displayed in Figure 3.3.

Post hoc analyses of achieved power found the ROI results reported above to be robust. Overall, power was high and consistent across analyses. Achieved power for the functionally defined IFG ROI was .92. Achieved power for the voxel analysis was .88. Achieved power for the structurally defined BA 9 ROI was .74. Together, *post hoc* analyses demonstrated sample size was not a significant concern, and that ROI findings in the current report can be interpreted with confidence.

To ensure that distractor related differences in activation in right PFC were not due to difference is global activation between groups or between task conditions, we evaluated patterns of activation in primary motor cortex. We hypothesized there would be no difference in overall activation between groups,

no difference in motor activation between dSAT and SAT trials, and no interaction. This was indeed the case. Controls and Ile89Val showed similar levels of motor activation, $F(1,24) = 0.33$, $p = .57$, $\eta^2_G = 0.01$. There was no enhancement of motor activation during distractor challenge, $F(1,24) = 1.00$, $p = .33$, $\eta^2_G < 0.01$, and no interaction, $F(1,24) = 0.02$, $p = .90$, $\eta^2_G < 0.01$.

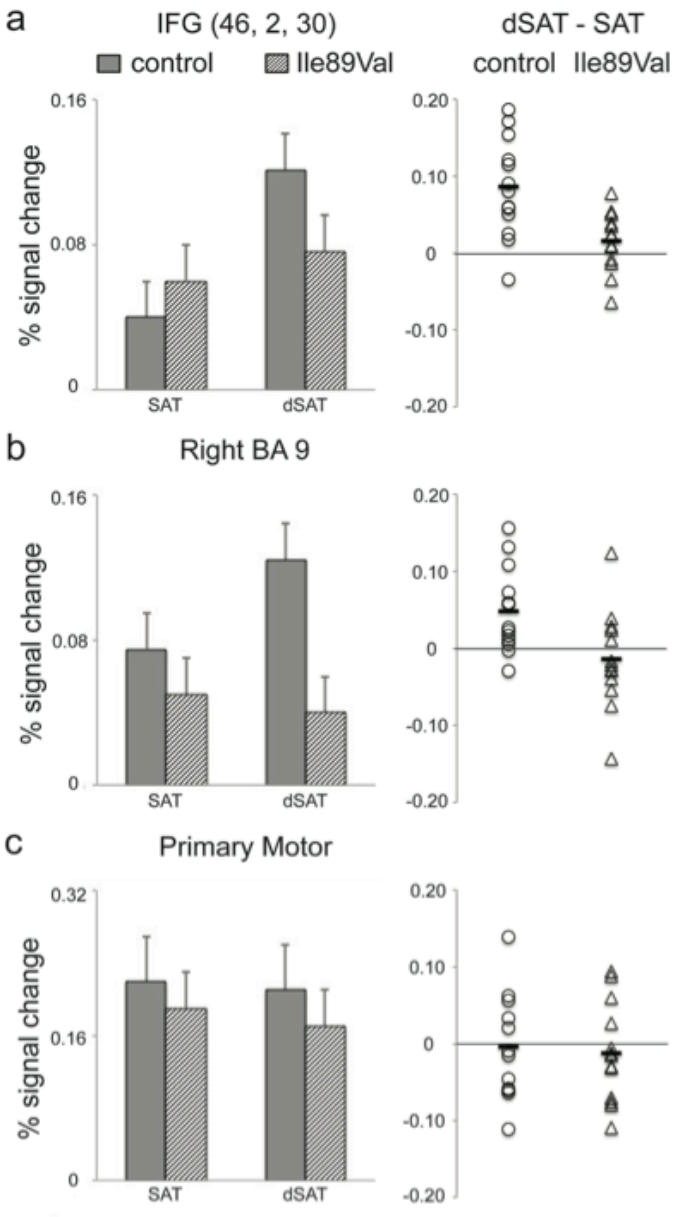

Figure 3.3. Controls, but not Ile89Val increase right BA 9 activation in the presence of distraction. Percent signal change was extracted from regions of interest for controls (gray bars, circles) and Ile89Val (pattern bars, triangles). Primary motor cortex was used as a control region. Percent signal change in the bar graphs (left) is reported relative to fixation baseline. Individual participant data (right) is plotted as percent signal change for the index dSAT – SAT. (a) A significant group by distraction interaction ($p = .003$) revealed controls increased activation during dSAT relative to SAT in the functionally defined right IFG region of interest ($p < .001$), but Ile89Val did not ($p = .18$). (b) Similarly, a significant group by distraction interaction ($p = .01$) revealed controls increased activation in the anatomically defined right BA 9 region of interest ($p = .008$), but Ile89Val did not ($p = .45$). (c) There was no difference between groups in overall activation in primary motor cortex ($p = .57$) and no increase with distraction ($p = .33$) suggesting global differences in activation between groups or across distraction condition were not driving group by distraction interactions.

Multivariate: multivoxel pattern analysis. We determined whether a binary support vector machine could discriminate Ile89Val and control participants based on activation patterns within the functionally defined right IFG ROI, and the structurally defined right BA 9 ROI. Confirming our hypothesis, we found significant classification of participants based on patterns of activation for the dSAT > SAT contrast. Classification within the right IFG functionally defined ROI was 76.9%, $p = .01$. Classification within the right BA 9 anatomically defined ROI was 84.6%, $p = .01$. Importantly, patterns of activation within M1 did not generate significant classification of groups indicating global differences in activation across groups did not drive classifier performance within right PFC. Analysis of motor activation demonstrated only chance levels of classification accuracy, 46.2 %, $p = .49$. Plots of classifier predictions are displayed for individual subjects in Figure 3.4.

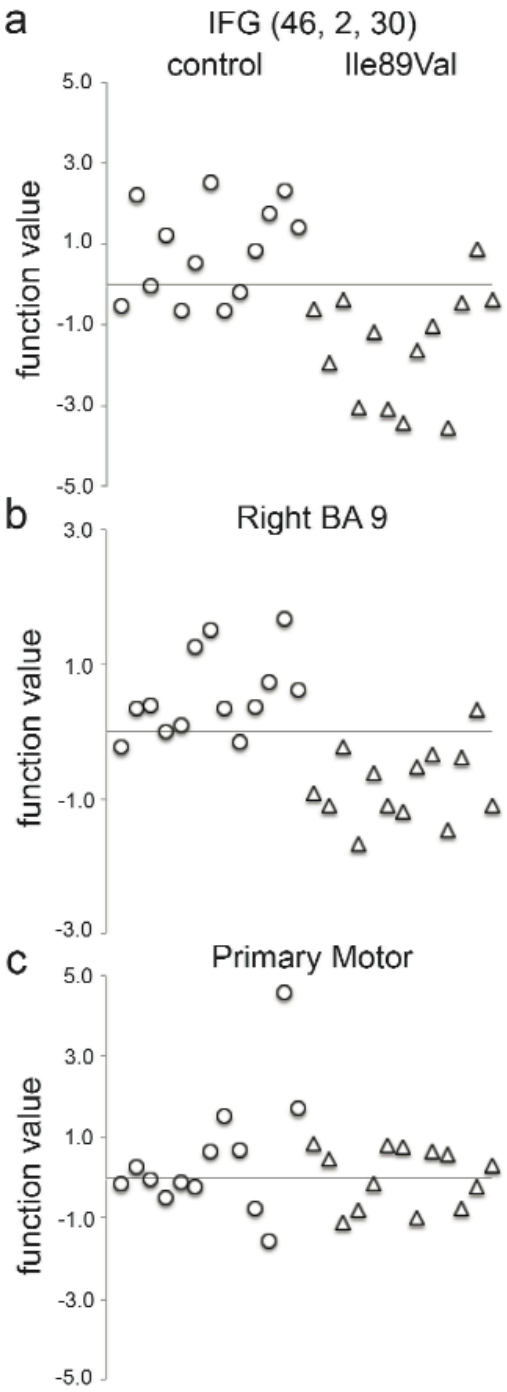

Figure 3.4. Patterns of activation in right BA 9 discriminate controls and Ile89Val. A binary support vector machine was used to test classification accuracy for controls (circles) vs Ile89Val (triangles) based on individual patterns of activation for the dSAT > SAT contrast within regions of interest. Scatter plots of group predictions for individual participants are displayed. (a) Classification accuracy based on the functionally defined region of interest was 76.9%, p = .01. (b) Classification accuracy based on the anatomically defined region of interest was 84.6%, p = .01. (c) Classification accuracy based on the control motor region of interest was at chance, 46.2%, p = .49.

Whole brain exploratory analyses

Univariate: voxel-wise analysis. Main effects of distraction were consistent with previous fMRI studies of SAT and dSAT (Berry et al., in prep; Demeter et al., 2011). Activation increases during dSAT were found in right IFG (MNI 48, 0, 30; 80 voxels), in close proximity to the right IFG peak identified in our previous event-related design study in healthy young adults, MNI 46, 2, 30 (Berry et al., in prep). Figure 3.5 displays significant right prefrontal activation for the contrast dSAT > SAT for both groups. There were no significant effects of genotype or genotype by distraction interactions.

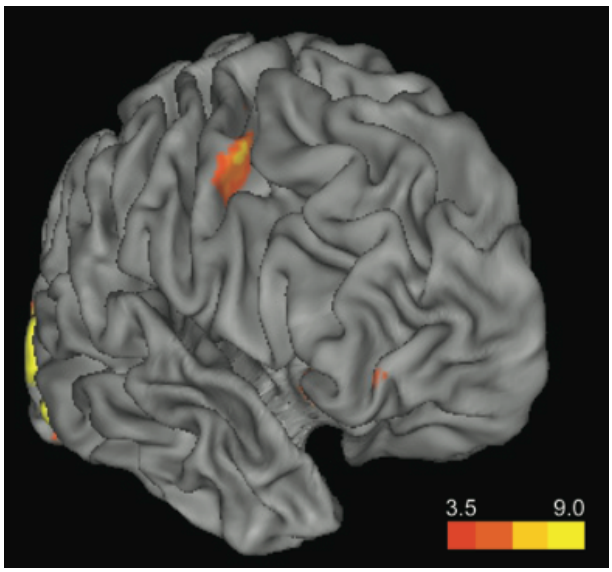

Figure 3.5. Activation in right BA 9 increases in the presence of distraction. T-map for the univariate contrast dSAT (hits + CRs) > SAT (hits + CRs) is displayed for controls and Ile89Val groups combined. The activation in right inferior frontal gyrus (IFG) approximating BA 9 (MNI 48, 0, 30) replicated our previous results using this task (Berry et al., in prep). Activation was also found in visual cortex, which may have been driven by visual stimulation caused by the flashing visual distractor. Activations are displayed on CARET slightly inflated surface representation with the t-value scale shown in the lower right.

Multivariate: multivoxel pattern analysis. To explore possible alternative neural mechanisms supporting Ile89Val performance during distractor challenge, we identified regions that more strongly discriminated dSAT vs SAT trials for Ile89Val participants relative to controls. Overall discrimination for dSAT vs SAT was similar across groups, within 4% accuracy (Ile89Val = 92.3%; control = 88.5%). By contrasting the voxel-wise classification weight maps for each group, we identified two candidate regions that may have been recruited more strongly by Ile89Val participants during distractor challenge: orbitofrontal cortex and parahippocampal gyrus (Figure 3.6). See Appendix II for contrast images at reduced thresholds.

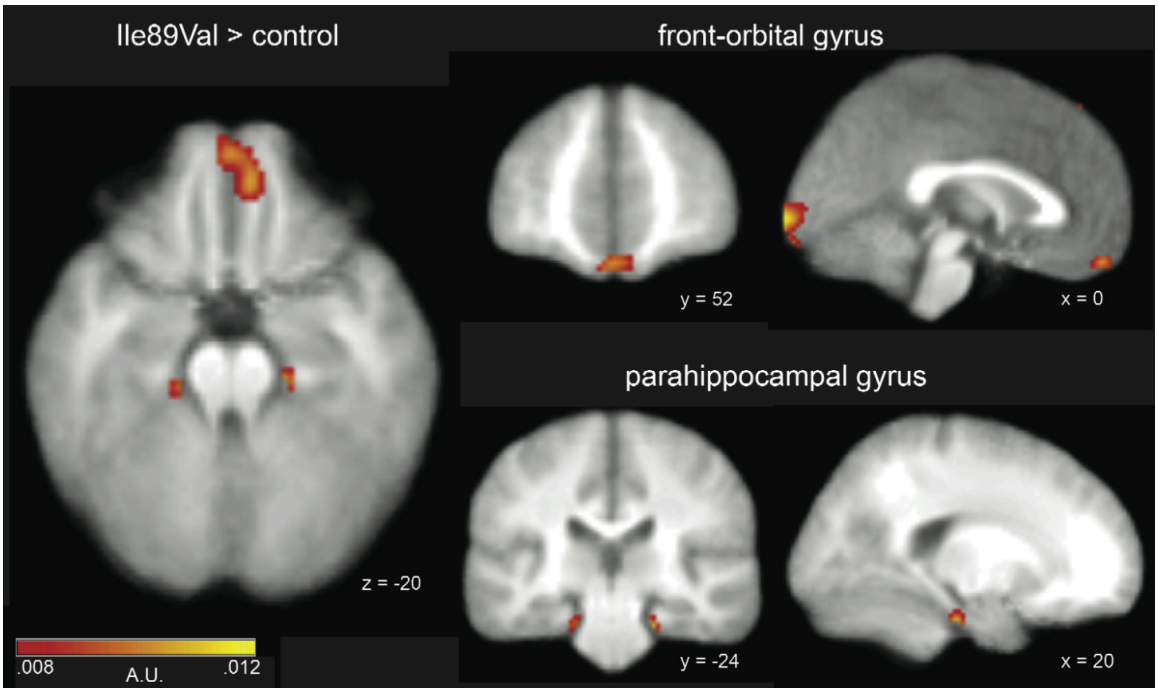

Figure 3.6. Regions more discriminating of distraction condition for Ile89Val than controls. To investigate whether there were regions differentially involved in dSAT performance for Ile89Val than controls, we generated weight maps for the classification of dSAT and SAT trials for controls and Ile89Val using a binary support vector machine. Displayed are regions showing greater discrimination for dSAT vs SAT for Ile89Val than controls: [Ile89Val dSAT > SAT weight map] – [control dSAT > SAT weight map]. Orbitofrontal cortex and parahippocampal gyrus may have been more strongly recruited by Ile89Val during distraction than controls. Weight maps are displayed on the average of each participant's normalized structural scan, and are displayed in arbitrary units (A.U., see Methods).

In addition to orbitofrontal and parahippocampal regions, visual cortex weighed more strongly in the discrimination of dSAT and SAT for Ile89Val than controls. When the occipital lobe was removed from the MVPA analysis, classification accuracy for Ile89Val was affected more than controls'. dSAT vs SAT discrimination accuracy for Ile89Val participants dropped from 92.3% to 73% while discrimination accuracy for controls only dropped from 88.5% to 84.6%. Increased classifier weighting of visual cortex activity suggested Ile89Val

patterns of activation for dSAT vs SAT outside of sensory cortex were more variable than activity for controls.

DISCUSSION

The present study took the first steps in determining how variation of endogenous cholinergic signaling modulates PFC function in humans. We found that a genetic polymorphism of the high affinity choline transporter (Ile89Val variant of the CHT gene *SLC5A7*), thought to limit cholinergic release capacity in PFC, was associated with attenuation of BOLD signal increases in a right-lateralized cognitive control region. Specifically, in Ile89Val heterozygotes, challenges to attention imposed by a global distractor did not evoke increases in activation in right BA 9, though robust activation increases were observed in controls homozygous for the dominant allele. These findings were predicted by findings from a growing body of cross-species research aimed to clarify links between cognitive functions, the neurotransmitter systems that underlie them, and functional correlates of these neural systems measured using fMRI (see also Berry et al., in press; Demeter et al., 2011; Demeter et al., 2008; Howe et al., 2013).

Our primary hypothesis, Ile89Val hypoactivation of the right BA 9 response to attentional challenge, was grounded in findings bridging molecular, systems, and cognitive neuroscience. Rodent studies of SAT and dSAT have

established the critical role of basal forebrain cholinergic inputs to right PFC for optimal attentional performance, particularly when attention is challenged by the presence of distraction. During dSAT performance, rodents and humans show parallel increases in right PFC activity: increased ACh release in rodents (Gill et al., 2000; St Peters et al., 2011), and increased fMRI activation in humans (Berry et al., in prep; Demeter et al., 2011). These complementary findings laid the groundwork for the suggestion that increased fMRI activation in humans is accompanied by, and possibly modulated by, increased cholinergic signaling in right PFC. Testing the impact of genetic variation of the cholinergic system on right PFC fMRI measures was the next step in investigating this possibility.

Previous human studies linking cholinergic function to fMRI measures have largely remained restricted to pharmacological manipulations. One exception is a previous imaging genetics study, which investigated a more common polymorphism of the CHT1 gene (G to T nucleotide base pair substitution located in the 3' untranslated region). Neumann and colleagues (2006) associated possible deficits in cholinergic signaling with greater corticolimbic reactivity implicated in depression and other mood disorders. Importantly, this study supports the feasibility of using CHT genetic variants to detect group differences in fMRI BOLD measures.

The feasibility of using CHT genetic variants to detect significant differences in cholinergic release in PFC was established by our own studies in mice with heterozygous deletion of the CHT transporter (CHT +/-). CHT transport

of choline into the presynaptic terminal is a critical step in the synthesis of ACh, and is thought to be rate limiting during high release periods. This predicts ACh release deficiencies driven by CHT variation are unveiled when the cholinergic system is most active. Supporting this prediction, levels of cholinergic neurotransmission appear to be the same for CHT +/- and wild-type controls (CHT +/+) at baseline, but prolonged, stimulated ACh neurotransmission induces significant release deficits in CHT +/- (Parikh, St Peters, Blakely, & Sarter, 2013). Most relevant to the present study, during SAT performance, CHT +/- mice released significantly less ACh than wild-type controls (Paolone et al., 2013). (ACh measurement during dSAT has not yet been performed, though a similar pattern of results would be predicted). Together, previous genetic manipulations in mice and genetics imaging studies in humans converge to predict the Ile89Val polymorphism would be associated with task-driven differences in PFC BOLD activation linked to presumed limitations in cholinergic release.

Confirming our primary hypothesis, univariate analyses showed Ile89Val heterozygotes did not significantly increase right BA 9 activation during performance of dSAT relative to SAT, while controls showed predicted increases. This was a robust finding, which replicated for functionally and structurally defined *a priori* ROIs, and showed consistent group differences with achieved power as high as .92. Further supporting univariate BOLD findings, multivariate patterns of activation within *a priori* ROIs significantly discriminated groups with accuracy as high as 84%. These findings suggest that Ile89Val and controls

showed both quantitative univariate and qualitative multivariate differences in right BA 9 activation.

Ile89Val heterozygotes in the present study showed equivalent task performance as controls. This finding was consistent with SAT studies conducted in CHT +/- mice, which, despite lower cortical ACh release, performed at comparable levels to controls. Receptor binding assays revealed CHT +/- mice displayed a higher density of postsynaptic cholinergic receptors in PFC, specifically α4β2* nicotinic ACh receptors. Such compensatory upregulation of receptors may have served to produce comparable cholinergic modulation of cortical circuitry and similar levels of performance. Though Ile89Val may also have upregulated ACh receptors in cortex, it was not possible to test such a compensatory mechanism in the present study. A first step for future studies will be to assess the impact of ACh receptor antagonists on performance. If Ile89Val maintain attentional performance via increased ACh receptor density, we would hypothesize that their performance would be more severely impacted by receptor blockade than controls. This differential susceptibility has been demonstrated in CHT +/- mice (Paolone et al., 2013).

Apart from structural compensatory changes, functional compensation may have served to maintain Ile89Val performance during distractor challenge. Two candidate regions, parahippocamal gyrus and orbitofrontal cortex, emerged from exploratory multivariate pattern analyses. It is not possible to determine, given the current evidence, how these regions supported performance (if at all),

and what “mental functions” they may reflect (see Aguirre, 2003; Poldrack, 2006, 2011 for discussion of pitfalls of “reverse inference” in neuroimaging). Here we make tentative conjectures based on evidence from the literature and our own hypotheses regarding the role of PFC cholinergic signaling in performance during attentional challenge. Specific predictions generated by these speculations will need further testing to assess their validity.

One proposal is that the recruitment of orbitofrontal PFC by Ile89Val reflected their increased reward-related processing during dSAT trials. In the present study, participants were given accuracy feedback following each response, and correct trials were associated with a small monetary reward. Orbitofrontal/ventromedial cortex is commonly activated in response to reward, including abstract rewards (O’Doherty, Kringelbach, Rolls, Hornak, & Andrews, 2001; O’Doherty et al., 2003; Rogers et al., 2004), and its activity during response/decision periods scales with the subjective value of the reward and predicted reward likelihood (Daw, O’Doherty, Dayan, Seymour, & Dolan, 2006; Valentin, Dickinson, & O’Doherty, 2007). We posit Ile89Val differentially relied on feedback and monetary reinforcement in order to maintain motivated task performance.

Ile89Val may have differentially focused on motivating factors if they perceived dSAT performance as more aversive or effortful relative to controls. If cholinergic capacity is deficient in Ile89Val, these effects would be felt most acutely during distractor challenge, where cholinergic release has been shown to

be highest and is directly related to preserved performance (St Peters et al., 2011). The increase in cognitive effort during dSAT, and potential disproportionate increase experienced by Ile89Val, may raise the participant's desire to disengage from the task (see Kurzban, Duckworth, Kable, & Myers, 2013 for discussion of the "opportunity cost" model of subjective effort, and Sarter et al., 2014 for discussion in relation to the cholinergic system). For Ile89Val, this desire may be alleviated by stronger engagement of reward processing to drive the continuation of on-task performance. Supporting this possibility, a recent study parametrically varied the effort required for task performance (calculation difficulty) and found increasing effort also increased the sensitivity to reward indexed by greater activation in a similar ventromedial PFC region (slightly more posterior to that identified in the present study; Hernandez Lallemant et al., 2014). Testing how increasing or eliminating reward during dSAT performance modulates activity in orbitofrontal/ventromedial PFC may shed light on the relationship between reward-based motivation and effort.

It is less clear how engagement of orbitofrontal cortex explicitly helped performance beyond its potential role in enabling Ile89Val to maintain performance at all.[2] However, it is feasible that in the present task, maintaining

[2] One possibility is that orbitofrontal cortex facilitates reward-driven learning during dSAT performance. Within-session learning may positively impact performance in the present task given the increased detection uncertainty imposed by the distractor. Orbitofrontal/ventromedial PFC is particularly implicated in in the establishment of stimulus-action-outcome associations (reviewed in Balleine & O'Doherty, 2010; Rangel & Hare, 2010; Rushworth, Noonan, Boorman, Walton, & Behrens, 2011). Within experimental session, these associations may act to optimize performance by guiding responding towards maximal reward.

focus and motivation to continue is sufficient to stabilize performance. The sudden onset signal may have an alerting effect, even with coincident presentation of the distractor, that may prohibit total task disengagement to an extent that would preclude the identification of significant group differences in healthy, motivated populations. Though orbitofrontal cortex may not have served to improve performance through task-specific processing, we maintain it is possible parahippocampal gyrus did via memory/medial temporal lobe functions supporting retrieval of task and response rules.

We have previously demonstrated increased vulnerability to distraction in Ile89Val heterozygotes (Berry et al., in press), though there was no performance decrement in the present study. Matching groups on performance can be beneficial in the interpretation of functional imaging data as one does not have to rule out nonspecific factors that can generate performance differences such as inability to perform the task, or lack of cooperativeness. Indeed, evidence of BOLD BA 9 differences in the face of equivalent behavior may serve to further specify a direct relationship between attenuated BOLD response and possible attenuated ACh release. However, the question of why Ile89Val report greater distractibility in everyday life and show significant decrements in performance in some tasks but not others is a question open to investigation.

Berry et al. (in press) found Ile89Val task performance was more severely impacted by the presence of an ecologically valid video distractor (similar to a television playing in the background). Importantly, participants did not receive

trial-to-trial feedback on the performance of the relevant task, an interval-timing task, and there was no monetary incentive. This task design precluded the use of an orbitofrontal, reward-based mechanism to maintain motivation (and performance) in the face of distractor challenge. Additionally, the use of socially and emotionally salient video distractors, which may have engaged orbitofrontal cortex, potentially interfered with the compensatory use of this region for processing of the relevant task. Future studies should examine the nature of orbitofrontal cortex recruitment during attentional challenge. Changes in functional connectivity in this region have been linked to a polymorphism of the serotonin transporter (5-HTT; Rao et al., 2007) and may be relevant to discovering the etiology of increased depression severity associated with the Ile89Val polymorphism (Hahn et al., 2008).

The present imaging genetics study, though limited by small sample size, tested hypotheses firmly grounded in cross-species research investigating the role of prefrontal cholinergic neurotransmission in controlled attention. Results of this research are relevant for understanding how variation in cholinergic function, independent of pathology, impacts individual difference factors in attentional function and common PFC BOLD measures. Additionally, this work may shed light on the risk and resiliency factors associated with suboptimal cholinergic function relevant to conditions such as schizophrenia (Demeter et al., 2013; Luck, Ford, Sarter, & Lustig 2012).

APPENDIX II

METHODS

Behavioral analysis d'

d' was calculated from the proportions of hits and FAs using the standard formula: d' = z(hits) – z(FAs) (Green & Swets, 1966). The following substitution was made for hit rates of 100%: 1-1/(2N) where N is the total number of signals. For FA rates of 0, we used the percentage equivalent to half a FA (1/2N) where N is the total number of nonsignal stimuli. Bias measures were calculated using the formula: $B"_D$ = [(1 -hits)(1 - FAs) – (hits x FAs)]/[(1 - hits)(1 - FAs) + (hits x FAs)] (Donaldson, 1992). Bias scores range from -1 to +1, with -1 indicating a liberal response bias, and + 1 indicating a conservative response bias.

RESULTS

Behavioral analysis

Table 3.A.1 reports hit and FA proportions which make up SAT score and d' indices. In agreement with SAT score analyses, d' measures and reaction time showed no main effects of group or group by distraction interactions. ANOVA results are reported in Table 3.A.2. There was a marginal effect of group for response bias such that Ile89Val were slightly more conservative than controls

(control SAT B"$_D$ M = 0.11 SD = .51; Ile89Val SAT B"$_D$ M = 0.38 SD = .39). Both groups became more conservative in the presence of distraction (control dSAT B"$_D$ M = 0.58 SD = .39; Ile89Val dSAT B"$_D$ M = 0.67 SD = .22), but there was no group by distraction interaction.

Table 3.A.1. Hit and false alarm proportions for SAT and dSAT trials. Data are means (standard error around the mean).

	hits	false alarms
control SAT	.88 (.03)	.10 (.13)
control dSAT	.72 (.06)	.06 (.10)
Ile89Val SAT	.88 (.03)	.05 (.06)
Ile89Val dSAT	.78 (.04)	.02 (.02)

Table 3.A.2. Mixed design ANOVA results. Results for the mixed design ANOVA analysis with within subjects factor Distraction (SAT, dSAT) and between subjects factor group (Ile89Val, control).

d' factors	*F*	*df*	*p*	*effect size*
GROUP	1.29	1,24	.27	0.04
DISTRACTION	2.39	1,24	.14	0.02
GROUP X DISTRACTION	.31	1,24	.58	<0.01
B"$_D$ factors	*F*	*df*	*p*	*effect size*
GROUP	1.83	1,24	.19	0.04
DISTRACTION	22.27	1,24	<.001	0.16
GROUP X DISTRACTION	1.18	1,24	.29	0.01
Hit RT factors	*F*	*df*	*p*	*effect size*
GROUP	.05	1,24	.82	<0.01
DISTRACTION	2.35	1,24	.14	<0.01
GROUP X DISTRACTION	1.35	1,24	.26	<0.01
CR RT factors	*F*	*df*	*p*	*effect size*
GROUP	.002	1,24	.96	<0.01
DISTRACTION	3.98	1,24	.06	<0.01
GROUP X DISTRACTION	.10	1,24	.76	<0.01

fMRI analysis

Multivariate: multivoxel pattern analysis. To complement the analysis suggesting orbitofrontal and parahippocampal regions discriminated distraction

condition more strongly for Ile89Val than controls, we present images at lower thresholds. These images are presented in Figure 3.A.1 in order to demonstrate the spread of “activation” at lowered thresholds is roughly symmetric. The symmetric spreading, particularly for the orbitofrontal region, counts against the possibility that MVPA group differences near the edge of the brain were artifactual and driven by participant head motion.

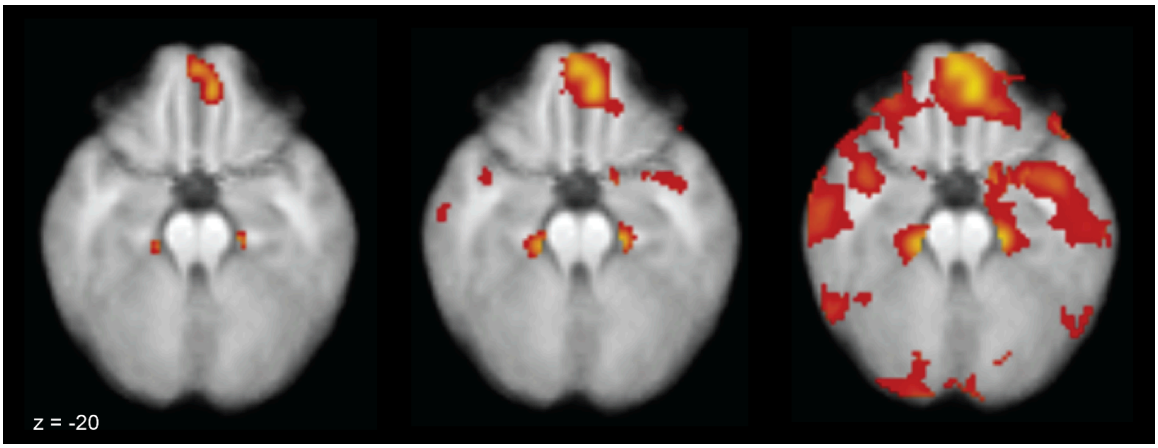

Figure 3.A.1. Decreasing threshold for Ile89Val > control MVPA results. To investigate whether group differences for the MVPA exploratory analysis were artifactual, we generated contrasted weight maps at three thresholds. Displayed are regions showing greater discrimination for dSAT vs SAT for Ile89Val than controls (Ile89Val dSAT > SAT weight map – control dAST > SAT weight map). The spreading of regions was largely symmetrical which supports the view that groups showed real functional differences in the pattern of brain activity in orbitofrontal cortex and parahippocampal gyrus.

Acknowledgements

This chapter presented research conducted in collaboration with Cindy Lustig, Martin Sarter, and Randy Blakely from Vanderbilt University. This research was supported by PHS grants R01MH086530 (MS, CL). Anne Berry was supported a NSF Graduate Research Fellowship. Additional thanks go to Elise Demeter for her efforts in helping to establish the University of Michigan Cognitive Genetics Program (COGENT), and to Brett English for performing genotyping analyses.

References

Aguirre, G. K. (2003). Functional imaging in behavioral neurology and cognitive neuropsychology. In T. E. Feinberg & M. J. Farah (Eds.), *Behavioral Neurology and Cognitive Neuropsychology* (pp. 85-96). New York: McGraw-Hill.

Apparsundaram, S., Martinez, V., Parikh, V., Kozak, R., & Sarter, M. (2005). Increased capacity and density of choline transporters situated in synaptic membranes of the right medial prefrontal cortex of attentional task-performing rats. *J Neurosci, 25*(15), 3851-3856.

Arnold, H. M., Burk, J. A., Hodgson, E. M., Sarter, M., & Bruno, J. P. (2002). Differential cortical acetylcholine release in rats performing a sustained attention task versus behavioral control tasks that do not explicitly tax attention. *Neuroscience, 114*(2), 451-460.

Bakeman, R. (2005). Recommended effect size statistics for repeated measures designs. *Behav Res Methods, 37*(3), 379-384.

Balleine, B. W., & O'Doherty, J. P. (2010). Human and rodent homologies in action control: corticostriatal determinants of goal-directed and habitual action. *Neuropsychopharmacology, 35*(1), 48-69.

Berry, A. S., Demeter, E., Sabhapathy, S., English, B. A., Blakely, R. D., Sarter, M., et al. (in press). Disposed to distraction: Genetic variation in the cholinergic system influences distractibility but not time-on-task effects. *J Cogn Neurosci*.

Berry, A. S., Sarter, M., & Lustig, C. (in prep). Frontoparietal correlates of attentional effort versus distractor resistance during challenges to attention.

Brett, M., Anton, J., Valabregue, R., & Poline, J. (2002). *Region of interest analysis using an SPM toolbox [abstract].* Paper presented at the 8th International Conference on Functional Mapping of the Human Brain.

Broussard, J. I., Karelina, K., Sarter, M., & Givens, B. (2009). Cholinergic optimization of cue-evoked parietal activity during challenged attentional performance. *Eur J Neurosci, 29*(8), 1711-1722.

Brown, V. J., & Bowman, E. M. (2002). Rodent models of prefrontal cortical function. *Trends Neurosci, 25*(7), 340-343.

Burges, C. J. C. (1998). A tutorial on support vector machines for pattern recognition. *Data Mining and Knowledge Discovery, 2*, 121-167.

Button, K. S., Ioannidis, J. P., Mokrysz, C., Nosek, B. A., Flint, J., Robinson, E. S., et al. (2013). Power failure: why small sample size undermines the reliability of neuroscience. *Nat Rev Neurosci, 14*(5), 365-376.

Counts, S. E., & Mufson, E. J. (2005). The role of nerve growth factor receptors in cholinergic basal forebrain degeneration in prodromal Alzheimer disease. *J Neuropathol Exp Neurol, 64*(4), 263-272.

Davis, T., & Poldrack, R. A. (2013). Measuring neural representations with fMRI: practices and pitfalls. *Annals of the New York Academy of Sciences, 1296*, 108-134.

Daw, N. D., O'Doherty, J. P., Dayan, P., Seymour, B., & Dolan, R. J. (2006). Cortical substrates for exploratory decisions in humans. *Nature, 441*(7095), 876-879.

Demeter, E., Guthrie, S. K., Taylor, S. F., Sarter, M., & Lustig, C. (2013). Increased distractor vulnerability but preserved vigilance in patients with schizophrenia: evidence from a translational Sustained Attention Task. *Schizophr Res, 144*(1-3), 136-141.

Demeter, E., Hernandez-Garcia, L., Sarter, M., & Lustig, C. (2011). Challenges to attention: a continuous arterial spin labeling (ASL) study of the effects of distraction on sustained attention. *Neuroimage, 54*(2), 1518-1529.

Demeter, E., Sarter, M., & Lustig, C. (2008). Rats and humans paying attention: cross-species task development for translational research. *Neuropsychology, 22*(6), 787-799.

English, B. A., Hahn, M. K., Gizer, I. R., Mazei-Robison, M., Steele, A., Kurnik, D. M., et al. (2009). Choline transporter gene variation is associated with attention-deficit hyperactivity disorder. *J Neurodev Disord, 1*(4), 252-263.

Everitt, B. J., & Robbins, T. W. (1997). Central cholinergic systems and cognition. *Annual Review of Psychology, 48*, 649-684.

Faul, F., Erdfelder, E., Buchner, A., & Lang, A.G. (2009). Statistical power analyses using G*Power 3.1: Tests for correlation and regression analyses. *Behavior Research Methods, 41*, 1149-1160.

Frey, P. W., & Colliver, J. A. (1973). Sensitivity and responsivity measures for discrimination learning. *Learning and Motivation, 4*, 327-342.

Fritz, C. O., Morris, P. E., & Richler, J. J. (2012). Effect size estimates: Current use, calculations, and interpretation. *Journal of Experimental Psychology. General, 141*, 2-18.

Gill, T. M., Sarter, M., & Givens, B. (2000). Sustained visual attention performance-associated prefrontal neuronal activity: evidence for cholinergic modulation. *J Neurosci, 20*(12), 4745-4757.

Hahn, M. K., Blackford, J. U., Haman, K., Mazei-Robison, M., English, B. A., Prasad, H. C., et al. (2008). Multivariate permutation analysis associates multiple polymorphisms with subphenotypes of major depression. *Genes Brain Behav, 7*(4), 487-495.

Hasselmo, M. E. (1995). Neuromodulation and Cortical Function - Modeling the Physiological-Basis of Behavior. *Behavioural Brain Research, 67*(1), 1-27.

Hasselmo, M. E., & McGaughy, J. (2004). High acetylcholine levels set circuit dynamics for attention and encoding and low acetylcholine levels set dynamics for consolidation. *Acetylcholine in the Cerebral Cortex, 145*, 207-231.

Hasselmo, M. E., & Sarter, M. (2011). Modes and models of forebrain cholinergic neuromodulation of cognition. *Neuropsychopharmacology, 36*(1), 52-73.

Hernandez Lallement, J., Kuss, K., Trautner, P., Weber, B., Falk, A., & Fliessbach, K. (2014). Effort increases sensitivity to reward and loss magnitude in the human brain. *Social cognitive and affective neuroscience, 9*(3), 342-349.

Howe, W. M., Berry, A. S., Francois, J., Gilmour, G., Carp, J. M., Tricklebank, M., et al. (2013). Prefrontal cholinergic mechanisms instigating shifts from monitoring for cues to cue-guided performance: converging electrochemical and fMRI evidence from rats and humans. *J Neurosci, 33*(20), 8742-8752.

Huba, G. J., Singer, J. L., Aneshensel, C. S., & Antrobus, J. S. (1982). *Short Imaginal Processes Inventory*. Port Huron, MI: Research Psychologists Press.

Jenkinson, M., Bannister, P., Brady, M., & Smith, S. (2002). Improved optimization for the robust and accurate linear registration and motion correction of brain images. *Neuroimage, 17*(2), 825-841.

Kamitani, Y., & Sawahata, Y. (2010). Spatial smoothing hurts localization but not information: pitfalls for brain mappers. *Neuroimage, 49*(3), 1949-1952.

Kozak, R., Bruno, J. P., & Sarter, M. (2006). Augmented prefrontal acetylcholine release during challenged attentional performance. *Cereb Cortex, 16*(1), 9-17.

Kurzban, R., Duckworth, A., Kable, J. W., & Myers, J. (2013). An opportunity cost model of subjective effort and task performance. *The Behavioral and brain sciences, 36*(6), 661-679.

Lancaster, J. L., Rainey, L. H., Summerlin, J. L., Freitas, C. S., Fox, P. T., Evans, A. C., et al. (1997). Automated labeling of the human brain: a preliminary report on the development and evaluation of a forward-transform method. *Hum Brain Mapp, 5*(4), 238-242.

Lancaster, J. L., Woldorff, M. G., Parsons, L. M., Liotti, M., Freitas, C. S., Rainey, L., et al. (2000). Automated Talairach atlas labels for functional brain mapping. *Hum Brain Mapp, 10*(3), 120-131.

Luck, S. J., Ford, J. M., Sarter, M., & Lustig, C. (2012). CNTRICS final biomarker selection: Control of attention. Schizophrenia bulletin, 38(1), 53-61.

Maldjian, J. A., Laurienti, P. J., Kraft, R. A., & Burdette, J. H. (2003). An automated method for neuroanatomic and cytoarchitectonic atlas-based interrogation of fMRI data sets. *Neuroimage, 19*(3), 1233-1239.

Martinez, V., & Sarter, M. (2004). Lateralized attentional functions of cortical cholinergic inputs. *Behav Neurosci, 118*(5), 984-991.

Mayka, M. A., Corcos, D. M., Leurgans, S. E., & Vaillancourt, D. E. (2006). Three-dimensional locations and boundaries of motor and premotor cortices as defined by functional brain imaging: a meta-analysis. *Neuroimage, 31*(4), 1453-1474.

McGaughy, J., Kaiser, T., & Sarter, M. (1996). Behavioral vigilance following infusions of 192 IgG-saporin into the basal forebrain: selectivity of the behavioral impairment and relation to cortical AChE-positive fiber density. *Behav Neurosci, 110*(2), 247-265.

Mesulam, M. (2004). The cholinergic lesion of Alzheimer's disease: pivotal factor or side show? *Learn Mem, 11*(1), 43-49.

Mufson, E. J., Ma, S. Y., Cochran, E. J., Bennett, D. A., Beckett, L. A., Jaffar, S., et al. (2000). Loss of nucleus basalis neurons containing trkA immunoreactivity in individuals with mild cognitive impairment and early Alzheimer's disease. *J Comp Neurol, 427*(1), 19-30.

Neumann, S. A., Brown, S. M., Ferrell, R. E., Flory, J. D., Manuck, S. B., & Hariri, A. R. (2006). Human choline transporter gene variation is associated with corticolimbic reactivity and autonomic-cholinergic function. *Biol Psychiatry, 60*(10), 1155-1162.

O'Doherty, J., Kringelbach, M. L., Rolls, E. T., Hornak, J., & Andrews, C. (2001). Abstract reward and punishment representations in the human orbitofrontal cortex. *Nat Neurosci, 4*(1), 95-102.

O'Doherty, J., Winston, J., Critchley, H., Perrett, D., Burt, D. M., & Dolan, R. J. (2003). Beauty in a smile: the role of medial orbitofrontal cortex in facial attractiveness. *Neuropsychologia, 41*(2), 147-155.

Okuda, T., Okamura, M., Kaitsuka, C., Haga, T., & Gurwitz, D. (2002). Single nucleotide polymorphism of the human high affinity choline transporter alters transport rate. *J Biol Chem, 277*(47), 45315-45322.

Op de Beeck, H. P. (2010). Against hyperacuity in brain reading: spatial smoothing does not hurt multivariate fMRI analyses? *Neuroimage, 49*(3), 1943-1948.

Oppenheim, A. V., Schafer, R. W., & Buck, J. R. (1999). *Discrete-time signal processing*. Englewood Cliffs, NJ: Prentice Hall.

Paolone, G., Mallory, C. S., Koshy Cherian, A., Miller, T. R., Blakely, R. D., & Sarter, M. (2013). Monitoring cholinergic activity during attentional performance in mice heterozygous for the choline transporter: A model of cholinergic capacity limits. *Neuropharmacology, 75*, 274-285.

Parikh, V., St Peters, M., Blakely, R. D., & Sarter, M. (2013). The presynaptic choline transporter imposes limits on sustained cortical acetylcholine release and attention. *J Neurosci, 33*(6), 2326-2337.

Poldrack, R. A. (2006). Can cognitive processes be inferred from neuroimaging data? *Trends in cognitive sciences, 10*(2), 59-63.

Poldrack, R. A. (2011). Inferring mental states from neuroimaging data: from reverse inference to large-scale decoding. *Neuron, 72*(5), 692-697.

Rangel, A., & Hare, T. (2010). Neural computations associated with goal-directed choice. *Curr Opin Neurobiol, 20*(2), 262-270.

Rao, H., Gillihan, S. J., Wang, J., Korczykowski, M., Sankoorikal, G. M., Kaercher, K. A., et al. (2007). Genetic variation in serotonin transporter alters resting brain function in healthy individuals. *Biol Psychiatry, 62*(6), 600-606.

Rogers, R. D., Ramnani, N., Mackay, C., Wilson, J. L., Jezzard, P., Carter, C. S., et al. (2004). Distinct portions of anterior cingulate cortex and medial prefrontal cortex are activated by reward processing in separable phases of decision-making cognition. *Biol Psychiatry, 55*(6), 594-602.

Rushworth, M. F., Noonan, M. P., Boorman, E. D., Walton, M. E., & Behrens, T. E. (2011). Frontal cortex and reward-guided learning and decision-making. *Neuron, 70*(6), 1054-1069.

Sarter, M., & Bruno, J. P. (1997). Cognitive functions of cortical acetylcholine: Toward a unifying hypothesis. *Brain Research Reviews, 23*(1-2), 28-46.

Sarter, M., Gehring, W. J., & Kozak, R. (2006). More attention must be paid: the neurobiology of attentional effort. *Brain Res Rev, 51*(2), 145-160.

Sarter, M., Lustig, C., & Taylor, S. F. (2012). Cholinergic contributions to the cognitive symptoms of schizophrenia and the viability of cholinergic treatments. *Neuropharmacology, 62*(3), 1544-1553.

Sarter, M., Lustig, C., Howe, W. M., Gritton, H., & Berry, A. S. (2014). Deterministic functions of cortical acetylcholine. *Eur J Neurosci*.

Schrouff, J., Rosa, M. J., Rondina, J. M., Marquand, A. F., Chu, C., Ashburner, J., et al. (2013). PRoNTo: pattern recognition for neuroimaging toolbox. *Neuroinformatics, 11*(3), 319-337.

Simon, J. R., Atweh, S., & Kuhar, M. J. (1976). Sodium-dependent high affinity choline uptake: a regulatory step in the synthesis of acetylcholine. *J Neurochem, 26*(5), 909-922.

Song, X. W., Dong, Z. Y., Long, X. Y., Li, S. F., Zuo, X. N., Zhu, C. Z., et al. (2011). REST: a toolkit for resting-state functional magnetic resonance imaging data processing. *PloS one, 6*(9), e25031.

St Peters, M., Demeter, E., Lustig, C., Bruno, J. P., & Sarter, M. (2011). Enhanced control of attention by stimulating mesolimbic-corticopetal cholinergic circuitry. *J Neurosci, 31*(26), 9760-9771.

Taylor, S. F., Martis, B., Fitzgerald, K. D., Welsh, R. C., Abelson, J. L., Liberzon, I., et al. (2006). Medial frontal cortex activity and loss-related responses to errors. *J Neurosci, 26*(15), 4063-4070.

Valentin, V. V., Dickinson, A., & O'Doherty, J. P. (2007). Determining the neural substrates of goal-directed learning in the human brain. *J Neurosci, 27*(15), 4019-4026.

Xie, J., & Guo, Q. (2004). Par-4 inhibits choline uptake by interacting with CHT1 and reducing its incorporation on the plasma membrane. *J Biol Chem, 279*(27), 28266-28275.

Yamamura, H. I., & Snyder, S. H. (1972). Choline: high-affinity uptake by rat brain synaptosomes. *Science, 178*(4061), 626-628.

Chapter IV

POSTPERCEPTUAL ELECTROPHYSIOLOGICAL CORRELATES OF SUCCESSFUL SIGNAL DETECTION DURING DISTRACTOR CHALLENGE

INTRODUCTION

Irrelevant stimuli can interfere with the detection of relevant signals in the environment. For example, during a rainstorm, the motion of the windshield wipers may distract a driver when she searches for a street sign. During motivated performance, cognitive control mechanisms may be engaged to overcome interference, promoting the maintenance of high levels of performance. Continuing the driving example, enhanced cognitive control allows the driver to ignore irrelevant inputs and can improve the detection of relevant signs allowing the driver to make the correct turn.

Here we tested the influence of irrelevant distraction on the neural correlates of signal detection. We used a visual signal detection task, the Sustained Attention Task (SAT), and its distractor condition (dSAT) to examine the influence of controlled attention on processing of relevant signals in occipital and parietal cortex. We hypothesized that the presence of a global distractor, a flashing background screen, decreases the perceptual salience of relevant signals, but that the engagement of cognitive control processes facilitates

performance in the distractor condition by enhancing postperceptual signal processing.

Previous fMRI studies using SAT and dSAT have been limited in their evaluation of the distractor's impact on signal-related processing in occipital and parietal cortex. The relatively low temporal resolution of fMRI imaging techniques coupled with the strong global visual distractor made it difficult to dissociate the potentially subtle differences in signal-related activity in occipital cortex between SAT and dSAT signals from the large hemodynamic response in occipital cortex evoked by the distractor. The EEG methods used in the present study circumvent these limitations through improved temporal resolution, which allows for the detection of small electrophysiological changes in signal-evoked neuronal responses on a millisecond timescale.

Our primary measure of visual perception was the N1 event-related potential (ERP). The N1 is an exogenous waveform that is always evoked by visual stimuli. It is a negative deflection occurring as early as 120 ms post stimulus onset and is maximal in lateral occipital electrodes. Larger and earlier N1 waveforms are thought to reflect enhanced perceptual processing of relevant targets, and N1 enhancement is associated with performance gains in detection and discrimination tasks (Anllo-Vento, 1995; Csibra, Johnson, & Tucker, 1997; Eimer, 1997; Luck et al., 1994). Interfering with the perceptual salience of a target by lowering its luminance delays the N1, increasing its latency in occipital cortex (Johannes, Munte, Heinze, & Mangun, 1995). We hypothesized the global,

flashing distractor would decrease the salience of dSAT signals relative to SAT signals, and that this could be measured in suppression of the N1 perceptual response.

An alternative hypothesis would be that the increased cognitive control demands imposed by the distractor may drive greater attentional selection for dSAT signals, leading to an enhanced N1 response. The N1 is the earliest visual component to show amplitude and latency enhancement by attentional selection (Luck & Hillyard, 1995; Luck et al., 1994)[1]. Specifically, targets presented in cued locations or containing selected features evoke larger and earlier N1 responses. It is thought the top-down control of attention mediates this modulation of perceptual markers in occipital cortex (reviewed in Hillyard, Teder-Salejarvi, & Munte, 1998). However, a previous study investigating the impact of variation in attentional selection (target location) and target salience (luminance) suggested attentional selection does not overcome the suppressive N1 effects of decreased target salience (Johannes et al., 1995). Though the manipulations of target salience and attentional selection used by Johannes and colleagues differ from our own, our favored prediction was that dSAT signals would evoke smaller and later N1 responses than SAT signals due to the distractor's degrading effect on signal salience.

[1] P1, an earlier visually-evoked ERP does not show enhancement by selection relative to neutral stimuli, but is often suppressed for stimuli presented at noncued locations or that contain irrelevant features (Berry, Zanto, Rutman, Clapp, & Gazzaley, 2009; Clapp, Rubens, & Gazzaley, 2010; Luck, Heinze, Mangun, & Hillyard, 1990).

Our ERP measure of postperceptual signal processing was the P3, a later waveform also modulated by attention. It is a positive deflection occurring as early as 300 ms post stimulus onset and is maximal at parietal/occipto-parietal midline electrodes. Specifically, the P3 is associated with continued evaluation of the signal and its amplitude increases with greater attentional allocation (Isreal, Chesney, Wickens, & Donchin, 1980). The P3 is associated with a number of cognitive processes, most notably context updating (Donchin, 1981). In this framework, the P3 reflects the updating or refinement of internally maintained representations of the environment in order to guide behavior. In the current study, the P3 may reflect the evaluation of perceptual representations to judge whether the signal occurred, the updating of the current trial identity as a signal trial, and the adjustment expectations of what will come next (e.g. the cue to respond). The latency of the P3 may index the efficiency of these processes. In the current study, if early attentional selection in the perceptual period is not present (or fails) during dSAT trials, increased modulation of the P3 could represent late, "just in time" increases in signal-related processing supporting the subsequent hit response.

Though the source of top-down cognitive control signals supporting dSAT performance is not known, right PFC approximating Brodmann's area (BA) 9 is a candidate region. This mid-dorsal/dorsolateral PFC region is part of the frontoparietal cognitive control network, and previous fMRI studies consistently show increases activation in this region during dSAT performance (Berry,

Blakely, Sarter, & Lustig, in prep; Berry, Sarter, & Lustig, in prep; Demeter et al., 2011). Supporting its role in cognitive control functions, stronger functional connectivity between right BA 9 and posterior parietal regions was associated with successful maintenance of performance during distraction (Berry, Sarter et al., in prep). Here we analyzed oscillatory coherence between prefrontal and posterior electrodes to examine the timecourse of these effects.

PFC oscillatory activity in the theta frequency range (4-7 Hz) is associated with cognitive control; it increases during attention demanding tasks (Anguera et al., 2013; Muller & Anokhin, 2012; Nigbur, Ivanova, & Sturmer, 2011; Onton, Delorme, & Makeig, 2005; Sauseng, Hoppe, Klimesch, Gerloff, & Hummel, 2007), and disruptions in theta power accompany cognitive deficits associated with schizophrenia (Kaser et al., 2013; Ranlund et al., 2014). Coordinated fluctuation in oscillatory activity (measured through phase-locking) is a measure of functional connectivity between brain regions, and may index long-range communication across regions and the engagement of cognitive control networks (Buzsaki & Draguhn, 2004; Fell & Axmacher, 2011; Uhlhaas et al., 2009). Fronto-posterior theta coherence increases in tasks demanding cognitive control in humans (Anguera et al., 2013; Onton et al., 2005; Sauseng et al., 2007) and rodents (Benchenane et al., 2010; Jones & Wilson, 2005), and has been implicated in the cognitive control deficits associated with schizophrenia (Sharma, Weisbrod, Kaiser, Markela-Lerenc, & Bender, 2011; Sigurdsson, Stark, Karayiorgou, Gogos, & Gordon, 2010). We aimed to determine the timecourse of

increases in phase-locking associated with signal detection, and to determine whether increases in connectivity were associated with optimal performance during distraction.

METHODS

Participants.

Final analyses included data from 22 healthy young adults (mean age, 21.4 years; range 19-29 years; 10 females). Participants scored at least 9 on the Extended Range Vocabulary Test (ERVT) (mean score = 20.89, SE = 5.13; range 9-29.5). EEG data for one additional participant were excluded because they were collected at a lower sampling frequency. All participants were right-handed, had normal or corrected to normal vision, did not have a history of learning disorders, anxiety, depression or ADHD, and did not take psychotropic medication. Participants gave informed consent to participate in the study approved by the Institution Review Board at the University of Michigan.

Behavioral task.

Participants performed the Sustained Attention Task (SAT) and its distractor condition (dSAT) as previously described (Demeter, Guthrie, Taylor,

Sarter, & Lustig; 2013; Demeter, Hernandez-Garcia, Sarter, & Lustig, 2011; Demeter, Sarter, & Lustig, 2008). Stimuli were presented through E-Prime software (Psychology Software Tools) and were displayed on a CRT monitor. Participants were seated 50 cm from the monitor in a dim, sound attenuated, and electrically shielded testing chamber.

Each trial of the SAT consisted of a variable-duration monitoring period (2-10 sec) at the end of which a signal (27-66 ms; varied randomly across signal trials) did or did not appear, with 50% probability (Figure 4.1). One second after the signal or nonsignal event, two horizontal lines representing levers appeared for 1.2 sec, indicating the start of the response period. This screen was displayed for the entire duration of the response window. Participants responded with a left ("z" key) or right ("/" key) index-finger keypress to indicate whether or not a signal had appeared on that trial, with left vs right key assignment to signal vs nonsignal events counterbalanced across subjects. At the end of the response window, feedback consisting of a green screen for correct responses or a red screen for incorrect responses was presented for 200 ms, after which the screen went blank, indicating the start of the next trial. Responses were classified as hits (correct signal trials), misses (incorrect signal trials), correct rejections (CR; correct nonsignal trials), false alarms (FA; incorrect nonsignal trials), and omissions. dSAT trials were identical to SAT trials except the background screen flashed from gray to black at 20 Hz[2]. Participants were provided monetary

[2] The 20 Hz distractor was used in favor of the 10 Hz distractor used in earlier studies so that analyses of oscillatory activity in the alpha range (8 – 12 Hz) would not be

incentive. For each task run, participants were paid 1 cent for each percent correct, but penalized 5 cents for the percent of missed trials.

Participants performed four task runs of SAT trials and four task runs of dSAT trials consisting of 70 trials per run. Trial types (signal vs nonsignal) were pseudorandomly intermixed with the restriction that signal and nonsignal trials followed each other with equal probability within a run.

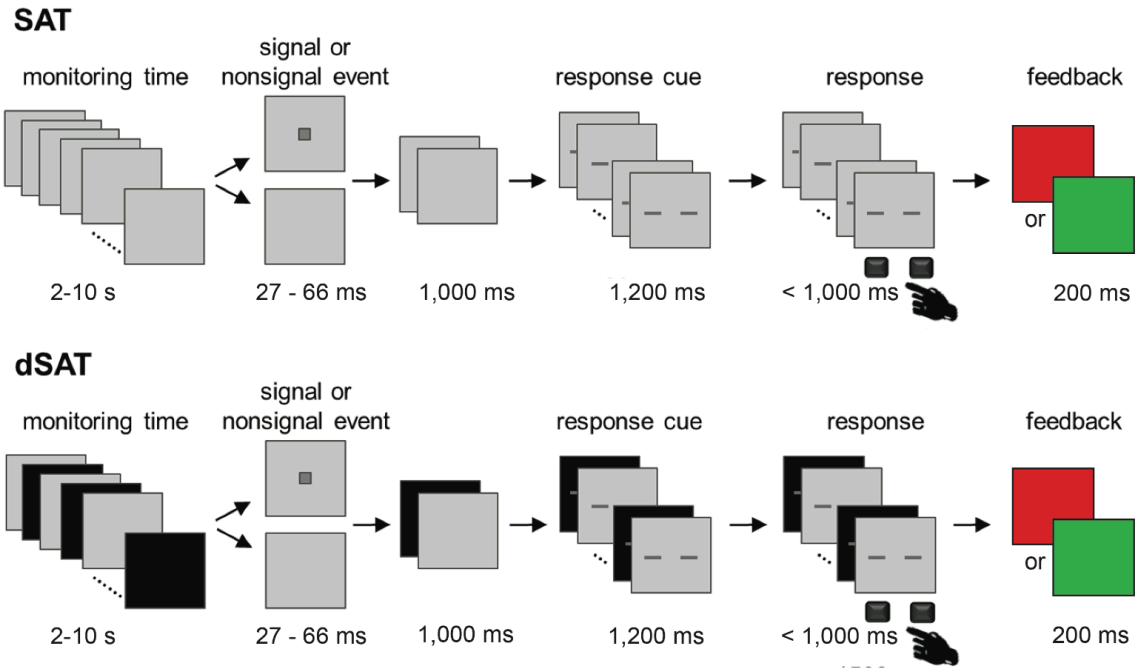

Figure 4.1. Sustained Attention Task (SAT). Each trial consisted of a variable duration monitoring interval followed by the presentation of a signal or nonsignal event. The signal was a gray square on a silver background and varied in duration. Signal and nonsignal events were pseudorandomized and occurred with equal frequency. Participants were cued to respond by the presentation of a screen with two gray bars. Participants responded via buttonpress using one index finger for signal trials and the other index finger for nonsignal trials (left-right key assignment counterbalanced across participants). The cue to respond remained on the screen for 1,200 ms until accuracy feedback was given. Correct responses were followed by a green screen; incorrect responses or omissions were followed by a red screen. During dSAT trials, the screen flashed from gray to black at 20 Hz. SAT and dSAT trials were presented in separate task runs.

---

contaminated. These analyses yielded largely null results that are not included in the present report.

Behavioral analysis.

We compared SAT score, a measure of performance across both signal and nonsignal trials, for SAT and dSAT trials. For completeness, Appendix III reports the standard signal-detection measures of sensitivity (d') and bias (Swets, Tanner, & Birdsall, 1961). SAT score was calculated for each condition (SAT, dSAT) using the formula SAT score = (hits – FAs)/[2(hits + FAs) – (hits + FAs)^2]. SAT score varies from + 1 to -1 with + 1 indicating all responses were hits or CRs and -1 indicating all responses were misses or FAs.

EEG data acquisition and preprocessing.

Electrophysiological signals were recorded with an ActiveTwo BioSemi 64-channel Ag-AgCl active electrode EEG acquisition system in conjunction with ActiView Software (BioSemi; Amsterdam, The Netherlands). Signals were amplified and digitized at 1,024 Hz with 24-bit resolution. All electrode offsets were between ± 20 mV. Data were recorded referenced to a ground formed from a common mode sense (CMS) active electrode and driven right leg (DRL) passive electrode (see http://www.biosemi.com/faq/cms&drl.htm). Data were referenced to the mastoids off-line. Electrooculogram was recorded from electrodes placed above, below, and on the outer canthi of both eyes.

Eye blink correction was made using the procedure described by Gratton, Coles and Donchin (Gratton, Coles, & Donchin, 1983). For ERP analysis, anti-aliasing and band-pass filters (0.1 and 30 Hz) were applied, whereas theta coherence analyses used only the 0.1 Hz high-pass filter. We removed noisy channels identified during the recording session and replaced them with averaged signal from the surrounding electrodes to minimize the number of trials removed due to artifacts. We removed individual trials containing artifacts with a voltage threshold ± 100 μV. Using EEGLAB Toolbox (Delorme & Makeig, 2004) and ERPLAB Toolbox (erpinfo.org/erplab), we extracted EEG epochs of 1,500 ms timelocked to signal onset.

Data analysis methods and rationale: Neural.

As described below, we analyzed ERP and phase-locking neural measures associated with successful signal detection (hits) during standard SAT performance and during dSAT performance. Main analyses tested for significant effects of distraction on signal-evoked neural measures. In addition, we performed Pearson correlations to assess the relationship between individual differences in these measures and performance. Hit rates for SAT and dSAT trials were used for correlational analyses rather than SAT score, an accuracy measure comprising signal and nonsignal trials, because neural measures reflected only signal-related processing. For correlation analyses, we eliminated

data for one participant whose hit rate for SAT and dSAT trials was greater than 3 SD below the mean. Though this participant was excluded from correlation analyses, we report r-values both including and excluding this subject for all significant and marginal correlations so the reader may interpret the results accordingly. Overall performance of this subject was comparable to the performance of fMRI participants (overall hit rate = 80%), and SAT score and d' indices were within 3 SD of the mean. Therefore, data from this participant was included in analyses of main effects.

ERP data. We focused our analyses on signal-evoked responses, and included only correct signal trials (hits). Before calculating the ERP, a 200 ms prestimulus baseline was subtracted from each trial. Because the global flashing distractor may cause differences in baseline noise in our recordings, we limited our investigation to large ERP components, occipital N1 and parietal P3, rather than smaller ones (such as the occipital P1 and frontal P3). Peak negative deflection values were chosen in the window between 120-300 ms for the N1 and peak positive deflection values were chosen in the window between 300-600 ms for the P3. Mean ERP amplitudes (+/- 5 ms) and latencies were analyzed for electrodes of interest in lateral occipital cortex (PO8, PO7) for the N1 and midline parietal cortex (POz) for the P3. These electrodes were selected based on within-experiment localization performed by averaging responses to all visual stimuli (including SAT and dSAT signals, cue to respond, and response feedback). On

the group level, the maximal N1 response was found at electrode PO8 on right lateral occipital cortex and the maximal P3 response at electrode POz on midline occipito-parietal cortex. PO7 on left lateral occipital cortex was included in analysis to assess possible laterality effects.

Theta phase-locking. Finally, we examined functional connectivity between right PFC and occipito-parietal cortex by measuring signal-evoked increases in theta (4-7 Hz) phase-locking. Functional connectivity analyses examined coherence following the signal, and included only correct signal trials (hits). Phase-locking values (PLVs) were calculated between right-lateralized prefrontal (FC4, F4, FC6, C4, FC2) and midline occipito-parietal (POz, Oz, O1, O2, Iz) electrodes. Our selection of these midline occipto-parietal electrodes was based on a recent study demonstrating increased theta phase-locking between occipito-parietal cortex and PFC was associated with optimal cognitive control performance (Anguera et al., 2013). We selected right PFC electrodes based on the location of right BA 9 activation increases during dSAT performance (MNI coordinates: 46, 3, 30). To guide the selection of right PFC electrodes corresponding with this region for coherence analysis, we used Brainsight frameless stereotaxic software (Rogue Research, Montreal, Canada) to co-register a separate volunteer's high-resolution anatomical T1-weighted anatomical MRI image with her head in a common digital workspace. While the volunteer wore the EEG cap, we identified the electrodes surrounding the right PFC coordinates.

To calculate PFC and occipito-parietal phase-locking values, EEG data were filtered using a two-way, zero phase-lag, finite impulse response filter (eegfilt.m fuction in EEGLAB Toolbox; Delorme & Makeig, 2004), and a Hilbert transform was applied to each time series (hilbert.m function). Results from the current analysis are comparable to data-dependent triangulation (DDT) and wavelet approaches (Bruns, 2004; Le Van Quyen et al., 2001). Phase-locking values range from 0-1 where 0 represents randomly distributed phases and 1 represents perfect phase-locking. We examined differences in phase-locking from the onset of the signal stimulus to the onset of the response cue (1 second). Data are displayed in 100 ms bins. We identified the timepoint of peak coherence for SAT and dSAT trials combined and used this timepoint for subsequent correlation analyses.

RESULTS

Statistical tests and effect-size calculation.

For analysis of behavioral, ERP, and phase-locking data, we used two-tailed paired *t* tests and repeated-measures ANOVA. For ANOVAs, we applied the Greenhouse-Geisser correction for sphericity when necessary (degrees of freedom reported as integers in the text for easier reading) and performed *post hoc* analyses using two-tailed paired *t* tests. The factors included in each

analysis are specified in the relevant subsections below. ANOVA effect sizes were calculated using η^2_G (Bakeman, 2005), which gives smaller values than the frequently-used η^2_P but is preferable as it reduces error when comparing across studies (Fritz, Morris, & Richler, 2012). Effect sizes for *t* tests were calculated using Cohen's d. We calculated neural-behavioral correlations using Pearson's r. Data were analyzed with SPSS, version 21.

Behavioral data.

Performance for SAT and dSAT conditions was high, though was not at ceiling for any trial type (all $t > 4.17$, $p < .001$). Omissions were generally low (SAT M = .03, SD = .03; dSAT M = .02, SD = .02), and did not differ across conditions, $t < 1$. Response accuracy was equivalent for SAT and dSAT conditions $t < 1$, though RT data revealed modest slowing with distraction.

Analysis of SAT score revealed no effect of distraction $t < 1$. Table 4.1 displays hit and FA values that make up SAT score, and d' indices.

Table 4.1. Hit and false alarm proportions for SAT and dSAT trials. Data are means (standard deviation).

	Hits	**False alarms**
SAT	.94 (.05)	.07 (.06)
dSAT	.96 (.04)	.06 (.07)

Analysis of RT data revealed modest slowing associated with distraction. Specifically, the presence of the distractor slowed CR responses $t(22) = 2.29$, $p =$

.03, dz = 0.42 (SAT RT M = 626.76 SD = 48.04, dSAT RT M = 614.43 SD = 49.90), but not hit responses, $F < 1$.

ERP data.

N1 amplitude. We conducted repeated measures ANOVA with factors distraction (SAT, dSAT) and laterality (right, left). dSAT signals evoked smaller N1 ERP amplitudes relative to SAT signals, $F(1, 21) = 5.39$, $p = .03$, $\eta^2_G = 0.02$ (Figure 4.2). Consistent with the bilateral distribution of the N1 displayed in Figure 4.2, there was no effect of laterality, $F < 1$. Additionally, there were no hemispheric interactions with distraction, $F < 1$. On an individual subject level, there was no correlation between SAT or dSAT hit rate and N1 amplitude (mean right and left hemisphere), both $r < .26$, $p = 26$.

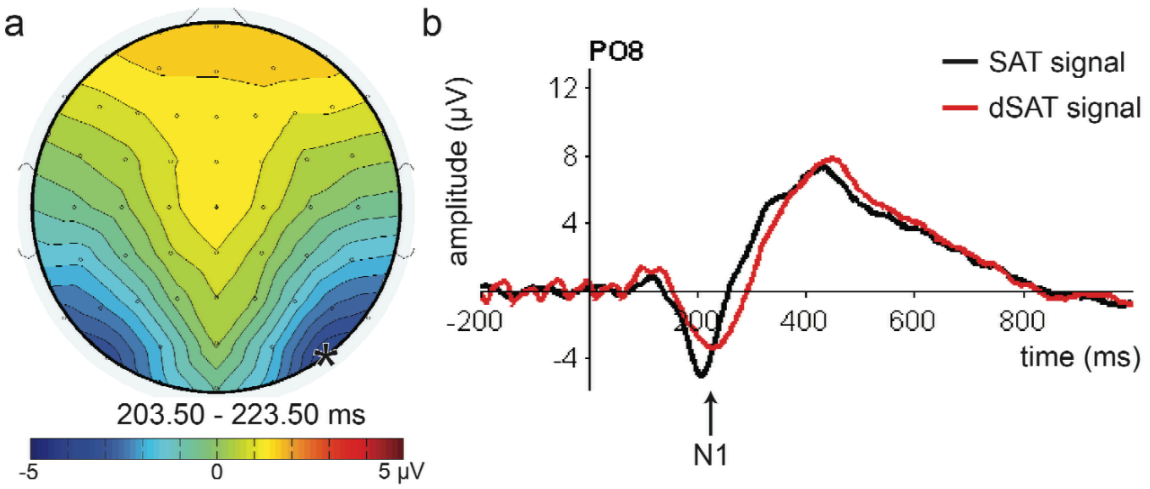

Figure 4.2. Signal-evoked N1 ERP: stimulus perception. For SAT and dSAT signals combined, the N1 waveform peaked approximately 214 ms post signal onset. (a) The N1 was maximal at lateral occipital electrodes and did not show right versus left hemispheric differences in amplitude or latency. Electrode of interest PO8 is indicated with an asterisk. (b) dSAT and SAT signal-evoked ERPs are displayed at electrode PO8, though equivalent effects were found at PO7. The N1 peak was significantly smaller and later for dSAT signals relative to SAT signals. The diminished N1 response suggests the distractor diminished the perceptual salience of dSAT signals.

N1 latency. Consistent with N1 amplitude findings, the ERP evoked by dSAT signals peaked later than SAT signals, $F(1, 21) = 34.20$, $p < .001$, $\eta^2_G = 0.16$, though the effect size was much greater (compare to $\eta^2_G = 0.02$). Latencies did not differ across hemispheres, $F < 1$, and there was no interaction with distraction, $F(1, 21) = 2.81$, $p = .11$, $\eta^2_G = 0.02$. On an individual subjects level, SAT hit rate and N1 latency showed a trend-level correlation in the expected direction. Participants with the earliest N1 peaks were more likely to detect the signal, $r = -.36$, $p = .11$ two-tailed, $p = .05$ one-tailed (outlier excluded), $r = -.32$, $p = .14$ two-tailed, $p = .07$ one-tailed (outlier included; Figure 4.3). There was no relationship between dSAT hit and N1 latency, $r = -.08$, $p = .73$.

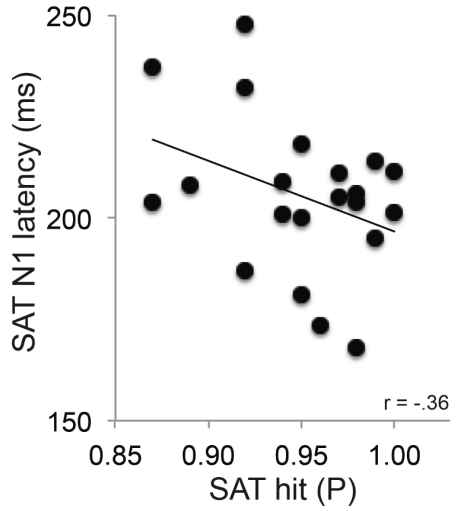

Figure 4.3. N1 latency neural-behavioral correlation. There was a modest relationship between N1 latency for SAT signals and SAT hit rate such that participants with the earliest N1 peaks detected the greatest percentage of signals. Earlier N1 responses may reflect stronger perceptual representations of the signal, which was associated with higher hit rates.

P3 amplitude. We next assessed modulation of the later P3 component by distraction to assess whether high levels of dSAT performance may be maintained by greater postperceptual processing of the signal. Figure 4.4 displays the scalp topography for the P3, indicating it was maximal for midline occipito-parietal electrodes. For the parietal P3, dSAT and SAT signals evoked ERPs with equivalent amplitudes, $t(21) = .83$, $p = .42$, $dz = 0.18$ (Figure 4.4). On an individual subjects level, there was no correlation between SAT or dSAT hit rate and P3 amplitude, both $r < .13$.

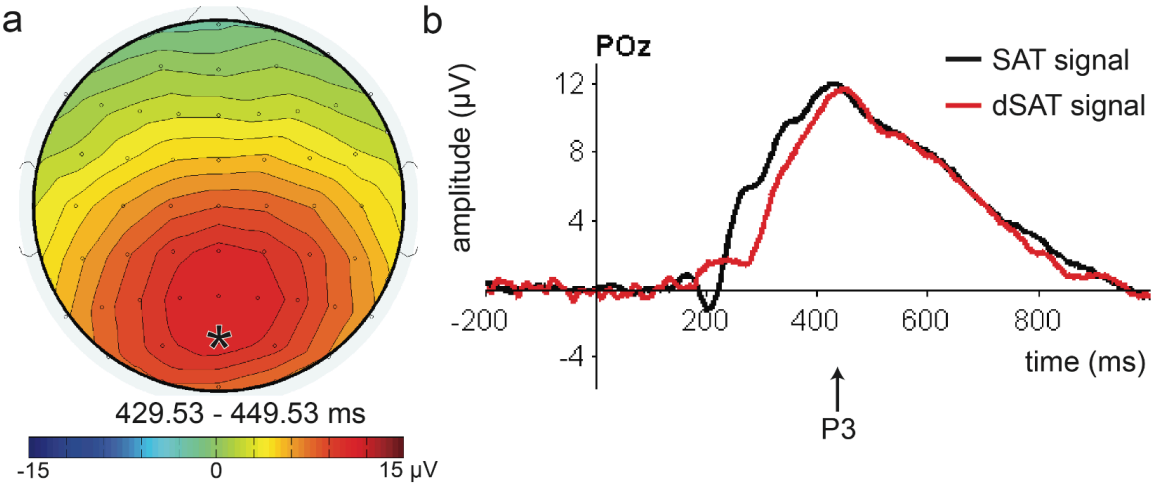

Figure 4.4. Signal-evoked P3 ERP: postperceptual processing. For SAT and dSAT signal combined, P3 waveform peaked approximately 240 ms post signal onset. (a) The P3 was maximal at midline occipito-parietal electrodes. Electrode of interest POz is indicated with an asterisk. (b) SAT and dSAT signal-evoked ERPs are displayed at electrode POz. There was no effect of distraction on P3 peak amplitude or latency despite early N1 perception-related differences measured in lateral occipital electrodes. A small downward N1 deflection (between 200 – 300 ms) can be seen for SAT and dSAT signal-evoked ERPs plotted above. Though the N1 response was small at POz, the dSAT signal-evoked N1 deflection appeared smaller and later than the SAT signal-evoked N1, as was demonstrated by the N1 statistical analysis above.

P3 latency. Consistent with P3 amplitude findings, there was no difference in P3 latency for dSAT and SAT signals, $t(21) = 1.19$, $p = .25$, $dz = .25$. These findings indicated that by the time of the P3 peak, approximately 450 ms post signal onset, processing of SAT and dSAT signals was statistically indistinguishable. On an individual subjects level, there was a significant correlation between dSAT hit rate and P3 latency such that participants with the earlier P3 peaks were more likely to detect the signal, $r = -.55$, $p = .01$ (outlier excluded), $r = -.18$, $p = .43$ (outlier included; Figure 4.5). There was no relationship between SAT hit rate and P3 latency, $r = .16$, $p = .48$.

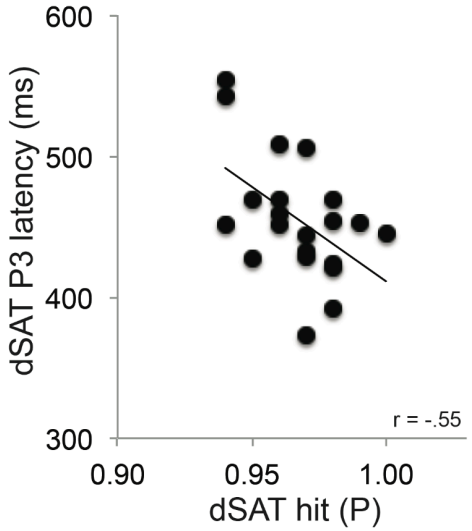

Figure 4.5. P3 latency neural-behavioral correlation. There was a significant correlation between P3 latency for dSAT signals and dSAT hit rate such that participants with the earliest P3 peaks detected the greatest percentage of signals. Earlier P3 responses may reflect greater postperceptual processing of the signal, which was associated with higher hit rates despite diminished perception-related N1 response for dSAT signals.

Theta coherence data.

Theta coherence between right PFC and midline occipito-parietal cortex was maximal for the 500-600 ms period post signal onset for both SAT and dSAT signals (Figure 4.6). Coherence for this timebin was significantly greater than baseline, $t(21) = 3.86$, $p = .001$, $dz = 0.82$. Though connectivity for this timebin was numerically greater following dSAT signals than SAT signals, differences did not reach statistical significance, $t(21) = 1.44$, $p = .16$, $dz = 0.31$.

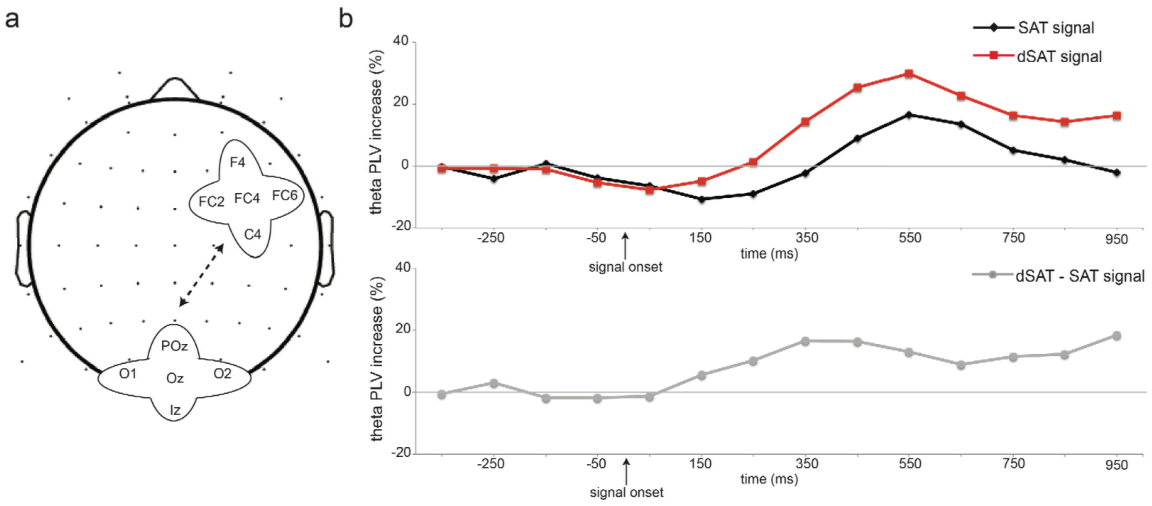

Figure 4.6. Functional connectivity: theta coherence. (a) We measured the degree of theta phase-locking between right PFC and occipito-parietal cortex following SAT and dSAT signals. Theta phase-locking is a measure of long-range functional connectivity that increases with greater demands on cognitive control. (b) Theta phase-locking peaked approximately 550 ms post stimulus onset for both SAT and dSAT signals. Though phase-locking was greater for dSAT signals at this timepoint on average, differences between conditions were not significant. Differences in phase-locking between conditions are plotted over time in gray to demonstrate mean differences between conditions begin to emerge as early as 150 ms post stimulus onset during the perceptual window.

On an individual subject level, dSAT hit performance correlated with dSAT coherence during the 500-600 ms timebin such that high performers had the strongest connectivity, $r = .56$, $p = .008$ (outlier excluded), $r = .57$, $p = .006$ (outlier included) (Figure 4.7). For SAT trials, there was no relationship between SAT hits and connectivity, $r = .06$, $p = .79$.

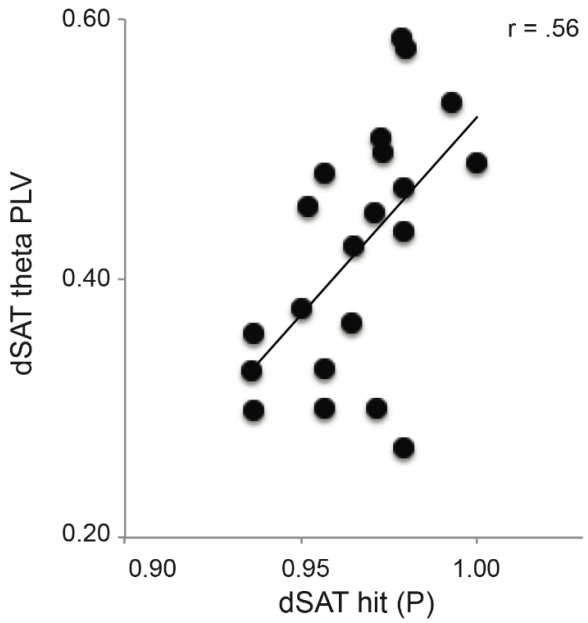

Figure 4.7. Postperceptual theta phase-locking and dSAT performance. Higher theta phase-locking following dSAT signals was positively correlated with higher dSAT hit rates. This relationship suggested the engagement of cognitive control processes via frontoparietal functional connectivity in the postperceptual period was associated with successful dSAT signal detection despite early perceptual interference.

DISCUSSION

The present study examined the effect of irrelevant distraction on signal detection. The results complement previous fMRI studies by defining the distractor's impact on neural activity with greater temporal precision. Specifically, our findings indicated the presence of distraction interfered with early perception of the relevant signal, but that successful detection performance may have been maintained via greater postperceptual signal processing starting approximately 440 ms post signal onset. Individual differences analyses suggested enhanced signal-related processing in occipito-parietal cortex and enhanced frontoparietal functional connectivity supported optimal detection performance during

distraction. The relationship between functional connectivity and performance found in the present study mirrors previous fMRI findings, and offers new insights regarding the timecourse of engagement of cognitive control during attentional challenge.

The presence of the flashing distractor during dSAT trials interfered with perception of the signal, as indexed by smaller and later N1 evoked potentials in occipital cortex. The effect of distraction on N1 latency was considerably stronger than its effect on N1 amplitude. This pattern is consistent with previous investigations that examined the impact that low target salience has on ERPs (Johannes et al., 1995). The similarity in N1 findings across studies suggests the N1 effects observed for dSAT signals stemmed from degradation of the signal's salience by the flashing distractor.

The diminished N1 perceptual response evoked by dSAT signals may have increased uncertainty as to whether the signal was presented. For SAT trials in which perceptual representations were stronger and "certainty" was greater, early N1 latency was associated with successful detection (though the relationship only reached one-tailed significance). Participants with the highest SAT hit rates had the earliest N1 signal-evoked potentials, which suggests successful detection was facilitated by enhanced perception of the signal. For SAT signals, enhancement of later postperceptual markers did not correlate with performance, which may indicate that the strong perceptual representation of the signal was sufficient to drive successful detection. In contrast to this, for dSAT

signals, N1 latency was not an indicator of subsequent performance. Instead, enhancement of postperceptual measures most strongly correlated with performance. Relationships between performance and postperceptual measures suggest this later processing may have acted to resolve uncertainty and preserve detection performance.

For the postperceptual P3 waveform, the responses for SAT and dSAT signals were equivalent. P3 latency correlated with dSAT performance, but not SAT performance, suggesting modulation of the P3 had greater functional relevance for dSAT trials. Though there is continued debate in the literature about the cognitive processes that underlie the P3 waveform, there is general agreement that it is associated with continued processing of the stimulus postperception. In the present study, the signal-evoked P3 may have reflected the continued evaluation of the perceptual representation in working memory, identification of the present trial as a signal trial, and updating of expectations of what will come next. These processes are broadly consistent with the influential "context updating" account of the P3 (Donchin, 1981), which posits the P3 reflects the updating or refinement of internally maintained representations in order to guide behavior. This account is also compatible with the cognitive functions associated with the neural generators of the P3: parietal cortex and medial temporal lobe structures (Ebmeier et al., 1995; Kirino, Belger, Goldman-Rakic, & McCarthy, 2000; Knight, Scabini, Woods, & Clayworth, 1989). Together, our findings suggest that when perceptual processing was limited, enhanced P3-

related processing may have compensated to maintain optimal detection performance.

A previous fMRI study of SAT and dSAT implicated increased frontoparietal functional connectivity in the successful preservation of high levels of performance during dSAT (Berry, Sarter, et al., in prep). dSAT is associated with increased activation in right PFC approximating BA 9, a region in the frontoparietal cognitive control network (Berry, Blakely, et al., in prep; Berry, Sarter et al., in prep; Demeter et al., 2011). Functional connectivity analyses (psychophysiological interaction) demonstrated participants with the strongest right BA 9 – posterior parietal connectivity showed the smallest decrements in performance during distraction (SAT – dSAT score). A test of the consistency of this relationship was to assess whether, for an electrophysiological dataset, increased functional connectivity was associated with optimal dSAT detection performance.

Complementing the previous fMRI findings, we found increased theta phase-locking between right PFC and occipito-parietal cortex positively correlated with dSAT performance. While there may be increases in synchrony within cognitive control networks that are maintained over time when attention is challenged, the temporal resolution of EEG allowed for the observation that frontoparietal connectivity increased transiently following presentation of the signal, peaking approximately 550 ms post signal onset. These findings suggest the signal itself evoked the strengthening of functional connections, and the

relationship between transient connectivity increases and performance leave open the possibility that long-range synchronization was associated with communication or the coordination of processing across region to facilitate successful detection performance.

Long-range frontoparietal theta phase-locking has been specifically implicated in the engagement of cognitive control, and is sensitive to individual differences in cognitive control function. A recent study by Anguera and colleagues (2013) demonstrated age-related differences in theta phase-locking between PFC and posterior cortices during target discrimination. Older adults showed diminished phase-locking accompanied by lower task performance relative to young adults. Suggesting theta phase-locking is sensitive to therapeutic intervention, older adults that took part in computerized training designed to improve cognitive control showed significant increases in theta phase-locking and task performance at post-training test. These findings support the use of frontoparietal connectivity as a useful, and sensitive marker for measuring cognitive control function. Indeed, our own fMRI resting state connectivity findings indicate frontoparietal network activity may be a relatively stable predictor of subsequent attentional control performance (Berry, Sarter et al., in prep), opening the possibility of using such connectivity measures as an index of cognitive control capacity from which to measure or predict post-intervention gains (c.f. Varkuti et al., 2013; Urner, Schwarzkopf, Friston, & Rees, 2013; reviewed in Guerra-Carrillo, Mackey, & Bunge, 2014).

Together our findings indicate that the dSAT distractor impaired early perceptual processing of the signal in lateral occipital cortex, but that later processing in occipito-parietal cortex may have resolved perceptual interference. Increases in frontoparietal connectivity, associated with engagement of cognitive control, are particularly implicated in the maintenance of optimal detection performance in the face of distraction. Future studies using dSAT may investigate possible disruption of frontoparietal connectivity in schizophrenia, a disorder associated with deficits in controlled attention (Demeter et al., 2013) as well as long-range theta coherence (Sharma et al., 2011; Sigurdsson et al., 2010). Frontoparietal connectivity, if deficient, may be an important target for future therapeutic intervention as gains in frontoparietal connectivity may benefit performance on a broad range of tasks that require cognitive control.

APPENDIX III

METHODS

Behavioral analysis d'

d' was calculated from the proportions of hits and FAs using the standard formula: d' = z(hits) – z(FAs) (Green & Swets, 1966). The following substitution was made for hit rates of 100%: 1-1/(2N) where N is the total number of signals. For FA rates of 0, we used the percentage equivalent to half a FA (1/2N) where N is the total number of nonsignal stimuli. Bias measures were calculated using the formula: $B"_D$ = [(1 -hits)(1 - FAs) – (hits x FAs)]/[(1 - hits)(1 - FAs) + (hits x FAs)] (Donaldson, 1992). Bias scores range from -1 to +1, with -1 indicating a liberal response bias, and + 1 indicating a conservative response bias.

RESULTS

Behavioral analysis d'

Similar to SAT score results, d' showed no effect of distraction on accuracy, $t < 1$. Additionally, there was no effect of distraction on bias, $t(22) = 1.42$, $p = .17$, $dz = 0.28$, though bias became slightly more conservative during dSAT (SAT M = -0.9, SD = .32; dSAT M = .01, SD = .08).

Acknowledgements

This chapter presented research conducted in collaboration with Cindy Lustig, Martin Sarter, and Bill Gehring. This research was supported by a Rackham research grant (AB). Anne Berry was supported a NSF Graduate Research Fellowship. Special thanks go to Bill Gehring for his enormous generosity in opening his lab to our collaboration! Additional thanks go to Jose Torres and Ursula Seals for their assistance data collection, to Joe Orr for his introduction to Gratton eye-bink correction, and to Joaquin Anguera for his training in phase-locking analyses.

References

Anguera, J. A., Boccanfuso, J., Rintoul, J. L., Al-Hashimi, O., Faraji, F., Janowich, J., et al. (2013). Video game training enhances cognitive control in older adults. *Nature, 501*(7465), 97-101.

Anllo-Vento, L. (1995). Shifting attention in visual space: the effects of peripheral cueing on brain cortical potentials. *The International journal of neuroscience, 80*(1-4), 353-370.

Bakeman, R. (2005). Recommended effect size statistics for repeated measures designs. *Behav Res Methods, 37*(3), 379-384.

Benchenane, K., Peyrache, A., Khamassi, M., Tierney, P. L., Gioanni, Y., Battaglia, F. P., et al. (2010). Coherent theta oscillations and reorganization of spike timing in the hippocampal- prefrontal network upon learning. *Neuron, 66*(6), 921-936.

Berry, A. S., Blakely, R. D., Sarter, M., & Lustig, C. (in prep). A choline transporter minor allele is associated with attenuated hemodynamic response in right prefrontal cortex during challenges to attention.

Berry, A. S., Sarter, M., & Lustig, C. (in prep). Frontoparietal correlates of attentional effort versus disttractor resistance during challenges to attention.

Berry, A. S., Zanto, T. P., Rutman, A. M., Clapp, W. C., & Gazzaley, A. (2009). Practice-related improvement in working memory is modulated by changes in processing external interference. *Journal of neurophysiology, 102*(3), 1779-1789.

Braver, T. S., Barch, D. M., Keys, B. A., Carter, C. S., Cohen, J. D., Kaye, J. A., et al. (2001). Context processing in older adults: evidence for a theory relating cognitive control to neurobiology in healthy aging. *J Exp Psychol Gen, 130*(4), 746-763.

Braver, T. S., Gray, J. R., & Burgess, G. C. (Eds.). (2007). *Explaining the many varieties of working memory variation: Dual mechanisms of cognitive control*: Oxford University Press.

Braver, T. S., Satpute, A. B., Rush, B. K., Racine, C. A., & Barch, D. M. (2005). Context processing and context maintenance in healthy aging and early stage dementia of the Alzheimer's type. *Psychol Aging, 20*(1), 33-46.

Bruns, A. (2004). Fourier-, Hilbert- and wavelet-based signal analysis: are they really different approaches? *J Neurosci Methods, 137*(2), 321-332.

Buzsaki, G., & Draguhn, A. (2004). Neuronal oscillations in cortical networks. *Science, 304*(5679), 1926-1929.

Clapp, W. C., Rubens, M. T., & Gazzaley, A. (2010). Mechanisms of working memory disruption by external interference. *Cereb Cortex, 20*(4), 859-872.

Csibra, G., Johnson, M. H., & Tucker, L. A. (1997). Attention and oculomotor control: a high-density ERP study of the gap effect. *Neuropsychologia, 35*(6), 855-865.

Delorme, A., & Makeig, S. (2004). EEGLAB: an open source toolbox for analysis of single-trial EEG dynamics including independent component analysis. *J Neurosci Methods, 134*(1), 9-21.

Demeter, E., Guthrie, S. K., Taylor, S. F., Sarter, M., & Lustig, C. (2013). Increased distractor vulnerability but preserved vigilance in patients with schizophrenia: evidence from a translational Sustained Attention Task. *Schizophr Res, 144*(1-3), 136-141.

Demeter, E., Hernandez-Garcia, L., Sarter, M., & Lustig, C. (2011). Challenges to attention: a continuous arterial spin labeling (ASL) study of the effects of distraction on sustained attention. *Neuroimage, 54*(2), 1518-1529.

Demeter, E., Sarter, M., & Lustig, C. (2008). Rats and humans paying attention: cross-species task development for translational research. *Neuropsychology, 22*(6), 787-799.

Desimone, R., & Duncan, J. (1995). Neural mechanisms of selective visual attention. *Annu Rev Neurosci, 18*, 193-222.

Donaldson, W. (1992). Measuring recognition memory. *J Exp Psychol Gen, 121*(3), 275-277.

Donchin, E. (1981). Presidential address, 1980. Surprise!...Surprise? *Psychophysiology, 18*(5), 493-513.

Ebmeier, K. P., Steele, J. D., MacKenzie, D. M., O'Carroll, R. E., Kydd, R. R., Glabus, M. F., et al. (1995). Cognitive brain potentials and regional cerebral blood flow equivalents during two- and three-sound auditory "oddball tasks". *Electroencephalogr Clin Neurophysiol, 95*(6), 434-443.

Eimer, M. (1997). Attentional selection and attentional gradients: an alternative method for studying transient visual-spatial attention. *Psychophysiology, 34*(3), 365-376.

Fell, J., & Axmacher, N. (2011). The role of phase synchronization in memory processes. *Nat Rev Neurosci, 12*(2), 105-118.

Fritz, C. O., Morris, P. E., & Richler, J. J. (2012). Effect size estimates: Current use, calculations, and interpretation. *Journal of Experimental Psychology. General, 141*, 2-18.

Gratton, G., Coles, M. G., & Donchin, E. (1983). A new method for off-line removal of ocular artifact. *Electroencephalogr Clin Neurophysiol, 55*(4), 468-484.

Green, D. M., & Swets, J. A. (1966). *Signal detection theory and psychophysics*. New York: Wiley.

Guerra-Carrillo, B., Mackey, A. P., & Bunge, S. A. (2014). Resting-State fMRI: A Window into Human Brain Plasticity. *The Neuroscientist : a review journal bringing neurobiology, neurology and psychiatry*.

Hillyard, S. A., Teder-Salejarvi, W. A., & Munte, T. F. (1998). Temporal dynamics of early perceptual processing. *Curr Opin Neurobiol, 8*(2), 202-210.

Isreal, J. B., Chesney, G. L., Wickens, C. D., & Donchin, E. (1980). P300 and tracking difficulty: evidence for multiple resources in dual-task performance. *Psychophysiology, 17*(3), 259-273.

Johannes, S., Munte, T. F., Heinze, H. J., & Mangun, G. R. (1995). Luminance and spatial attention effects on early visual processing. *Brain research. Cognitive brain research, 2*(3), 189-205.

Jones, M. W., & Wilson, M. A. (2005). Theta rhythms coordinate hippocampal-prefrontal interactions in a spatial memory task. *PLoS biology, 3*(12), e402.

Kaser, M., Soltesz, F., Lawrence, P., Miller, S., Dodds, C., Croft, R., et al. (2013). Oscillatory underpinnings of mismatch negativity and their relationship with cognitive function in patients with schizophrenia. *PloS one, 8*(12), e83255.

Kirino, E., Belger, A., Goldman-Rakic, P., & McCarthy, G. (2000). Prefrontal activation evoked by infrequent target and novel stimuli in a visual target detection task: an event-related functional magnetic resonance imaging study. *J Neurosci, 20*(17), 6612-6618.

Knight, R. T., Scabini, D., Woods, D. L., & Clayworth, C. C. (1989). Contributions of temporal-parietal junction to the human auditory P3. *Brain research, 502*(1), 109-116.

Le Van Quyen, M., Foucher, J., Lachaux, J., Rodriguez, E., Lutz, A., Martinerie, J., et al. (2001). Comparison of Hilbert transform and wavelet methods for the analysis of neuronal synchrony. *J Neurosci Methods, 111*(2), 83-98.

Luck, S. J., Heinze, H. J., Mangun, G. R., & Hillyard, S. A. (1990). Visual event-related potentials index focused attention within bilateral stimulus arrays. II. Functional dissociation of P1 and N1 components. *Electroencephalogr Clin Neurophysiol, 75*(6), 528-542.

Luck, S. J., & Hillyard, S. A. (1995). The role of attention in feature detection and conjunction discrimination: an electrophysiological analysis. *The International journal of neuroscience, 80*(1-4), 281-297.

Luck, S. J., Hillyard, S. A., Mouloua, M., Woldorff, M. G., Clark, V. P., & Hawkins, H. L. (1994). Effects of spatial cuing on luminance detectability: psychophysical and electrophysiological evidence for early selection. *J Exp Psychol Hum Percept Perform, 20*(4), 887-904.

Miller, E. K., & Cohen, J. D. (2001). An integrative theory of prefrontal cortex function. *Annu Rev Neurosci, 24*, 167-202.

Muller, V., & Anokhin, A. P. (2012). Neural synchrony during response production and inhibition. *PloS one, 7*(6), e38931.

Nigbur, R., Ivanova, G., & Sturmer, B. (2011). Theta power as a marker for cognitive interference. *Clinical neurophysiology : official journal of the International Federation of Clinical Neurophysiology, 122*(11), 2185-2194.

Onton, J., Delorme, A., & Makeig, S. (2005). Frontal midline EEG dynamics during working memory. *Neuroimage, 27*(2), 341-356.

Ranlund, S., Nottage, J., Shaikh, M., Dutt, A., Constante, M., Walshe, M., et al. (2014). Resting EEG in psychosis and at-risk populations - A possible endophenotype? *Schizophr Res*.

Sauseng, P., Hoppe, J., Klimesch, W., Gerloff, C., & Hummel, F. C. (2007). Dissociation of sustained attention from central executive functions: local activity and interregional connectivity in the theta range. *Eur J Neurosci, 25*(2), 587-593.

Sharma, A., Weisbrod, M., Kaiser, S., Markela-Lerenc, J., & Bender, S. (2011). Deficits in fronto-posterior interactions point to inefficient resource allocation in schizophrenia. *Acta psychiatrica Scandinavica, 123*(2), 125-135.

Sigurdsson, T., Stark, K. L., Karayiorgou, M., Gogos, J. A., & Gordon, J. A. (2010). Impaired hippocampal-prefrontal synchrony in a genetic mouse model of schizophrenia. *Nature, 464*(7289), 763-767.

Uhlhaas, P. J., Pipa, G., Lima, B., Melloni, L., Neuenschwander, S., Nikolic, D., et al. (2009). Neural synchrony in cortical networks: history, concept and current status. *Frontiers in integrative neuroscience, 3*, 17.

Urner, M., Schwarzkopf, D. S., Friston, K., & Rees, G. (2013). Early visual learning induces long-lasting connectivity changes during rest in the human brain. *Neuroimage, 77*, 148-156.

Varkuti, B., Guan, C., Pan, Y., Phua, K. S., Ang, K. K., Kuah, C. W., et al. (2013). Resting state changes in functional connectivity correlate with movement recovery for BCI and robot-assisted upper-extremity training after stroke. *Neurorehabilitation and neural repair, 27*(1), 53-62.

Vogel, E. K., & Luck, S. J. (2000). The visual N1 component as an index of a discrimination process. *Psychophysiology, 37*(2), 190-203.

Chapter V

DISCUSSION

Summary of Chapters II-IV.

Collectivity, the research presented here supports a role of right BA 9 in the control of attention during distractor challenge. Two of our main findings directly link to our previous research. First, we found enhanced activation in right BA 9 during dSAT that correlated with the distractor's effect on performance. Participants with the greatest performance impairment during dSAT showed the highest increases in right BA 9 activation. This neural-behavioral relationship supports our previous account that activation in this region likely reflects increases in attentional effort—the activation of attentional systems in an effort to maintain performance (Demeter et al., 2011). Second, complementing previous rodent studies, we found that a genetic variant thought to limit cholinergic release (Ile89Val variant of CHT gene *SLC5A7*) was associated with dampening of the right BA 9 response to attentional challenge. These findings are an approximate replication of studies in mice with genetically imposed reductions in CHT expression (Paolone et al., 2013), and support the possibility that human cholinergic signaling contributed to right BA 9 activation increases.

In addition to findings complementing or replicating our previous research, the three studies presented here offer a number of new insights. These insights lead to new predictions to be tested in future experiments and are discussed at greater length below. Briefly, our major new contributions concern 1) the role of functional connectivity between right BA 9 and posterior parietal cortices in the successful rescue of performance during distractor challenge, and 2) the lack of behavioral deficit in Ile89Val participants and possible compensatory mechanisms.

Future directions: functional connectivity between right BA 9 and parietal cortex.

Functional connectivity analyses described in Chapter II revealed increased connectivity between right BA 9 and posterior parietal cortex was associated with preserved performance during dSAT. Specifically, multivariate regression analyses demonstrated that participants with the greatest BA 9 – precuneus/SPL PPI connectivity showed greatest resistance to distraction (smallest drops in dSAT performance relative to SAT). The strength of these functional network connections may be a relatively stable predictor of successful cognitive control. Supporting this view, the pattern of connectivity measured at rest between BA 9 and precuneus/SPL significantly predicted subsequent behavioral effects of distraction.

Functional connectivity measured in the EEG study described in Chapter IV added further support for the suggestion that right BA 9 exerted its protective effects on performance via functional network connections with posterior cortices. Analyses of theta coherence between right PFC and occipito-parietal cortex revealed participants with the greatest long-range phase locking had the highest rates of successful signal detection during dSAT. Adding temporal specificity to this observation, we found the connectivity measures peaked approximately 550 ms after the presentation of the relevant signal.

These patterns of findings suggest that the successful maintenance of performance in the face of distraction was facilitated by network interactions with posterior parietal cortices. A different pattern was found for distractor-related increases in frontal measures: right BA 9's activation and its functional connectivity with ACC. Increases in PFC measures were greatest for participants most affected by distraction (largest drops in dSAT performance relative to SAT). These regions showed the greatest enhancement where the demands on cognitive control to rescue or stabilize performance were greatest. The dissociation between the functional role of frontal connectivity and frontoparietal connectivity in the present study generally support a framework in which frontal regions control the effortful maintenance of task goals while processing in posterior cortex supports their execution (Doesnbach et al., 2006; Miller and Cohen, 2001).

An important test of the role of posterior cortices in dSAT performance will be to determine whether the perturbation of activity in parietal cortex affects the distractor's impact on performance. Such a test in humans can be achieved via transcranial magnetic stimulation (TMS). TMS is a noninvasive approach, which, depending on stimulation parameters, is thought to temporarily enhance or suppress the ability of cortical neurons to fire. I would predict that suppressive 1 Hz repetitive TMS (rTMS) of precuneus/SPL would disrupt the ability of this region to be engaged in task performance and would lead to greater performance decrements during dSAT. A complementary experiment could test the ability of excitatory short burst rTMS of precuneus/SPL to boost performance—further protecting against the effects of distraction. Experimental support for these hypotheses would strengthen our interpretation of the functional connectivity finding in Chapter II, which suggested network-level engagement of precuneus/SPL underlay distractor resistance.

An interesting test of the temporal information provided in Chapter IV and its relationship with fMRI findings would implement a different, non-repetitive form of TMS: theta burst stimulation. Unlike repetitive stimulation, which is generally applied continuously for 10 – 20 minutes prior to task performance, theta burst stimulation can be applied at specific times during task performance and may transiently increase excitability in a targeted region. I would hypothesize that stimulation of parietal cortex approximately 500 ms post signal onset would boost

detection during dSAT, but that later stimulation coincident with the response cue would not boost detection.

Though careful piloting would be required for the proposed studies, the results would be highly informative, particularly if stimulation experiments could be performed in conjunction with fMRI or EEG imaging to demonstrate disruption of functional connectivity with right BA 9. To date, TMS experiments targeting stimulation to right BA 9 have failed to reveal consistent effects of suppressive 1 Hz rTMS on performance (Berry, Meehan, Sarter, & Lustig, unpublished observation). It is possible the null results were due to compensatory engagement of other regions (including parietal cortex) following rTMS. However, such compensatory mechanisms may only be revealed through imaging (e.g. Zanto, Chadick, Satris, & Gazzaley, 2013). In addition, other nonspecific task factors (e.g. practice effects, non-optimized stimulation time) may have contributed to the lack of observable TMS effect. Nonetheless, future experiments targeting posterior parietal cortex may reveal this region to be the most sensitive target for perturbing task-relevant processing directly impacting performance.

Rodent studies lend general support for the involvement of posterior parietal cortex in SAT and dSAT performance. Successful detection is associated with greater signal-evoked parietal single unit activity (Broussard, Sarter, & Givens, 2006). Similar to effects in right PFC, increased cholinergic release in parietal cortex during task performance appears to facilitate successful signal

detection; removal of parietal cholinergic inputs reduces parietal signal-evoked activity and decreases hit rates (Broussard, Karelina, Sarter, & Givens, 2009). Relevant to the functional connectivity findings of Chapters II and IV, there is evidence of functional connectivity between right PFC and posterior parietal cortex in rodents. In fact, right PFC-parietal functional connectivity may mediate the acetylcholine (ACh) increases in parietal cortex relevant to performance. Specifically, stimulation of right PFC (with glutamatergic and cholinergic agonists) increased ACh release in posterior parietal cortex (Nelson, Sarter, & Bruno, 2005). These cross-species findings implicating parietal cortex activity, and right PFC-parietal connectivity in SAT and dSAT performance suggest that further investigation specifying the role of posterior parietal cortex during distractor challenge should continue in parallel across species.

Future directions: Ile89Val behavioral findings.

In Chapter III we hypothesized that people with a polymorphism of the high-affinity transporter thought to limit cholinergic release capacity (Ile89Val) would show greater sensitivity to the distractor, but found no behavioral deficit. However, similar to null results in Chapter III, studies in mice with a deleted copy of the high-affinity transporter (CHT +/-) did not reveal consistent attentional deficits (Paolone et al., 2013). These behavioral findings in humans and mice are somewhat perplexing given previous demonstrations of the necessity of the

cholinergic system for optimal attentional performance (Martinez & Sarter, 2004; McGaughy et al., 1999; McGaughy et al., 1996; McGaughy & Sarter, 1998, 1999). Follow-up studies in mice and humans are needed to address these seemingly inconsistent findings.

A first set of experiments could address possible upregulation of post-synaptic cholinergic receptors in response to genetic limitations on transport capacity. In mice, receptor-binding assays suggest that post-synaptic nicotinic ACh receptors were unregulated in CHT +/- mice. Supporting the hypothesis that receptor upregulation compensated for reduced cholinergic release during task performance, antagonizing these receptors differentially impaired CHT +/- performance (Paolone et al., 2013). A parallel antagonist study in humans would lend additional support for this compensatory mechanism of preserved dSAT performance. Another possible avenue of research would be to attempt to limit the possible compensatory upregulation of receptors in mice by selectively inducing CHT knockdown through a viral vector prior to behavioral testing (rather than using mice born with the deleted CHT gene, presumably allowing for the development of compensatory mechanisms throughout development). Evidence of greater sensitivity to distraction in virally-induced CHT knockdowns relative to mice receiving a control vector would be consistent with our understanding of the role of ACh in controlled attention, and support our hypothesis that previous null findings were associated with compensatory receptor upregulation.

Our previous research in humans with the Ile89Val polymorphism revealed selective vulnerability to distraction using a different behavioral task: a continuous performance test with video distraction (Berry et al., in press). Both the nature of the distractor as well as the primary relevant task varied from dSAT, and thus it is difficult to know which element was the primary factor that allowed for the detection of group performance differences. Future experiments manipulating just one variable would be necessary for such a distinction to be made. See Chapter III for a discussion of a number of factors that may have caused the difference in findings between tasks.

Multivariate pattern classification analysis in Chapter III took the first steps in evaluating possible alternative cognitive strategies employed by Ile89Val to maintain attentional performance. Our findings suggest the Ile89Val polymorphism was associated with greater reward-related processing in orbitofrontal cortex during distractor challenge relative to controls. We proposed increases in cognitive effort induced by the distractor led to enhanced sensitivity to reward, and may have served to motivate continued performance. A possible avenue of future research not discussed in Chapter III would be to further examine possible differential sensitivity to cognitive effort associated with the Ile89Val polymorphism.

ACh-related differences in sensitivity to cognitive effort may be unveiled behaviorally using the AX-CPT task, which can be used to distinguish between participants using “high-effort” cognitive control strategies and those using “low-

effort" cognitive control strategies (Braver et al., 2007; Braver, Paxton, Locke, & Barch, 2009). Specifically, the reliance on high-effort *proactive* control versus low-effort *reactive* control can be revealed bi-directionally by reaction time priming effects[1]. The distinction between these alternative control mechanisms is made by the Dual Mechanisms of Control (DMC) account, which posits proactive control is established and maintained in anticipation of the onset of task stimuli, whereas reactive control acts *post hoc* after task stimuli are presented to resolve interference (Braver, 2012). Though proactive control is generally more effective, it is hypothesized to be more effortful than reactive control. Evidence that Ile89Val rely more heavily on low-effort reactive control mechanisms than controls would suggest greater sensitivity to cognitive effort.

Demonstrating sensitivity of the AX-CPT to group differences, differential reliance on reactive control has been shown for people with schizophrenia (Barch & Braver, 2005; Edwards, Barch, & Braver, 2010). Relevant to our own research, lower reliance on proactive control in people with schizophrenia is accompanied by reduced activation in right BA 9 (Edwards et al., 2010; Lesh et al., 2013; Yoon et al., 2012). Behavioral and imaging studies using the AX-CPT task may reveal the Ile89Val polymorphism is associated with an inability or resistance to engage effortful proactive cognitive control, and may be particularly fruitful in linking such limitations to reduced right BA 9 activation.

[1] Participants are presented with a stream of letters. One type of response is required for target letter X only when the letter A precedes it (AX), and another type of response is required for all other letters. The proactive control strategy is characterized by reaction time slowing for non-targets preceded by the "cue" letter A (AY). The reactive control strategy is characterized by reaction time slowing for BX trials relative to BY trials.

Final remarks.

While the three experiments presented here offer replications of previous findings and support for longstanding hypotheses, they also present new questions ripe for further investigation. An exciting avenue of new research is underway in Parkinson's disease patients with possible deficits in cholinergic function identified via Positron Emission Tomography (PET) imaging. In these patients, specific associations between the integrity of cholinergic function in posterior parietal cortex and vulnerability to distraction are beginning to emerge (Kim, Muller, Bohnen, Sarter, & Lustig, 2014). Together, connections are strengthening between studies in rodent models and human neuroimaging findings in healthy adults, genetic populations, and patients. In summary, this growing body of research converges to specify a role of right PFC, posterior parietal cortices, and the cholinergic system in attentional control that may contribute to our understanding of the neural mechanisms underlying attentional dysfunction.

References

Barch, D. M., & Braver, T. S. (2005). Cognitive control in schizophrenia: cognitive and neural mechanisms. In R. W. Engle, G. Sedek, U. von Hecker & D. N. McIntosh (Eds.), *Cognitive Limitations in Aging and Psychopathology: Attention, Working Memory, and Executive Functions* (pp. 122-159). Cambridge: Cambridge University Press.

Berry, A. S., Demeter, E., Sabhapathy, S., English, B. A., Blakely, R. D., Sarter, M., et al. (in press). Disposed to distraction: Genetic variation in the cholinergic system influences distractibility but not time-on-task effects. *J Cogn Neurosci*.

Braver, T. S. (2012). The variable nature of cognitive control: a dual mechanisms framework. *Trends in cognitive sciences, 16*(2), 106-113.

Braver, T. S., Gray, J. R., & Burgess, G. C. (Eds.). (2007). *Explaining the many varieties of working memory variation: Dual mechanisms of cognitive control*: Oxford University Press.

Braver, T. S., Paxton, J. L., Locke, H. S., & Barch, D. M. (2009). Flexible neural mechanisms of cognitive control within human prefrontal cortex. *Proc Natl Acad Sci U S A, 106*(18), 7351-7356.

Broussard, J., Sarter, M., & Givens, B. (2006). Neuronal correlates of signal detection in the posterior parietal cortex of rats performing a sustained attention task. *Neuroscience, 143*(2), 407-417.

Broussard, J. I., Karelina, K., Sarter, M., & Givens, B. (2009). Cholinergic optimization of cue-evoked parietal activity during challenged attentional performance. *Eur J Neurosci, 29*(8), 1711-1722.

Demeter, E., Hernandez-Garcia, L., Sarter, M., & Lustig, C. (2011). Challenges to attention: a continuous arterial spin labeling (ASL) study of the effects of distraction on sustained attention. *Neuroimage, 54*(2), 1518-1529.

Dosenbach, N. U., Visscher, K. M., Palmer, E. D., Miezin, F. M., Wenger, K. K., Kang, H. C., et al. (2006). A core system for the implementation of task sets. *Neuron, 50*(5), 799-812.

Edwards, B. G., Barch, D. M., & Braver, T. S. (2010). Improving prefrontal cortex function in schizophrenia through focused training of cognitive control. *Frontiers in human neuroscience, 4*, 32.

Fritz, C. O., Morris, P. E., & Richler, J. J. (2012). Effect size estimates: Current use, calculations, and interpretation. *Journal of Experimental Psychology. General, 141*, 2-18.

Kim, K., Muller, M., Bohnen, N., Sarter, M., & Lustig, C. (2014). *Vulnerability to distraction in patients with Parkinson's disease is linked to low cortical cholinergic function*. Paper presented at the Annual meeting of the Cogntive Neuroscience Society.

Lesh, T. A., Westphal, A. J., Niendam, T. A., Yoon, J. H., Minzenberg, M. J., Ragland, J. D., et al. (2013). Proactive and reactive cognitive control and dorsolateral prefrontal cortex dysfunction in first episode schizophrenia. *NeuroImage. Clinical, 2*, 590-599.

Martinez, V., & Sarter, M. (2004). Lateralized attentional functions of cortical cholinergic inputs. Behav Neurosci, 118(5), 984-991.

McGaughy, J., Decker, M. W., & Sarter, M. (1999). Enhancement of sustained attention performance by the nicotinic acetylcholine receptor agonist ABT-418 in intact but not basal forebrain-lesioned rats. Psychopharmacology, 144(2), 175-182.

McGaughy, J., Kaiser, T., & Sarter, M. (1996). Behavioral vigilance following infusions of 192 IgG-saporin into the basal forebrain: selectivity of the behavioral impairment and relation to cortical AChE-positive fiber density. Behav Neurosci, 110(2), 247-265.

McGaughy, J., & Sarter, M. (1998). Sustained attention performance in rats with intracortical infusions of 192 IgG-saporin-induced cortical cholinergic deafferentation: effects of physostigmine and FG 7142. Behav Neurosci, 112(6), 1519-1525.

McGaughy, J., & Sarter, M. (1999). Effects of ovariectomy, 192 IgG-saporin-induced cortical cholinergic deafferentation, and administration of estradiol on sustained attention performance in rats. Behav Neurosci, 113(6), 1216-1232.

Miller, E. K., & Cohen, J. D. (2001). An integrative theory of prefrontal cortex function. *Annu Rev Neurosci, 24*, 167-202.

Nelson, C. L., Sarter, M., & Bruno, J. P. (2005). Prefrontal cortical modulation of acetylcholine release in posterior parietal cortex. *Neuroscience, 132*(2), 347-359.

Paolone, G., Mallory, C. S., Koshy Cherian, A., Miller, T. R., Blakely, R. D., & Sarter, M. (2013). Monitoring cholinergic activity during attentional performance in mice heterozygous for the choline transporter: A model of cholinergic capacity limits. *Neuropharmacology, 75*, 274-285.

Swets, J., Tanner, W. P., Jr., & Birdsall, T. G. (1961). Decision processes in perception. *Psychol Rev, 68*, 301-340.

Yoon, J. H., Nguyen, D. V., McVay, L. M., Deramo, P., Minzenberg, M. J., Ragland, J. D., et al. (2012). Automated classification of fMRI during cognitive control identifies more severely disorganized subjects with schizophrenia. *Schizophr Res, 135*(1-3), 28-33.

Zanto, T. P., Chadick, J. Z., Satris, G., & Gazzaley, A. (2013). Rapid functional reorganization in human cortex following neural perturbation. *J Neurosci, 33*(41), 16268-16274.